

Optical/ γ -ray blazar flare correlations: understanding the high-energy emission process using ASAS-SN and Fermi light curves

T. de Jaeger¹★, B. J. Shappee¹, C. S. Kochanek^{2,3}, J. T. Hinkle¹, S. Garrappa⁴,
I. Liodakis⁵, A. Franckowiak⁴, K. Z. Stanek^{2,3}, J. F. Beacom^{6,2,3}, J. L. Prieto^{7,8}

¹ Institute for Astronomy, University of Hawaii, 2680 Woodlawn Drive, Honolulu, HI 96822, USA.

² Department of Astronomy, The Ohio State University, 140 W. 18th Avenue, Columbus, OH 43210, USA.

³ Center for Cosmology and AstroParticle Physics (CCAPP), The Ohio State University, 191 W. Woodruff Avenue, Columbus, OH 43210, USA.

⁴ Fakultät für Physik & Astronomie, Ruhr-Universität Bochum, D-44780 Bochum, Germany.

⁵ Finnish Centre for Astronomy with ESO, 20014 University of Turku, Finland.

⁶ Department of Physics, The Ohio State University, 191 W. Woodruff Ave., Columbus, OH 43210, USA.

⁷ Núcleo de Astronomía de la Facultad de Ingeniería y Ciencias, Universidad Diego Portales, Av. Ejército 441, Santiago, Chile.

⁸ Millennium Institute of Astrophysics, Nuncio Monsenor Sotero Sanz 100, Providencia 8320000, Santiago, Chile.

ABSTRACT

Using blazar light curves from the optical All-Sky Automated Survey for Supernovae (ASAS-SN) and the γ -ray *Fermi*-LAT telescope, we performed the most extensive statistical correlation study between both bands, using a sample of 1,180 blazars. This is almost an order of magnitude larger than other recent studies. Blazars represent more than 98% of the AGNs detected by *Fermi*-LAT and are the brightest γ -ray sources in the extragalactic sky. They are essential for studying the physical properties of astrophysical jets from central black holes. However, their γ -ray flare mechanism is not fully understood. Multi-wavelength correlations help constrain the dominant mechanisms of blazar variability. We search for temporal relationships between optical and γ -ray bands. Using a Bayesian Block Decomposition, we detect 1414 optical and 510 γ -ray flares, we find a strong correlation between both bands. Among all the flares, we find 321 correlated flares from 133 blazars, and derive an average rest-frame time delay of only $1.1^{+7.1}_{-8.5}$ days, with no difference between the flat-spectrum radio quasars, BL Lacertae-like objects or low, intermediate, and high-synchrotron peaked blazar classes. Our time-delay limit rules out the hadronic proton-synchrotron model as the driver for non-orphan flares and suggests a leptonic single-zone model. Limiting our search to well-defined light curves and removing 976 potential but unclear “orphan” flares, we find 191 (13%) and 115 (22%) clear “orphan” optical and γ -ray flares. The presence of “orphan” flares in both bands challenges the standard one-zone blazar flare leptonic model and suggests multi-zone synchrotron sites or a hadronic model for some blazars.

Key words: galaxies: jets — relativistic processes — galaxies: active

1 INTRODUCTION

Blazars are a subclass of radio-loud active galactic nuclei (AGNs) characterised by a jet pointing within a few degrees of the observer’s line of sight (Blandford & Ostriker 1978; Antonucci 1993; Urry & Padovani 1995). Due to the nearly-aligned viewing angle, we observe strong relativistic effects such as beaming of the emitted power, causing blazars to be the brightest γ -ray sources in the extragalactic sky. They represent more than 98% of the AGNs detected by the Large Area Telescope (LAT) onboard the *Fermi* γ -ray space observatory (Atwood et al. 2009; Acero et al. 2015; Abdollahi et al. 2020) and are ideal objects for studying the poorly understood physics of astrophysical jets.

Based on the strength of their optical emission lines, blazars are subdivided into flat-spectrum radio quasars (FSRQs) and BL Lacertae (BL Lac) objects (Urry & Padovani 1995). FSRQs have prominent broad emission lines, while BL Lacs have blue nearly featureless optical spectra with emission line equivalent width $< 5\text{\AA}$ (Stickel et al. 1991). Padovani & Giommi (1995) proposed an independent classification based on the peak of their spectral energy distribution (SED; see also Abdo et al. (2010) and Ghisellini et al. (2011)): low-synchrotron peaked blazars (LSP; $\nu_{\text{peak}} \leq 10^{14}$ Hz), intermediate synchrotron peaked blazars (ISP; $10^{14} \leq \nu_{\text{peak}} \leq 10^{15}$ Hz), and high-synchrotron peaked blazars (HSP; $\nu_{\text{peak}} > 10^{15}$ Hz). The HSP and ISP blazar groups are mostly BL Lacs, while the LSP class is dominated by FSRQs.

★ E-mail: dejaeger@hawaii.edu

All blazars emit across the electromagnetic spectrum. Their

SED consists of two broad non-thermal peaks, one at radio to ultra-violet wavelengths and the second at X-ray to γ -ray energies (Impey & Neugebauer 1988; Fossati et al. 1998; Marscher et al. 2008). The low-frequency peak is generally agreed to be synchrotron emission from relativistic electrons spiralling in the jet magnetic field (Urry & Mushotzky 1982; Impey & Neugebauer 1988). However, the origin of the higher-energy peak is not fully understood. It can be explained by leptonic, hadronic (Mücke et al. 2003; Böttcher et al. 2013; Madejski & Sikora 2016), or hybrid models (see Böttcher 2019 for a review).

In the leptonic model, electron pairs dominate the high-energy emissions, as the protons within the outflow are either not accelerated to sufficiently high energies or the injected energy in relativistic protons is much less than that in relativistic electrons to make a significant contribution. Therefore, GeV-TeV γ -rays are due to inverse Compton scattering (ICS) of low-energy (IR-optical-UV) target photons by the same ultra-relativistic electrons producing the synchrotron emission at lower frequencies (Maraschi et al. 1992; Sikora et al. 1994). Since the low and high-energy peaks are produced by the same population of electrons, the leptonic model predicts strong correlations between the optical and γ -ray emission. The origin of the seed photons is not clear. They could be produced within the jet (synchrotron self-Compton, SSC; e.g., Marscher & Gear 1985; Ghisellini & Maraschi 1989; Maraschi et al. 1992; Bloom & Marscher 1996; Mastichiadis & Kirk 1997; Chiang & Böttcher 2002; Arbeiter et al. 2005) or from external sources (external Compton, EC) such as the accretion disk, the “dusty torus”, or the broad-line region (Dermer & Schlickeiser 1993; Sikora et al. 1994; Ghisellini & Madau 1996; Boettcher et al. 1997; Błażejowski et al. 2000; Dermer et al. 2009).

The absence of thermal emission in BL Lac blazar flares favours a one-zone leptonic SSC model, where a single emitting region with constant and homogeneous parameters dominates the emission (Costamante & Ghisellini 2002). One-zone leptonic SSC models are interesting because of their simplicity and their limited number of free parameters. However, unlike BL Lac, the FSRQ SED is not easily described by a simple one-zone SSC model. It is best modelled with a sum of the contribution from the SSC and the scattering of external photons with the EC contribution dominant during strong γ -ray flares (Sikora et al. 1994; Ghisellini et al. 2012; Williamson et al. 2014; Böttcher 2019).

In hadronic models, the high-energy emission is associated with ultra-relativistic protons emitted by proton-synchrotron radiation (Aharonian 2000; Mücke & Protheroe 2001; Mücke et al. 2003; Liodakis & Petropoulou 2020) or photo-pion production (Mannheim 1993). A strong long-term correlated variability between the low-energy bands and γ -rays is generally not expected for the hadronic model. However, we expect a correlation between the γ -ray and the neutrino fluxes, when the γ -rays from pion decay are emitted in a similar energy range as the neutrinos. Note that for GeV γ -rays and PeV neutrinos, a correlation is not always expected (Kelner et al. 2006; Gao et al. 2017; IceCube Collaboration et al. 2018). Note also, there could still be some correlation between optical and γ -ray emission, because the hadronic processes that produce high-energy γ -rays also produce high-energy electrons, which act just like those in leptonic models. However, the corresponding low-energy emission can be overwhelmed by other sources.

Understanding the dominant process for blazar’s γ -ray emissions and the physics of the astrophysical jets can be done through two complementary approaches:

i) The first is broadband SED modelling of individual objects such as 3C 454.3, Mrk 421, Mrk 501 or PKS 2155-304. Unfortu-

nately, for almost all blazars, leptonic, hadronic, and lepto-hadronic scenarios have all been able to reproduce the SEDs of blazars successfully (e.g., Punch et al. 1992; Dermer & Schlickeiser 1993; Mannheim 1993; Urry et al. 1997; Ghisellini et al. 1998; Mücke & Protheroe 2001; Błażejowski et al. 2005; Aharonian et al. 2007; Albert et al. 2007; Jorstad et al. 2010; Böttcher et al. 2013; Cerruti et al. 2019), so it has been difficult to constrain the dominant process. Note that in the case of TXS 0506+056, the SED modelling showed that lepto-hadronic models could not reproduce simultaneously the EM and neutrino observations (Keivani et al. 2018; Gao et al. 2019; Rodrigues et al. 2019). Obtaining the SED also requires intensive multi-wavelength observational campaigns for each source.

(ii) An alternative method is to study flux variations and search for temporal correlations between the two major emission components (optical and γ -ray). This method can now be applied to a large number of blazars thanks to the well-sampled γ -ray light curves from *Fermi*-LAT and the optical light curves from new generations of optical surveys like the All-Sky Automated Survey for Supernovae (ASAS-SN; Shappee et al. 2014; Kochanek et al. 2017). This allows a significant expansion in the number of optically monitored blazars compared to previous campaigns studying individual objects such as Yale/SMARTS (Chatterjee et al. 2012; Bonning et al. 2012) or the Katzman Automatic Imaging Telescope (KAIT; Filippenko et al. 2001; Cohen et al. 2014; Liodakis et al. 2019).

Recent multi-wavelength correlation investigations of large blazar samples have constrained the dominant mechanisms driving blazar variability. For example, Liodakis et al. (2019) studied 178 *Fermi*-LAT blazars regularly monitored by KAIT and SMARTS and found strong optical/ γ -ray correlations with time delays of only a few days (1 to 30 days), supporting the leptonic models and confirming previous studies with smaller samples (Bonning et al. 2012; Chatterjee et al. 2012; Hovatta et al. 2014; Cohen et al. 2014; Liodakis et al. 2018a). However, the presence of γ -ray flares without a low-energy counterpart and optical flares without a high-energy counterpart (known as “orphan” flares) in the same blazar sample challenges the standard one-zone leptonic blazar flare model (Chatterjee et al. 2012; Böttcher et al. 2013; Cohen et al. 2014; Liodakis et al. 2019). There are several models for the origin of orphan flares (see Böttcher 2019 for a review), including a hadronic synchrotron mirror model in which a flare is due to the interaction of relativistic protons within the jet with external photons from the reflected electron-synchrotron emission from a nearby external obstacle (Böttcher 2005), a two-zone model with a site of γ -ray production situated between the broad-line region and the jet recollimation shock (MacDonald et al. 2015), an encounter between relativistic blobs in the jet and a luminous star (Banasieński et al. 2016), the effects of the magnetic fields (Joshi et al. 2016), or a stochastic dissipation model (Wang et al. 2022).

In this work, we investigate the question of the high-energy emission process by looking for optical/ γ -ray flare correlations for 1,180 blazar light curves from the *Fermi*-LAT Collaboration database (Abdollahi et al. 2022). This sample represents the most extensive and homogeneous statistical study of blazar flares. Our paper is organised as follows. Section 2 describes our optical and γ -ray data. Section 3 presents our methodology to search for optical- γ -ray flares and measure rest-frame time lag. Section 4 presents our our results. Finally, Section 5 contains a summary and conclusions. Appendix A and B present the sample and “orphan” flare information.

2 DATA SAMPLES

We selected all the sources from the 12-year *Fermi*-LAT point source (4FGL-DR3) catalogue (Abdollahi et al. 2022) with a variability index greater than 24.725. For these sources, the chance of being a steady source is $< 1\%$. This leads to a sample of 1,695 sources ($\sim 25\%$ of the 4FGL-DR3 6,659 source catalogue). Then, we remove all sources with any non-zero entry in the analysis flags column indicating that they are affected by systematic errors (Abdollahi et al. 2022). Finally, we select only the blazars and blazar candidates — the sources classified as FSRQ, BL Lac, or blazar candidates of uncertain type (BCU) — with light curves in the *Fermi* LAT Light Curve Repository (LCR¹). This leads to a final sample of 1,180 sources consisting of 503 FSRQs, 437 BL Lacs, and 240 BCU (814 LSP, 123 ISP, and 127 HSP) sources. This source list is provided in Table A1.

2.1 γ -ray light curves

The γ -ray light curves were obtained from the LAT Light Curve Repository website and included data binned at three-day, one-week, and one-month intervals. For our analysis, we use the three-day binning to detect short flares, on a day scale. Using a daily binned light curves for the brightest sources would be useful for our analysis, however, is required a full likelihood analysis which is beyond the scope of this paper. A full description of the data reduction is found on the *Fermi*-LAT Light Curve Repository website and in Abdollahi et al. (2022). Therefore, we present only a brief description here.

The LAT sources are characterised using an unbinned maximum likelihood analysis (Abdo et al. 2009) in which the complete spatial and spectral information of each photon is used in the maximum likelihood optimisation. Light curves from the LCR were created using the standard *Fermi* Tools 1.4.7 analysis suite with the *P8R3_SOURCE_V2* instrument response functions on *P8R3_SOURCE* class photons selected over an energy range spanning 100 MeV–100 GeV. To select the photons, a region of interest with a radius of 12° is centred on the source localisation with a zenith angle cut of 90° to prevent contamination from γ -rays from the Earth limb. Then, the region of interest is fitted as a point source plus a model including the diffuse γ -ray emission from our Galaxy (template: *gll_iem_v07*), the isotropic template to account for all remaining isotropic emission (template: *iso_P8R3_SOURCE_V2_v1.txt*), the Sun and Moon steady emission templates, and all point-like and extended sources from DR3. The significance of the source detections are quantified by a test statistic (TS). Here, we select a detection criterion such that the maximum-likelihood TS exceeds four ($\sim 2\sigma$). Note that no assumptions about the spectral shape of the gamma-ray sources is made and the photon index fits are fixed.

2.2 Optical light curves

ASAS-SN is a ground-based survey able to observe the entire visible sky daily to a depth of $g = 18.5$ mag (Shappee et al. 2014; Kochanek et al. 2017). Starting in 2013, with its first unit (Brutus) located on Haleakalā in Hawaii (USA), ASAS-SN is now composed of five stations in both hemispheres. Two units at the Cerro Tololo International Observatory in Chile (Cassius and Paczynski), one

at McDonald Observatory in Texas, USA (Leavitt), and finally, one at the South African Astrophysical Observatory in Sutherland, South Africa (Payne-Gaposchkin). Each unit consists of four 14-cm aperture Nikon telephoto lenses with back-illuminated, 2048² CCD cameras having a 4.47 by 4.47-degree field of view. Until late 2018, Brutus and Cassius units used a V-band filter and were switched to g-band filters after roughly one year of V- and g-band overlap with the three new units.

For each ASAS-SN field, we take three dithered 90-second exposures. All the images are processed by the *ISIS* (Alard & Lupton 1998; Alard 2000) image subtraction ASAS-SN pipeline (Shappee et al. 2014; Kochanek et al. 2017; de Jaeger et al. 2022; Hart et al. in prep). For photometry, we use the subtracted image with the reference flux of the source added back to the light curve (see <https://www.astronomy.ohio-state.edu/asassn/public/examples.shtml>). With a 2-pixel radius ($\sim 16''$) and the *IRAF* *apphot* package, we conduct aperture photometry on the coadded image-subtracted data for each nightly epoch. Note that the blazar flux in the reference image leads to small offsets in the light curve for each ASAS-SN camera. To correct the light curves, we derive an average offset by comparing the average flux of each camera during the overlapping period. As the “reference” flux, we choose the camera with a longer time coverage range. Then, we apply the different cameras’ offsets to the rest of the light curve. Finally, we bin all the light curves to a three-day cadence to be consistent with the γ -ray light curves. No Milky Way or host-galaxy extinctions have been applied to the optical photometry as the extinction does not affect our methodology to detect flares. If we apply a dust correction, all the magnitudes will be offset but the ratio between the peak of the flares and the continuum will remain the same, therefore we will detect the same flares. For the blazars near the Galactic plane, affected by dust extinction, we will observe flares for only the brightest events.

ASAS-SN is ideal for searching for blazar flare correlations as it has two unique advantages over other optical surveys:

- i) Its observational baseline begins in 2013, covering the entire sky. For comparison, ZTF has observed only the Northern hemisphere since 2018 (Bellm et al. 2019). As seen in Figure 1, there are at least 1,970 and up to 8,100 observations² of every point in the sky.
- ii) Unlike targeted optical blazar monitoring programs, it has observations of all the *Fermi*-LAT sources.

Those two unique features allow us to do the most extensive statistical study of blazar flares to date with minimal selection biased, as we observe all the blazars independently of their properties or localisation.

3 SEARCH FOR OPTICAL/ γ -RAY CORRELATIONS

In this section, we detail our methodology to search for flares and how we derive the time lag between the optical and the γ -ray emissions.

3.1 Flares

In blazar studies, one of the most important goals is to search for and characterise flares. Flares are prominent outbursts lasting for days to months surrounded by period of relative quiescence. Unfortunately,

¹ <https://fermi.gsfc.nasa.gov/ssc/data/access/lat/LightCurveRepository/about.html>.

² One epoch consists of three observations of 90 seconds.

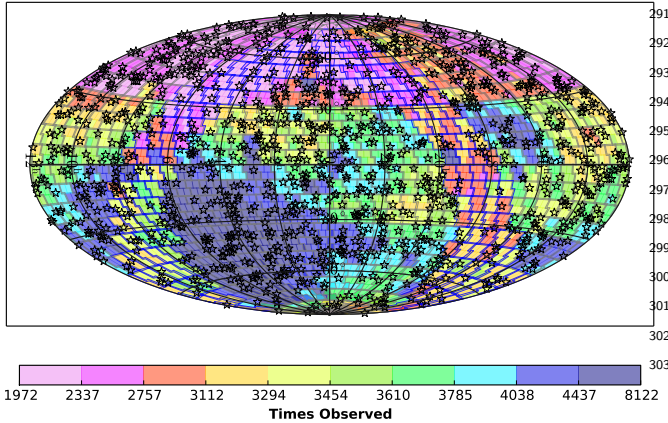


Figure 1. The all-sky, high-cadence, decade-long coverage of both ASAS-SN and *Fermi*-LAT makes the pairing of these two observational datasets compelling. ASAS-SN covers the entire visible sky with at least 1,970 epochs and more than 8,100 for some number of sky regions (as of October 11, 2022). The colour bar indicates the number of ASAS-SN epochs and the black stars indicate the 1,180 *Fermi*-LAT sources.

there is no a consensus on a quantitative definition of a flare. Here, we give a non-exhaustive list of the approaches used in the literature:

(i) A flare is simply defined as the period when the flux level exceeds $\langle F \rangle + 3\sigma_w$ where $\langle F \rangle$ is the average flux and σ_w is the weighted standard deviation (Williamson et al. 2014).

(ii) A flare is a contiguous period of time associated with a given flux peak, during which the flux exceeds half of the peak value, and this lower limit is attained exactly twice at the beginning and the end (Nalewajko 2013).

(iii) The blazar light curves are decomposed into individual flares (Valtaoja et al. 1999), each described by an exponential rise and decay (Chatterjee et al. 2008; Jorstad et al. 2010; Chatterjee et al. 2012; Liodakis et al. 2018b; Roy et al. 2019).

(iv) A flare is defined using the Bayesian block algorithm (Scargle 1998; Scargle et al. 2013). First, the Bayesian block algorithm is used to segment the blazar light curve into blocks with statistically constant fluxes. Then, we choose a flux threshold above which a block is designated as a flare (Liodakis et al. 2018a; Meyer et al. 2019; Adams et al. 2022; Stathopoulos et al. 2022).

(v) A flare is the period of time where the fractional variability amplitude (Fvar), which characterises the flux variability properties of a blazar, is above a threshold (Vaughan et al. 2003).

For this study, we use Bayesian Block Decomposition (BBD; Scargle et al. 2013; Scargle 1998), as it seems to be the most objective way to identify strong flares, for both the γ -ray and optical light curves. Additionally, it can identify significant data series changes independently of gaps or exposure variations and does not need a prior for the flare timescale. BBD determines an optimal binning for the data, where the bin sizes do not have the same width but each bin has no statistically significant flux variations. This method requires a false-positive rate (p_0) associated with the prior estimate of the number of bins, ncrprior , defined as $4 - \log(73.53p_0N^{-0.478})$, where N is the number of photometric points. We choose a false-positive rate for the optical and the γ -ray data of $p_0=0.01$.

After running the BBD, the non-flaring and flaring levels are identified using a three-step procedure following Meyer et al. (2019, see also Wagner et al. 2022 for *Python* codes).

i) We select all the local maxima³ with a peak higher than $\tilde{F} + \sigma_F$ where \tilde{F} is the median flux and σ_F is the standard deviation of the whole light curve. Note that a block peak is defined as the average flux in the block ($\overline{F_{blocks}}$).

ii) We regroup blocks using the HOP algorithm (Eisenstein & Hut 1998) based on a bottom-up hill-climbing concept. We proceed downward from the peak, and every block subsequently lower in both directions (left and right) belongs to that peak. The flux exceeding our quiescent level ($\tilde{F} + \sigma_F$) determines the start/end of the flare. Note that using the median flux for our quiescent level yields an upward bias for the true quiescent level estimate. However, this has little effect for our results, as we focus only on the most prominent flares (see Section 4.2).

iii) Finally, for our work, we study only the prominent flares. First, from all the flares defined above, we select only the flares with at least two flux points ($N > 2$). Then, we apply a threshold which depends on the number of points in the flare (See equation 1).

$$\overline{F_{blocks}} > 3 \times \frac{\overline{F_{blocks}} - \tilde{F}}{\sigma_F} \times \sqrt{N}. \quad (1)$$

Finally, we visually inspect all the flare candidates and remove the bad candidates: flares with large photometric errors, optical flares due to seasonal gap edges (e.g., higher airmass), or optical flares seen only in one optical band (V or g) during the V/g band overlap period. Then, we classify each source as:

- (i) Having at least one flare in both bands (both).
- (ii) Only in optical (opt).
- (iii) Only in γ -ray (gam).
- (iv) Without flares (none).

Table A1 shows a summary of the results of our visual inspections. Figure 2 shows an example of a blazar with flares detected in both bands after applying our methodology. We highlight correlated flares, “orphan” flares, candidate “orphan” flares, and the flares removed after our visual inspection in different colours. We select only the clearest examples for our “orphan” flare analysis, as explained in Section 4.3. For example, we do not consider the first “orphan” flare candidate at \sim MJD 58050 as a true “orphan” flare. At the same epoch, the γ -ray light curve presents a small flux rise, not enough to be considered a flare according to our definition but enough to consider the optical flare as not an “orphan”. Note also that the two “orphan” γ -ray flares detected by our methodology (magenta) are removed from the sample because they occurred during an optical observational gap.

3.2 Time lags

To resolve the structure of relativistic jets and the localisation of the emission along the length of the jet, we can study the time lags between flares in different energy bands. For example, in the leptonic single-zone model (SSC and EC), one expects time delays of only a few days because the same electrons produce flares in both bands. For example, we find short delays (on hour-day scale) when the EC is the dominant mechanism due to the stratification with the distance from the black hole of the jet regarding the amount of emitted energy and the profile of the magnetic field (Janiak et al. 2012). For some hadronic models, the low- and high-energy SED peaks vary independently and we do not expect a correlation between the optical

³ All the blocks that are higher than both the previous and subsequent blocks.

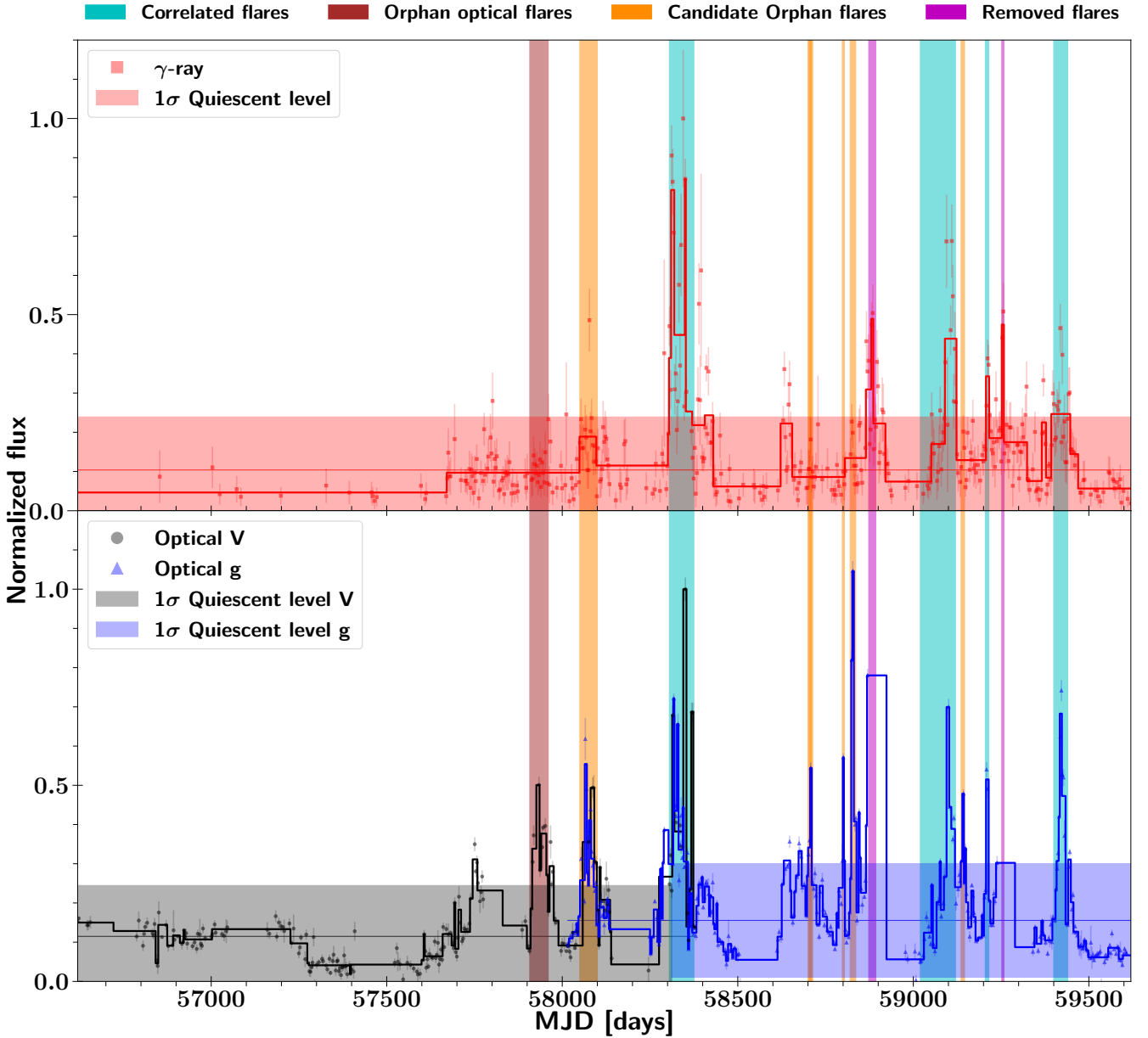


Figure 2. *Upper panel:* Fermi-LAT γ -ray light curves for J0038.2-2459 and its Bayesian Block Decomposition (solid line), together with the identified HOP groups shown by the shaded regions. *Bottom panel:* Optical V and g light curves from ASAS-SN and their BBD are shown respectively in red and black. In both panels, the vertical cyan, brown, orange and magenta-shaded regions represent the correlated flares, the flares seen in optical but not in γ -rays (“orphan” optical flares), the “orphan” candidate flares, and the flares removed after visual inspection, respectively.

and gamma-ray flares. This is the case for the proton-synchrotron model (Sikora et al. 1994; Sokolov et al. 2004; Cohen et al. 2014; Lioudakis et al. 2019; Böttcher 2019) but not for photo-hadronic cascade models (Mastichiadis et al. 2013) or purely hadronic models (Mastichiadis & Petropoulou 2021). Different works using different techniques and samples have found a strong temporal correlation between optical and γ -ray flares ruled out the proton-synchrotron model for the blazar flares. In particular, Bonning et al. (2012), Cohen et al. (2014), Lioudakis et al. (2019), and Bhatta (2021) only found short time delays of the order of days to tens of days.

In the literature, two methods are commonly used to study the cross-correlation between time series and estimate lags:

(i) Discrete Correlation Function (DCF): this method is based

on the discrete correlation function (Edelson & Krolik 1988), which, unlike the auto-correlation function, allows an estimates from unevenly sampled data.

(ii) Z-transformed discrete correlation function (ZDCF): this is a modified version of the DCF (Alexander 1997, 2013) where the cross-correlation coefficients, r , are z-transformed using Fisher transformations. Unlike the DCF, the data are rebinned with an equal numbers of data points in each lag bin. The ZDCF reduces biases and gives better estimates of the uncertainties.

In general, one computes the DCF and the ZDCF for a range of time lags. Then, the correlation peak is fit with a Gaussian to determine the time lag and its uncertainty.

Here, we focus on the lags for individual correlated flares in-

stead of cross correlations the entire light curve. By looking only at flares, we are less sensitive to seasonal systematics, especially for sources near the detection limits of ASAS-SN and Fermi. This technique is better for objects where the DCF or the ZDCF curves do not show a peak in the correlation function, but the optical and γ -ray light curves clearly have correlated flares. An example is shown in Figure 3. For this source, both DCF and ZDCF correlation functions lack a well-defined peak. However, both light curves clearly have correlated flares. For example, around MJD 56550, a flare is visible in both bands, with the γ -ray emission leading the optical. Another possible less significant correlated flare is visible around MJD 57250 but it was not detected by the Bayesian Block Decomposition of the γ -ray light curve.

For all the blazars, we define the rest-frame time lag (τ_{lag}) as the difference in the epochs of the Bayesian block peaks (the middle of the block) and the associated uncertainty as half the block widths. For the object presented in Figure 3, the γ -ray and optical observed flare epochs are respectively MJD 56557.25 ± 42.8 and MJD 56574.12 ± 38.2 . So the rest-frame is $\tau_{lag} = 8.8 \pm 21.1$ days. A positive τ_{lag} corresponds to the γ -ray emission leading to the optical emission.

4 RESULTS

In this section, we investigate if flaring activities are stronger in one of the bands. One metric for this is the number of flares (correlated and “orphan”) observed in each band and for each blazar class. Then, we measure the time lag between optical and γ -ray emissions.

4.1 Flares

After applying our search methodology from Section 3.1, we end up with a total of 2584 flares in 421 blazars⁴: 1624 optical and 960 γ -ray flares. If we remove all the flares in observational gaps (at least 50 days without data) to keep only flares with overlapping optical and γ -ray observation periods—the total decreases to 1924 flares: 1414 optical and 510 γ -ray flares. Roughly $\sim 50\%$ of γ -ray flares occur during optical observing gaps. This is consistent with the 43% found by Liodakis et al. (2019).

Finally, we investigate how the statistics are affected by our instrument limiting magnitude. Figure 4 shows the histogram of a rough estimate of the g -band magnitude for blazars with (red) or without optical flares (blue). The g -band magnitudes are derived using an average weighted g -band flux over all the years (negative and positive values) and a zero point of 16.4. As expected, blazars without optical flares are on average fainter than those with flares, almost one magnitude. Also, as seen in Figure 4 (right panel), brighter blazars have more detected flares than fainter objects (~ 6 versus 3 flares). Therefore, as a conservative approach, we select only the optical flares in blazars with a mean $m_g < 18.5$ mag. This corresponds to our limiting magnitude and the magnitude where the number of flares per object flattens (see Figure 4). This is a conservative approach and some of the optical flares detected in fainter blazars are well defined and also correlated with the γ -ray emission (see Section 4.2). In Figure 5, we present examples of two clear optical flares and two correlated flares in fainter blazars.

After all the cuts, we end up with 1230 optical and 510 γ -ray flares, so, we detect $\sim 42\%$ more flares in optical than in γ -ray.

Liodakis et al. (2018a) found the same trend and obtained ~ 3.5 times more optical flares than γ -ray events. However, in a more recent study, Liodakis et al. (2019) increased their previous sample (178 versus 145 blazars) and derived a similar number of flares for each band: 4277 for optical and 4384 for γ -ray. It is important to note that with the BBD method, the number of flares varies with binning, with more flares for smaller temporal bins (Liodakis et al. 2019). The flare number is also sensitive to the photometric uncertainties, so the flare numbers change for different bin size and methodologies. This could explain our differences with Liodakis et al. (2019) and the different flare numbers between the optical and γ -ray bands. For example, the BBD method can explain the larger optical flare rate, as it creates several small false flares due to the smaller photometric errors and higher dispersion of the optical light curves. If we concentrate our study on only the strongest flares and increase our threshold in Equation 1 from 3 to 10 (i.e., the flare flux must exceed ten times our quiescent level), we only detect 273 optical flares and 161 γ -ray flares.

We also investigate the number of flares for each blazar class. In our sample of 421 blazars (with at least one flare), there are 220 FSRQs, 160 BL Lacs, and 41 BCU. We detect 874, 774, and 92 flares for the FSRQ, BL Lac, and BCU classes. Like Liodakis et al. (2018a), we find that FSRQs tend to exhibit more γ -ray flares per source than the BL Lacs with 520/650 optical and 354/124 γ -ray flares for the FSRQ/BL Lac classes. The trend is not statistically significant to conclude if the difference between the two sub-classes is intrinsic or because FSRQs are on average brighter in γ -rays than BL Lacs. However, the BL Lacs seem to have more optical flares than the FSRQs. Finally, we consider all the FSRQs and BL Lacs of our sample and not only those with at least one flare. We obtain a rate of 1.73/1.77 flares per source (503/437) for FSRQ/BL Lac classes. For optical and γ -ray, the rates are 1.03/1.48 and 0.70/0.28 flares per source for FSRQ/BL Lac classes, respectively.

4.2 Time lags

Time lags between optical and γ -ray flares are of the order of only a few days (Bonning et al. 2012; Cohen et al. 2014; Liodakis et al. 2019; Bhatta 2021), so we look for correlated flares within a 30-day rest-frame window. For each of these 175 objects with flares in both bands, the final rest-frame τ_{lag} is the average of correlated flare lags, and the error is the quadratic sum of the block widths. In the cases where two flares in one band could be correlated with a simple flare in the other band (i.e., within 30 days), we include both time lags. Our final rest-frame τ_{lag} and their associated errors are in Table A1. Unlike Section 4.1, here we do not remove the optical flares seen in faint blazars because we only consider correlated flares. Even in faint blazars, if a γ -ray emission is seen at roughly the same epoch as the optical flares, it is likely that the optical flare is real. An example of two correlated flares in faint blazars are displayed in Figure 5.

From the 175 objects with flares in both bands, we found 133 blazars with correlated flares and a redshift. Figure 6 shows the rest-frame time lag distribution between both bands. We obtain an average rest-frame time lag of $1.1^{+7.1}_{-8.5}$ days, and the quoted uncertainties (hereafter) represent the 68% confidence interval obtained from a bootstrapping simulation of 10,000 events. To estimate the uncertainties from the bootstrapping, we select 133 random rest-frame time lags for each event from our distribution and measure the standard deviation. Finally, from those 10,000 measurements, we derive our 68% confidence interval. Note that, if we simply use the scatter in the 10,000 median lags, the dispersion is only \sim

⁴ Blazars labeled as “opt”, “both” or “gam” in Table A1.

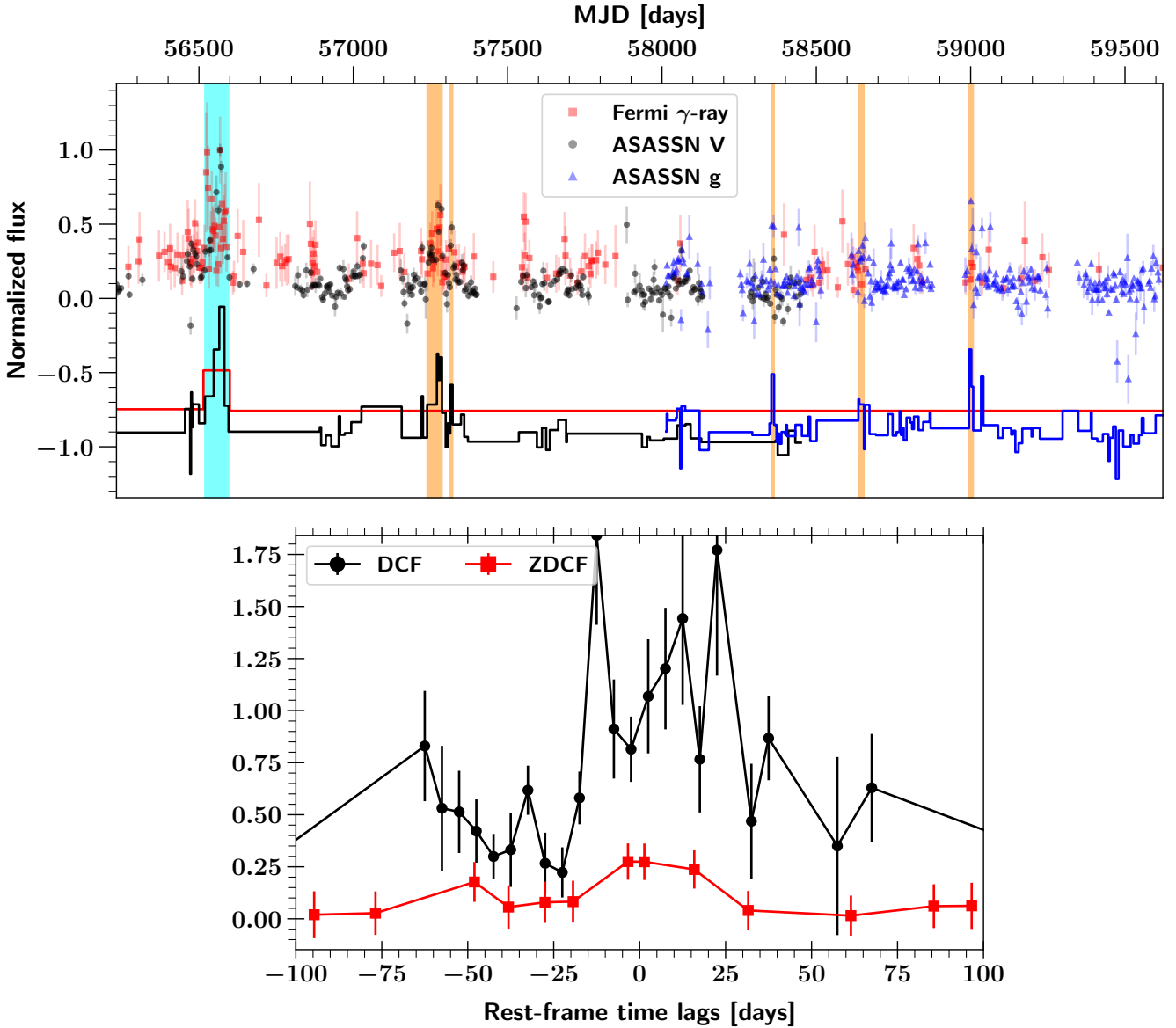


Figure 3. *Upper panel:* Correlated flares in the normalised light curves of J0050.4-0452 between the *Fermi*-LAT γ -ray (red squares) and the optical V-band (black dots), and g-band (blue triangles). The cyan shaded region indicates the flares in both bands and used to derive the time lag. The orange shaded regions represent the flare detected in the optical light curves but not in the γ -ray light curve. The black, red and blue lines are the Bayesian Block Decompositions for each band shifted downwards for clarity. *Bottom panel:* Discrete correlation function (DCF; in black) and Z-transformed discrete correlation function (ZDCF; in red) between the optical and γ -ray light curves. A positive observed time lag corresponds to the γ -ray emission leading to the optical emission.

1 day which it is not representative of our distribution (standard deviation ~ 7 –8 days). Among the 133 objects, only three have a rest-frame time lag greater than 20 days and are not consistent with 0 (20J0133.1–5201, 20J1006.7–2159, 20J1604.6+5714). Our distribution is almost centred on 0 days and it is consistent with previous works (Bonning et al. 2012; Cohen et al. 2014; Liodakis et al. 2019; Bhatta 2021). For example, Liodakis et al. (2019) derived a median time lag of -0.24 ± 20.5 days using 117 objects, so, it is consistent with no time lag. Their time lag distribution is similar to ours but has a tail towards longer time lags (see Figure 6). However, the difference may be due to our 30 day search window. If we increase our window to 60 days, the number of objects increases to 143, extending the distribution from -55 days to 56 days. However, the median value changes only to $2.9^{+15.9}_{-13.1}$ days. We

also find no correlations between our time lags and the redshift or the synchrotron peak frequency. If we remove the 17 blazars with $m_g > 18.5$ mag, we do not see significant difference in our average rest-frame time lag ($0.2^{+5.0}_{-10.1}$).

Investigating time lags between flares in different energy bands probes the origin of the seed photon for the leptonic model. For example, using 13 FSRQs and 17 BL Lacs, Cohen et al. (2014) found that FSRQs tend to have γ -rays leading the optical by a few days, while for the BL Lacs, they did not find a clear offset. This suggests that the seed photons for FSRQs are from external sources, while it is within the jet for BL Lacs (Böttcher et al. 2013). However, Liodakis et al. (2019) did not find such differences using a larger sample (53 FSRQs and 67 BL Lacs).

Figure 6 shows the time lag distribution of our 100 FSRQs

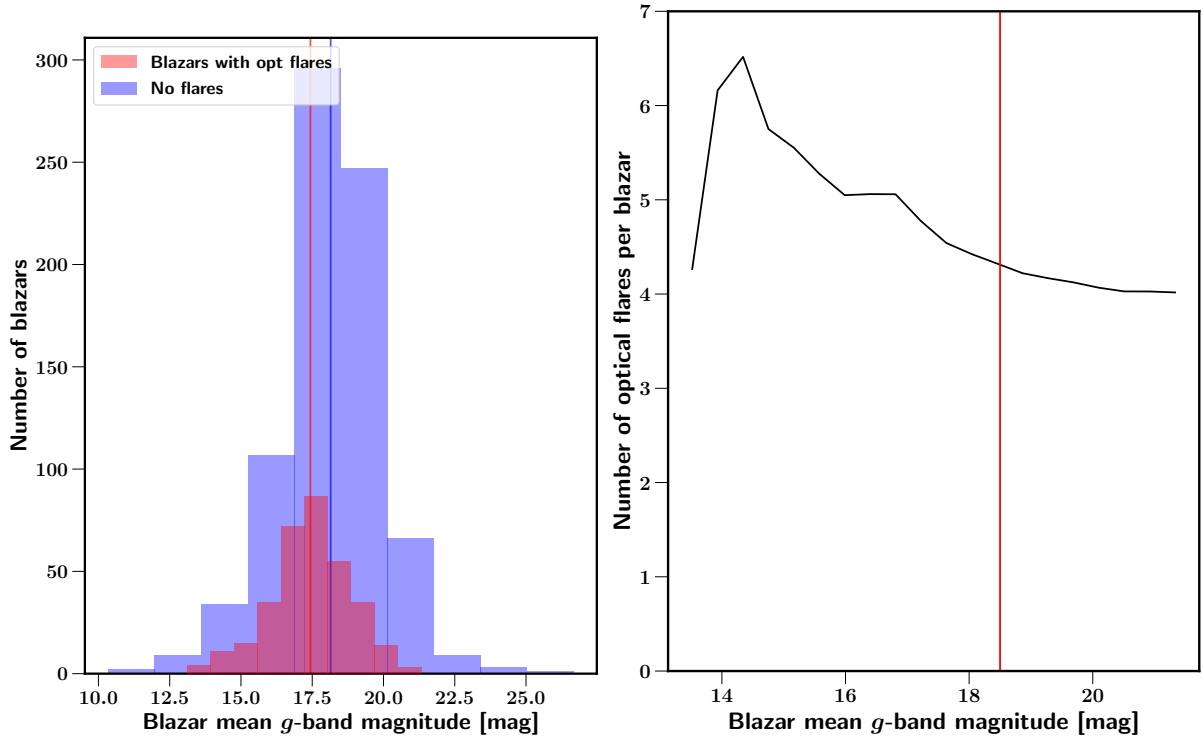


Figure 4. Optical flaring versus optical magnitude. *left:* Histogram of the mean g -band blazar magnitude for the objects with at least one optical flare (red) and the sources without flares (blue). The vertical lines correspond to the average values. *right:* Number of optical flares versus the mean g -band blazar magnitude. The red vertical line represents our magnitude cut at $g = 18.5$ mag.

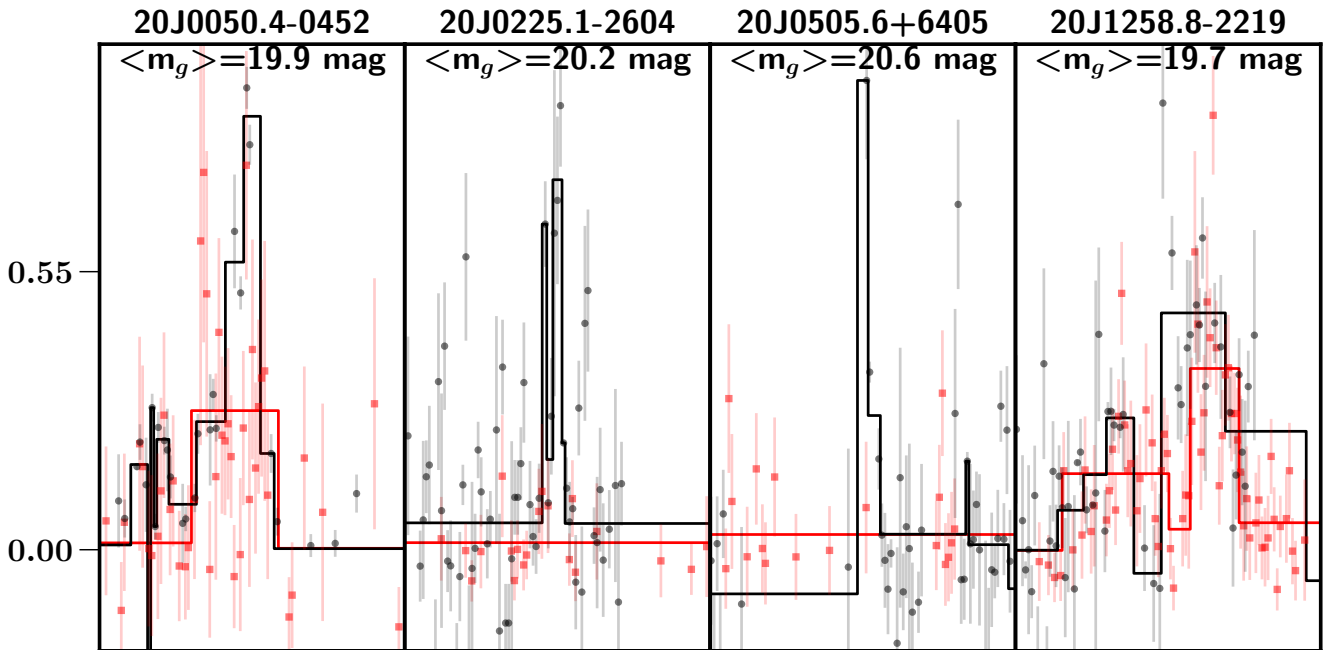


Figure 5. Example of optical flares observed in faint optical blazars ($m_g > 18.5$ mag). In each panel the optical blazar magnitude is shown. Black dots and red squares represent the V-band and γ -ray light curves and the red and black lines are the Bayesian Block Decompositions for each band. For 20J0050.4-0452 and 20J1258.8-2219 we clearly see a γ -ray counterpart.

and 30 BL Lacs with median values of $0.9^{+6.3}_{-8.0}$ and $1.5^{+8.2}_{-10.9}$ days for FSRQs and BL Lacs, respectively. A Kolmogorov-Smirnov test also confirms the distribution are consistent with each other. These results support [Liodakis et al. \(2019\)](#) in finding no evidence for a difference in the seed photon source of the two blazar classes. However, this is only a statistical statement; individual objects could have different high-energy emission mechanisms, as has already been seen for individual blazars (e.g., [Punch et al. 1992](#); [Dermer & Schlickeiser 1993](#); [Mannheim 1993](#); [Urry et al. 1997](#); [Ghisellini et al. 1998](#); [Mücke & Protheroe 2001](#); [Błażewski et al. 2005](#); [Aharonian et al. 2007](#); [Albert et al. 2007](#); [Jorstad et al. 2010](#); [Böttcher et al. 2013](#); [Cerruti et al. 2019](#)).

We also separate our sample based on their SED class (LSP, ISP, and HSP). Of 133 objects with τ_{lag} measurements, we have 118 LSP (96 FSRQs, 19 BL Lacs, 3 BCU), five ISP (1 FSRQ, 4 BL Lacs), and seven HSP (all BL Lacs), and three without an SED class. We derive a median lags of τ_{lag} of $0.90^{+6.2}_{-8.1}$ days, $3.6^{+1.8}_{-4.6}$ days, and $5.6^{+15.1}_{-10.3}$ days for the LSP, ISP, and HSP classes, respectively. We do not see any significant lags between the optical and γ -ray flares for the three SED classes. All are consistent with no lag given their uncertainties.

Finally, as different studies have used the DCF to derive time lags, Figure 6 shows our DCF lag distribution for the 113 objects with well measured DCF peaks. The DCF sample is smaller because 20 sources have correlated flares, but the DCF does not show a well-defined peak (e.g., Figure 3). Note that the lack of well-defined peak in the DCF could be due to the methodology. With the DCF, we analyse the entire light curve while with our methodology, we look only at correlated flares. Therefore, if there is only 1 flare in each band but the rest of the light curve is noisy, it will be difficult for the DCF to find a strong correlation between both signals. The DCF lag distribution is also statistically consistent with the lag distribution from the correlated peak analysis (Pearson correlation factor of 0.33, p-value of 0.009) and it has a median rest-frame τ_{lag} of $0.6^{+4.8}_{-6.2}$ days.

To summarise our time lag analysis, we find that the majority of blazars, have a strong optical/ γ -ray correlation with timescales on the order of days to tens of days, and are on average consistent with no delay for all blazar classes. Our results are in good agreement with previous studies ([Bonning et al. 2012](#); [Cohen et al. 2014](#); [Liodakis et al. 2019](#); [Bhatta 2021](#)) and our work rules out the hadronic proton-synchrotron model as the driver for non-orphan flares and supports leptonic single-zone model.

4.3 Orphan flares

Our study of time lags presented in Section 4.2 supports a leptonic single-zone model for the non-orphan flares. However, some blazars show behaviours not expected in such a model. One of the most peculiar is the presence of “orphan” flares – γ -ray flares with no visible counterpart or optical flares without γ -ray counterparts ([Krawczynski et al. 2004](#); [Błażewski et al. 2005](#)). As in Section 4.1, we remove all the “orphan” flare candidates which occur during optical or γ -ray observational gaps⁵ (see Figure 2). This cut removes 979 “orphan” flare candidates: 500 optical (29%) and 479 γ -ray (48%).

To be sure that the existence of “orphan” flares is not due to sensitivity limitations, we compare the optical and γ -ray flare amplitudes using all the correlated flares from Section 4.2. The

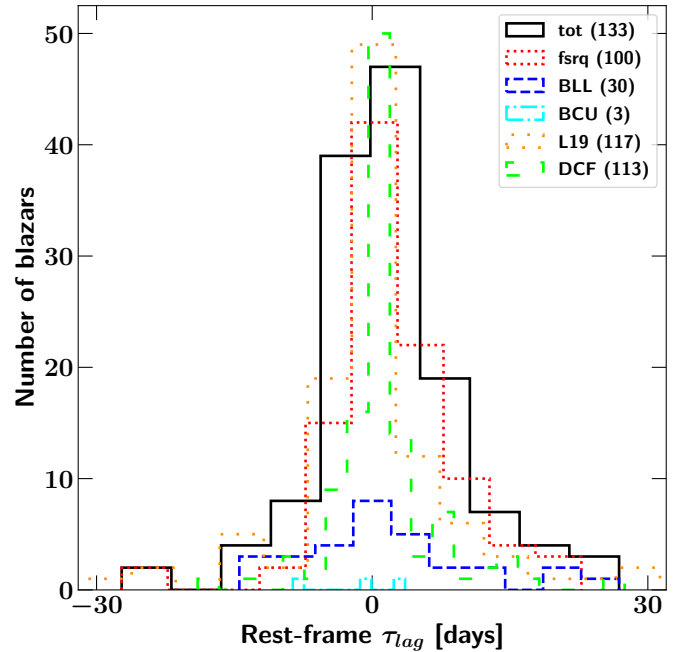


Figure 6. Distribution of all rest-frame time lags between the optical and γ -ray flares (solid black). The distributions for the classes are also shown: FSRQ (dotted red), BL Lac (dashed blue), and BCU (dash-dotted cyan). For comparison, the result obtained by [Liodakis et al. \(2019\)](#) is shown in loosely dotted orange, and the DCF lag distribution derived from the DCF is the loosely dashed lime. A positive τ_{lag} corresponds to the γ -ray emission leading the optical emission.

flare amplitude is defined as the difference between the height of the block and the median flux of the light curve. Then, we measure the amplitude ratio A_{opt}/A_{γ} . This ratio could give information regarding the structure of the jet as it expected to be different for different mechanisms. For example, for PKS 1510–089 [Marscher et al. \(2010\)](#) have shown that the dichotomy in the ratio suggests that as the emission feature moves down the jet, different sources of seed photons dominate the inverse Compton scattering. For another object, [Bonoli et al. \(2011\)](#), demonstrated that larger variation in the flux of the γ -ray light curve with respect to the optical can be explained by a decreasing magnetic field when the observed γ -ray luminosity increases. We do not find a strong correlation between the amplitudes (Pearson factor of 0.18, p-value of 0.002). Thus to estimate the expected γ -ray flux amplitude for any “orphan” optical flare candidate, we assume the median of $1.3^{+1.6}_{-1.2}$ of the A_{opt}/A_{γ} distribution. This value is consistent with [Liodakis et al. \(2019\)](#), who also found that optical flares have a larger average amplitude than γ -ray flares ($A_{opt}/A_{\gamma} \sim 2.7$).

Next, we visually inspect all the “orphan” flare candidates and select only the clearest ones, those with at least 2 points, not close to observational gaps, not likely due to photometric noise (see Figure 2), and seen only in one optical band during V/g bands overlap period. We found a total of ~ 306 “orphan” flares: 191 “orphan” optical flares and 115 “orphan” γ -ray flares. From those 306 “orphan” flares, we also construct a “gold” sample of flares for future individual analysis. Figure 7 shows those 28 “orphan” optical flares and 28 “orphan” γ -ray flares. Our fraction of “orphan” γ -ray flares (115) relative to the total number of γ -ray flares (507) is consistent with [Liodakis et al. \(2019\)](#). We estimate that $\sim 22\%$ of γ -ray flares are “orphan” events compared to $\sim 20\%$ in [Liodakis et al.](#)

⁵ We have only upper limits.

(2019). This is not surprising as we use the same photometric data for the γ -ray light curves (from *Fermi*-LAT). However, we find a different fraction percentage of “orphan” optical flares. We find that $\sim 13.5\%$ (191/1414) of optical flares are orphan events as compared to $\sim 54\%$ in Liodakis et al. (2019). A difference in methodology and photometric data could explain the difference. First, we only use the strongest flares, while Liodakis et al. (2019) considered all local maxima (centre of three Bayesian blocks) as flares, independent of their amplitudes. With a blazar sample roughly three times larger, we find only $\sim 2,000$ flares while they detected more than 8,600 flares. Second, unlike the γ -ray data, we are using optical photometry from different telescopes with different limiting magnitudes. We use data from ASAS-SN, which has a limiting magnitude of 18.5 mag (Kochanek et al. 2017). Most of the optical light curves used in Liodakis et al. (2019) are from the KAIT telescope (Filippenko et al. 2001) with a limiting magnitude of 19.5 mag, which allows Liodakis et al. (2019) to detect fainter optical flares which presumably leads to more “orphan” optical flares. Liodakis et al. (2018a) also found that “orphan” optical flares in their sample have lower amplitudes and are likely random fluctuations, not real flares. Note also, if we remove all the “orphan” optical flares in the blazars with $m_g > 18.5$ mag, our “orphan” optical flare fraction decreases to 12% (from 191 to 153).

We also estimate the “orphan” flare fraction for each blazar class. We obtained a similar optical “orphan” flare number for the two classes (91/91) but we see a different rates of “orphan” γ -ray flares (85/18) for the FSRQ/B LLac classes. Given the number of FSRQs (220) and BL Lacs (160) in our sample (+ 41 BCU), we find more “orphan” γ -ray flares among the FSRQs than among the BL Lacs: 0.38/0.11 “orphan” γ -ray flare per object for FSRQ/BL Lac classes. However, we obtain more “orphan” optical flares in BL Lacs than FSRQs: 0.41/0.57 “orphan” optical flare per object for FSRQ/BL Lac classes. The presence of “orphan” flares argues for multi-zone synchrotron sites or a hadronic origin for some blazar flares. However, as suggested by Liodakis et al. (2019), the small orphan γ -ray flare fraction favours a single-zone leptonic mechanism for the high-energy emission in most blazars.

4.4 Fractional Variability

We use the fractional variability to characterise the average variability of the blazars (Vaughan et al. 2003). It is defined as

$$F_{var} = \sqrt{\frac{S^2 - \langle \sigma_{err}^2 \rangle}{\langle F \rangle^2}}, \quad (2)$$

where $S^2 = (N-1)^{-1} \sum_{i=1}^N (F_i - \langle F \rangle)^2$ is the variance, $\langle F \rangle$ is the mean flux, and $\langle \sigma_{err}^2 \rangle$ is the mean square uncertainty. First, we compare the variability properties using the whole light curves. We measure the variability for 166 objects among the 175 with flares in both bands (for 9 blazars S^2 is smaller than $\langle \sigma_{err}^2 \rangle$). We obtain a mean value and a standard deviation of $F_{var} = 0.60 \pm 0.42$ and $F_{var} = 0.66 \pm 0.34$ for the optical and γ -ray bands, respectively. Even if both bands have a consistent fractional variability, a Kolmogorov-Smirnov test indicates that the fractional variability distributions are not the same ($p = 0.0078$). For the different blazar classes, we find $F_{var} = 0.66 \pm 0.44$ and $F_{var} = 0.73 \pm 0.33$ for FSRQs and the optical and γ -ray bands, respectively and $F_{var} = 0.45 \pm 0.27$ and $F_{var} = 0.49 \pm 0.25$ for BL Lacs. For the γ -ray band and FSRQs, our fractional variability values are higher but consistent with the value of 0.55 ± 0.33 found by Rajput et al. (2020). We also find that the FSRQ class has a higher fractional variability than the BL

Lac class in both the γ -ray and optical. A Kolmogorov-Smirnov test shows that FSRQ and BL Lac distributions are not from the same distribution at 95% confidence with statistics of 0.39/0.34 and a p-value of 0.00006/0.0008 (for γ -ray/optical).

Finally, because F_{var} is sensitive to the photometric uncertainties, we checked our analysis by doubling the uncertainties of both bands. We find different values for F_{var} but the FSRQs still have larger variability in both bands (Opt: FSRQs: 0.63 ± 0.45 , BL Lacs: 0.55 ± 0.24 ; γ -ray FSRQs: 0.79 ± 0.35 , BL Lacs: 0.65 ± 0.27).

5 CONCLUSIONS

Using blazar light curves from the optical All-Sky Automated Survey for Supernovae and the γ -ray *Fermi*-LAT telescope, we performed the most extensive statistical correlation study between both bands to date for a sample of 1,180 blazars. This is almost an order of magnitude larger than other recent studies (Cohen et al. 2014; Liodakis et al. 2019). We decompose both light curves into histograms using the Bayesian Block Decomposition method. Then, we select only the prominent flares to study the time delays and the relative rates of “orphan” flares. Of the 1,180 blazars, 421 objects have at least one flare and 133 sources have at least one correlated flare within a 30-day window. Our six main conclusions are:

(i) Based on the 143 sources with correlated flares, the time lag distribution between both bands is consistent with no lags (16th, 50th, and 84th percentiles of -8.5 , 1.1 , and 7.1 days).

(ii) We do not find differences in the time lags for different blazar classes. Both distributions are consistent, with median value of $0.9^{+6.3}_{-8.0}$ and $1.5^{+8.2}_{-10.9}$ days for our 100 FSRQs and 30 BL Lacs, respectively.

(iii) In the 421 blazars with flares, we detect ~ 1400 optical and 500 γ -ray flares. The exact numbers are sensitive to parameter choices but FSRQs tend to exhibit more γ -ray flares per source than the BL Lacs while BL Lacs have more optical flares than FSRQs.

(iv) We measure a median amplitude ratio between optical and γ -ray flares of $A_{opt}/A_{\gamma} = 1.3^{+1.6}_{-1.2}$.

(v) We search for good example of “orphan” flares and found a total of 306 “orphan” flares: 191 “orphan” optical flares and 115 “orphan” γ -ray flares. These represent $\sim 13\%$ of optical and $\sim 22\%$ of γ -ray flares. We find more “orphan” γ -ray flares in FSRQs than BL Lacs but, more “orphan” optical flares in BL Lacs than FSRQs.

(vi) We compare the variability properties in the optical and γ -ray bands. Both bands have a consistent fractional variability amplitude, but FSRQs have higher a fractional variability in both the γ -ray and optical than BL Lacs.

Our work rules out the hadronic proton-synchrotron model and supports the leptonic single-zone models where the low and high-energy emissions come from the same population of electrons as the dominant driver of blazar flares. However, the presence of “orphan” flares in some blazars argues for the occasional presence of a more complex emission mechanism, such as multi-zone synchrotron models or another hadronic models for some flares.

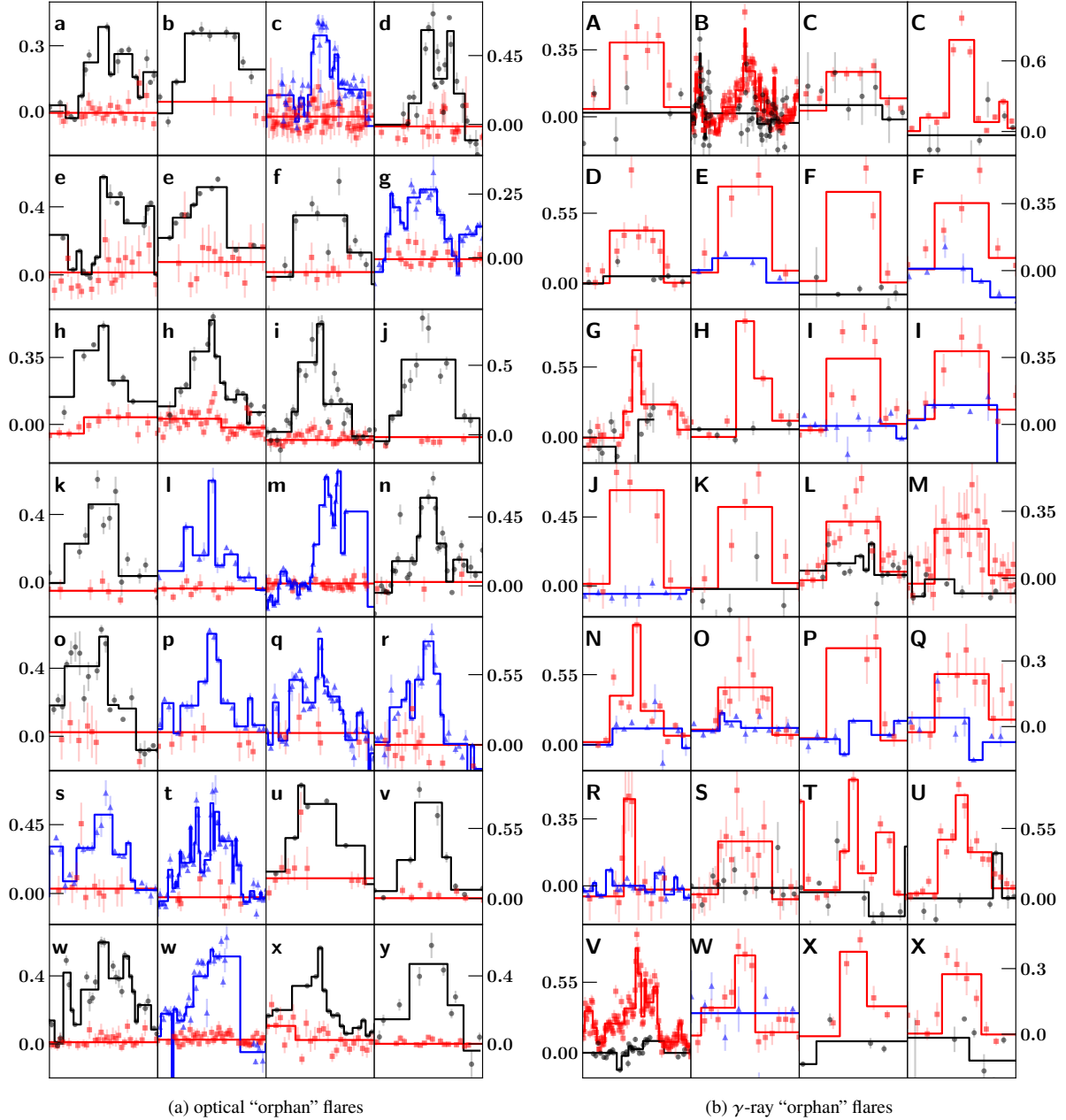


Figure 7. Gold sample of optical (left) and γ -ray (right) “orphan” flares. Black dots, blue triangles, and red squares are optical V, optical g, and γ -ray fluxes, respectively. The letter in each panel corresponds to the blazar name in Table B1.

Even if we performed the largest statistical study and independently confirmed previous work with a smaller sample, our work does not help distinguishing between SSC or EC models. The main reason is the signal-to-noise ratio of our optical light curves due to the limiting magnitude of ASAS-SN. However, it has been shown in the literature that the distinction between different models is doable for individual well studied blazar. For this reason, to put better constraints on the models and derive more precise time delays, instead of increasing the sample size, we need to obtain optical light curves with a better signal-to-noise ratio.

ACKNOWLEDGEMENTS

We thank the referee for the comments on the manuscript. We thank Las Cumbres Observatory and its staff for their continued support of ASAS-SN. ASAS-SN is funded in part by the Gordon and Betty Moore Foundation through grants GBMF5490 and GBMF10501 to the Ohio State University, and also funded in part by the Alfred P. Sloan Foundation grant G-2021-14192.

T.d.J thanks Colby Haggerty for discussions and Jedidah Isler for useful discussions in the early stages of this work. Support for T.d.J has been provided by NSF grants AST-1908952 and AST-1911074. B.J.S. is supported by NSF grants AST-1907570, AST-1908952, AST-1920392, and AST-1911074. C.S.K and K.Z.S are supported by NSF grants AST-1814440 and AST-1908570. A.F ac-

knowledges funding from the German Science Foundation DFG, via the Collaborative Research Center SFB1491 “Cosmic Interacting Matters - From Source to Signal”. Support for TW-SH was provided by NASA through the NASA Hubble Fellowship grant HST-HF2-51458.001-A awarded by the Space Telescope Science Institute, which is operated by the Association of Universities for Research in Astronomy, Inc., for NASA, under contract NAS5-265. J.F.B. is supported by National Science Foundation grant No. PHY-2012955.

This work is based on observations made by ASAS-SN. We wish to extend our special thanks to those of Hawaiian ancestry on whose sacred mountains of Maunakea and Haleakalā, we are privileged to be guests. Without their generous hospitality, the observations presented herein would not have been possible.

Facilities: Fermi-LAT telescope, Haleakala Observatories (USA), Cerro Tololo International Observatory (Chile), McDonald Observatory (USA), South African Astrophysical Observatory (South Africa).

Software: astropy (Astropy Collaboration et al. 2013), Matplotlib (Hunter 2007), Numpy (Harris et al. 2020), Scipy (Virtanen et al. 2020), Z-transformed discrete correlation function (Alexander 1997, 2013)

DATA AVAILABILITY STATEMENTS

The optical and γ -ray light curves have already been made available to the community. γ -ray light curves can be downloaded from <https://fermi.gsfc.nasa.gov/ssc/data/access/lat/LightCurveRepository/source.html> while optical light-curves from ASAS-SN can be obtained via their ASAS-SN sky patrol webpage (<https://asas-sn.osu.edu/>). All the datasets used in this work will be also available on the author’s Github (<https://github.com/tdejaeger>).

REFERENCES

Abdo A. A., et al., 2009, *ApJS*, **183**, 46
 Abdo A. A., et al., 2010, *ApJ*, **716**, 30
 Abdollahi S., et al., 2020, *ApJS*, **247**, 33
 Abdollahi S., et al., 2022, *ApJS*, **260**, 53
 Acero F., et al., 2015, *ApJS*, **218**, 23
 Adams C. B., et al., 2022, *ApJ*, **924**, 95
 Aharonian F. A., 2000, *New Astron.*, **5**, 377
 Aharonian F., et al., 2007, *ApJ*, **664**, L71
 Alard C., 2000, *A&AS*, **144**, 363
 Alard C., Lupton R. H., 1998, *ApJ*, **503**, 325
 Albert J., et al., 2007, *ApJ*, **669**, 862
 Alexander T., 1997, in Maoz D., Sternberg A., Leibowitz E. M., eds, *Astrophysics and Space Science Library* Vol. 218, Astronomical Time Series. p. 163, doi:10.1007/978-94-015-8941-3_14
 Alexander T., 2013, arXiv e-prints, p. arXiv:1302.1508
 Antonucci R., 1993, *ARA&A*, **31**, 473
 Arbeiter C., Pohl M., Schlickeiser R., 2005, *ApJ*, **627**, 62
 Astropy Collaboration et al., 2013, *A&A*, **558**, A33
 Atwood W. B., et al., 2009, *ApJ*, **697**, 1071
 Ballet J., Burnett T. H., Digel S. W., Lott B., 2020, arXiv e-prints, p. arXiv:2005.11208
 Banasiński P., Bednarek W., Sitarek J., 2016, *MNRAS*, **463**, L26
 Bellm E. C., et al., 2019, *PASP*, **131**, 018002
 Bhatta G., 2021, *ApJ*, **923**, 7
 Blandford R. D., Ostriker J. P., 1978, *ApJ*, **221**, L29

Błażejowski M., Sikora M., Moderski R., Madejski G. M., 2000, *ApJ*, **545**, 107
 Błażejowski M., et al., 2005, *ApJ*, **630**, 130
 Bloom S. D., Marscher A. P., 1996, *ApJ*, **461**, 657
 Boettcher M., Mause H., Schlickeiser R., 1997, *A&A*, **324**, 395
 Bonning E., et al., 2012, *ApJ*, **756**, 13
 Bonnoli G., Ghisellini G., Foschini L., Tavecchio F., Ghirlanda G., 2011, *MNRAS*, **410**, 368
 Böttcher M., 2005, *ApJ*, **621**, 176
 Böttcher M., 2019, *Galaxies*, **7**, 20
 Böttcher M., Reimer A., Sweeney K., Prakash A., 2013, *ApJ*, **768**, 54
 Cerruti M., Zech A., Boisson C., Emery G., Inoue S., Lenain J. P., 2019, *MNRAS*, **483**, L12
 Chatterjee R., et al., 2008, *ApJ*, **689**, 79
 Chatterjee R., et al., 2012, *ApJ*, **749**, 191
 Chiang J., Böttcher M., 2002, *ApJ*, **564**, 92
 Cohen D. P., Romani R. W., Filippenko A. V., Cenko S. B., Lott B., Zheng W., Li W., 2014, *ApJ*, **797**, 137
 Costamante L., Ghisellini G., 2002, *A&A*, **384**, 56
 de Jaeger T., et al., 2022, *MNRAS*, **509**, 3427
 Dermer C. D., Schlickeiser R., 1993, *ApJ*, **416**, 458
 Dermer C. D., Finke J. D., Krug H., Böttcher M., 2009, *ApJ*, **692**, 32
 Edelson R. A., Krolik J. H., 1988, *ApJ*, **333**, 646
 Eisenstein D. J., Hut P., 1998, *ApJ*, **498**, 137
 Filippenko A. V., Li W. D., Treffers R. R., Modjaz M., 2001, in Paczynski B., Chen W.-P., Lemme C., eds, *Astronomical Society of the Pacific Conference Series* Vol. 246, IAU Colloq. 183: Small Telescope Astronomy on Global Scales. p. 121
 Fossati G., Maraschi L., Celotti A., Comastri A., Ghisellini G., 1998, *MNRAS*, **299**, 433
 Gao S., Pohl M., Winter W., 2017, *ApJ*, **843**, 109
 Gao S., Fedynitch A., Winter W., Pohl M., 2019, *Nature Astronomy*, **3**, 88
 Ghisellini G., Madau P., 1996, *MNRAS*, **280**, 67
 Ghisellini G., Maraschi L., 1989, *ApJ*, **340**, 181
 Ghisellini G., Celotti A., Fossati G., Maraschi L., Comastri A., 1998, *MNRAS*, **301**, 451
 Ghisellini G., Tavecchio F., Foschini L., Ghirlanda G., 2011, *MNRAS*, **414**, 2674
 Ghisellini G., Tavecchio F., Foschini L., Sbarrato T., Ghirlanda G., Maraschi L., 2012, *MNRAS*, **425**, 1371
 Harris C. R., et al., 2020, *Nature*, **585**, 357
 Hovatta T., et al., 2014, *MNRAS*, **439**, 690
 Hunter J. D., 2007, *Computing in Science & Engineering*, **9**, 90
 IceCube Collaboration et al., 2018, *Science*, **361**, 147
 Impey C. D., Neugebauer G., 1988, *AJ*, **95**, 307
 Janiak M., Sikora M., Nalewajko K., Moderski R., Madejski G. M., 2012, *ApJ*, **760**, 129
 Jorstad S. G., et al., 2010, *ApJ*, **715**, 362
 Joshi M., Marscher A., Böttcher M., 2016, *Galaxies*, **4**, 45
 Keivani A., et al., 2018, *ApJ*, **864**, 84
 Kelner S. R., Aharonian F. A., Bugayov V. V., 2006, *Phys. Rev. D*, **74**, 034018
 Kochanek C. S., et al., 2017, *PASP*, **129**, 104502
 Krawczynski H., et al., 2004, *ApJ*, **601**, 151
 Liodakis I., Petropoulou M., 2020, *ApJ*, **893**, L20
 Liodakis I., Romani R. W., Filippenko A. V., Kiehlmann S., Max-Moerbeck W., Readhead A. C. S., Zheng W., 2018a, *MNRAS*, **480**, 5517
 Liodakis I., Hovatta T., Huppenkothen D., Kiehlmann S., Max-Moerbeck W., Readhead A. C. S., 2018b, *ApJ*, **866**, 137
 Liodakis I., Romani R. W., Filippenko A. V., Kocevski D., Zheng W., 2019, *ApJ*, **880**, 32
 MacDonald N. R., Marscher A. P., Jorstad S. G., Joshi M., 2015, *ApJ*, **804**, 111
 Madejski G. G., Sikora M., 2016, *ARA&A*, **54**, 725
 Mannheim K., 1993, *A&A*, **269**, 67
 Maraschi L., Ghisellini G., Celotti A., 1992, *ApJ*, **397**, L5
 Marscher A. P., Gear W. K., 1985, *ApJ*, **298**, 114
 Marscher A. P., et al., 2008, *Nature*, **452**, 966

Marscher A. P., et al., 2010, arXiv e-prints, [p. arXiv:1002.0806](#)
 Mastichiadis A., Kirk J. G., 1997, *A&A*, **320**, 19
 Mastichiadis A., Petropoulou M., 2021, *ApJ*, **906**, 131
 Mastichiadis A., Petropoulou M., Dimitrakoudis S., 2013, *MNRAS*, **434**, 2684
 Meyer M., Scargle J. D., Blandford R. D., 2019, *ApJ*, **877**, 39
 Mücke A., Protheroe R. J., 2001, *Astroparticle Physics*, **15**, 121
 Mücke A., Protheroe R. J., Engel R., Rachen J. P., Stanev T., 2003, *Astroparticle Physics*, **18**, 593
 Nalewajko K., 2013, *MNRAS*, **430**, 1324
 Padovani P., Giommi P., 1995, *ApJ*, **444**, 567
 Punch M., et al., 1992, *Nature*, **358**, 477
 Rajput B., Stalin C. S., Rakshit S., 2020, *A&A*, **634**, A80
 Rodrigues X., Gao S., Fedynitch A., Palladino A., Winter W., 2019, *ApJ*, **874**, L29
 Roy N., Chatterjee R., Joshi M., Ghosh A., 2019, *MNRAS*, **482**, 743
 Scargle J. D., 1998, *ApJ*, **504**, 405
 Scargle J. D., Norris J. P., Jackson B., Chiang J., 2013, *ApJ*, **764**, 167
 Shappee B. J., et al., 2014, *ApJ*, **788**, 48
 Sikora M., Begelman M. C., Rees M. J., 1994, *ApJ*, **421**, 153
 Sokolov A., Marscher A. P., McHardy I. M., 2004, *ApJ*, **613**, 725
 Stathopoulos S. I., Petropoulou M., Giommi P., Vasilopoulos G., Padovani P., Mastichiadis A., 2022, *MNRAS*, **510**, 4063
 Stickel M., Padovani P., Urry C. M., Fried J. W., Kuehr H., 1991, *ApJ*, **374**, 431
 Urry C. M., Mushotzky R. F., 1982, *ApJ*, **253**, 38
 Urry C. M., Padovani P., 1995, *PASP*, **107**, 803
 Urry C. M., et al., 1997, *ApJ*, **486**, 799
 Valtaoja E., Lähteenmäki A., Teräsranta H., Lainela M., 1999, *ApJS*, **120**, 95
 Vaughan S., Edelson R., Warwick R. S., Uttley P., 2003, *MNRAS*, **345**, 1271
 Virtanen P., et al., 2020, *Nature Methods*, **17**, 261
 Wagner S. M., et al., 2022, in 37th International Cosmic Ray Conference. 12-23 July 2021. Berlin. p. 868 ([arXiv:2110.14797](#))
 Wang Z.-R., Liu R.-Y., Petropoulou M., Oikonomou F., Xue R., Wang X.-Y., 2022, *Phys. Rev. D*, **105**, 023005
 Williamson K. E., et al., 2014, *ApJ*, **789**, 135

APPENDIX A: PROPERTIES OF BLAZARS USED IN OUR SAMPLE

In this appendix, we list relevant information from [Abdollahi et al. \(2022\)](#) and [Ballet et al. \(2020\)](#) of our blazar sample together with the results obtained in Section 4.

Table A1: Blazar properties.

| 4FGL Name | RA deg | Dec deg | Association | Class | SED class | redshift | Flares | Lags days |
|--------------|-----------|------------|----------------------------|--------|-----------|----------|--------|-----------------|
| J0001.2-0747 | 0.315100 | -7.797100 | PMN J0001-0746 | BL Lac | LSP | ... | opt | ... |
| J0001.5+2113 | 0.381500 | 21.218300 | TXS 2358+209 | FSRQ | ISP | 1.106 | both | 0.25 (4.64) |
| J0003.3-1928 | 0.846500 | -19.467600 | PKS 0000-197 | BCU | LSP | ... | none | ... |
| J0004.3+4614 | 1.075700 | 46.242699 | MG4 J000421+4615 | FSRQ | LSP | 1.810 | none | ... |
| J0004.4-4737 | 1.109100 | -47.623299 | PKS 0002-478 | FSRQ | LSP | 0.880 | none | ... |
| J0005.9+3824 | 1.498600 | 38.401001 | S4 0003+38 | FSRQ | LSP | 0.229 | none | ... |
| J0007.7+4008 | 1.927500 | 40.133999 | NVSS J000741+400830 | BCU | ... | ... | none | ... |
| J0009.3+5030 | 2.346600 | 50.511501 | NVSS J000922+503028 | BL Lac | HSP | ... | none | ... |
| J0010.6+2043 | 2.650200 | 20.733200 | TXS 0007+205 | FSRQ | LSP | 0.600 | none | ... |
| J0010.6-3025 | 2.667500 | -30.425800 | PKS 0008-307 | FSRQ | LSP | 1.190 | none | ... |
| J0011.4+0057 | 2.855100 | 0.964600 | RX J0011.5+0058 | FSRQ | LSP | 1.492 | gam | ... |
| J0014.1+1910 | 3.536800 | 19.171301 | MG3 J001356+1910 | BL Lac | LSP | 0.477 | none | ... |
| J0014.9+3212 | 3.726800 | 32.216202 | 3C 6 | BCU | LSP | ... | none | ... |
| J0016.2-0016 | 4.061000 | -0.280600 | S3 0013-00 | FSRQ | LSP | 1.576 | none | ... |
| J0017.0-0649 | 4.263500 | -6.831700 | PMN J0017-0650 | BCU | LSP | ... | none | ... |
| J0017.5-0514 | 4.394900 | -5.234700 | PMN J0017-0512 | FSRQ | LSP | 0.227 | both | 16.38 (26.92) |
| J0019.2-5640 | 4.810600 | -56.682598 | PMN J0019-5641 | BCU | LSP | ... | none | ... |
| J0019.6+7327 | 4.903100 | 73.456001 | S5 0016+73 | FSRQ | LSP | 1.781 | both | 999.90 (999.90) |
| J0021.5-2552 | 5.391200 | -25.868099 | CRATES J002132.55-255049.3 | BL Lac | ISP | ... | opt | ... |
| J0021.9-5140 | 5.498500 | -51.672798 | 1RXS J002159.2-514028 | BL Lac | ISP | 0.250 | opt | ... |
| J0022.5+0608 | 5.637600 | 6.134300 | PKS 0019+058 | BL Lac | LSP | ... | both | 999.90 (999.90) |
| J0023.7-6820 | 5.934700 | -68.338097 | PKS 0021-686 | FSRQ | LSP | 0.354 | none | ... |
| J0024.4+4647 | 6.121200 | 46.797001 | B3 0021+464 | BCU | ... | ... | none | ... |
| J0024.7+0349 | 6.197500 | 3.832100 | GB6 J0024+0349 | FSRQ | ... | 0.545 | none | ... |
| J0025.7-4801 | 6.435100 | -48.019100 | SUMSS J002545-480356 | BCU | LSP | ... | none | ... |
| J0028.4+2001 | 7.126200 | 20.017000 | TXS 0025+197 | FSRQ | LSP | 1.552 | both | -5.19 (12.89) |
| J0029.0-7044 | 7.250900 | -70.741402 | PKS 0026-710 | BL Lac | LSP | ... | none | ... |
| J0030.2-1647 | 7.564300 | -16.797501 | 2MASS J00302045-1647130 | BL Lac | HSP | 0.237 | none | ... |
| J0030.3-4224 | 7.595800 | -42.412701 | PKS 0027-426 | FSRQ | LSP | 0.495 | both | 0.78 (29.93) |
| J0030.6-0212 | 7.655800 | -2.201400 | PKS B0027-024 | FSRQ | LSP | 1.804 | both | 999.90 (999.90) |
| J0032.3-5522 | 8.077800 | -55.366798 | SUMSS J003210-552228 | BCU | ... | ... | none | ... |
| J0033.5-1921 | 8.395400 | -19.359301 | KUV 00311-1938 | BL Lac | HSP | 0.610 | none | ... |
| J0033.9+3858 | 8.483000 | 38.971600 | MG3 J003408+3901 | BCU | LSP | ... | opt | ... |
| J0034.0-4116 | 8.514200 | -41.270802 | PKS 0031-415 | BCU | LSP | ... | none | ... |
| J0035.2+1514 | 8.812300 | 15.240500 | RX J0035.2+1515 | BL Lac | ISP | 1.090 | none | ... |
| J0035.9+5950 | 8.982300 | 59.833401 | IES 0033+595 | BL Lac | HSP | ... | none | ... |
| J0036.9+1832 | 9.234000 | 18.542400 | CRATES J003659.39+183203.7 | BCU | ... | 1.595 | gam | ... |
| J0037.8+1239 | 9.469500 | 12.652700 | NVSS J003750+123818 | BL Lac | HSP | 0.089 | none | ... |
| J0038.2-2459 | 9.558900 | -24.994101 | PKS 0035-252 | FSRQ | LSP | 1.196 | both | 0.22 (9.16) |
| J0039.1+4330 | 9.799400 | 43.512199 | NVSS J003907+433015 | BCU | ISP | ... | opt | ... |
| J0043.8+3425 | 10.971700 | 34.431599 | GB6 J0043+3426 | FSRQ | LSP | 0.966 | none | ... |
| J0044.2-8424 | 11.071100 | -84.401604 | PKS 0044-84 | FSRQ | LSP | 1.032 | none | ... |
| J0045.1-3706 | 11.293600 | -37.106499 | PKS 0042-373 | FSRQ | LSP | ... | none | ... |
| J0045.3+2128 | 11.339600 | 21.466801 | GB6 J0045+2127 | BL Lac | HSP | ... | none | ... |
| J0045.7+1217 | 11.430900 | 12.292000 | GB6 J0045+1217 | BL Lac | ... | ... | none | ... |
| J0047.0+5657 | 11.753500 | 56.960098 | GB6 J0047+5657 | BL Lac | LSP | 0.747 | none | ... |
| J0047.9+2233 | 11.998100 | 22.563200 | GB6 J0048+2234 | FSRQ | LSP | 1.161 | opt | ... |
| J0047.9+3947 | 11.976300 | 39.797501 | B3 0045+395 | BL Lac | ... | 0.252 | none | ... |
| J0049.7+0237 | 12.437700 | 2.627300 | PKS 0047+023 | BL Lac | LSP | 1.474 | none | ... |
| J0050.4-0452 | 12.612100 | -4.880600 | PKS 0047-051 | FSRQ | LSP | 0.920 | both | 8.79 (21.13) |
| J0050.7-0929 | 12.675300 | -9.493600 | PKS 0048-09 | BL Lac | ISP | 0.635 | opt | ... |
| J0051.1-0648 | 12.782400 | -6.809600 | PKS 0048-071 | FSRQ | LSP | 1.975 | none | ... |
| J0051.2-6242 | 12.824300 | -62.703701 | 1RXS J005117.7-624154 | BL Lac | HSP | 0.300 | none | ... |
| J0055.1-1219 | 13.780500 | -12.320400 | TXS 0052-125 | BCU | LSP | ... | none | ... |
| J0056.3-0935 | 14.087400 | -9.599700 | TXS 0053-098 | BL Lac | ISP | 0.103 | none | ... |
| J0056.4-2118 | 14.120400 | -21.302900 | PMN J0056-2117 | BL Lac | ISP | ... | opt | ... |
| J0056.6-5317 | 14.159100 | -53.295601 | CRATES J005630.93-531931.5 | BCU | ISP | ... | none | ... |
| J0058.0-0539 | 14.510800 | -5.655000 | PKS 0055-059 | FSRQ | LSP | 1.246 | none | ... |
| J0058.0-3233 | 14.513200 | -32.565800 | PKS 0055-328 | BL Lac | LSP | ... | none | ... |
| J0058.4+3315 | 14.610100 | 33.250500 | MG3 J005830+3311 | FSRQ | LSP | 1.369 | none | ... |
| J0100.3+0745 | 15.093200 | 7.764700 | GB6 J0100+0745 | BL Lac | ISP | ... | none | ... |
| J0102.4+4214 | 15.606900 | 42.237099 | GB6 J0102+4214 | FSRQ | LSP | 0.874 | none | ... |
| J0102.8+5824 | 15.701000 | 58.409199 | TXS 0059+581 | FSRQ | LSP | 0.644 | opt | ... |
| J0103.5+5337 | 15.878700 | 53.626202 | RX J0103.3+5337 | BL Lac | ... | ... | none | ... |
| J0103.8+1321 | 15.969000 | 13.353600 | NVSS J010345+132346 | BL Lac | ... | 0.490 | none | ... |
| J0104.8-2416 | 16.214600 | -24.280800 | PKS 0102-245 | FSRQ | LSP | 1.747 | none | ... |
| J0105.1+3929 | 16.291300 | 39.496300 | GB6 J0105+3928 | BL Lac | LSP | 0.440 | opt | ... |
| J0107.4+0334 | 16.850800 | 3.569100 | PMN J0107+0333 | BL Lac | LSP | ... | none | ... |
| J0108.6+0134 | 17.169500 | 1.581900 | 4C +01.02 | FSRQ | LSP | 2.099 | both | 3.99 (23.06) |
| J0109.7+6133 | 17.445000 | 61.561501 | TXS 0106+612 | FSRQ | LSP | 0.783 | gam | ... |
| J0112.0-6634 | 18.023600 | -66.575203 | PKS 0110-668 | FSRQ | LSP | 1.189 | none | ... |
| J0112.1+2245 | 18.029400 | 22.751499 | S2 0109+22 | BL Lac | LSP | 0.265 | both | 7.53 (19.94) |
| J0112.8+3208 | 18.222700 | 32.139900 | 4C +31.03 | FSRQ | LSP | 0.603 | both | -2.40 (6.93) |
| J0113.1-3553 | 18.289301 | -35.894001 | PMN J0113-3551 | FSRQ | LSP | 1.220 | none | ... |
| J0113.4+4948 | 18.368200 | 49.805401 | S4 0110+49 | FSRQ | LSP | 0.389 | both | -8.96 (40.15) |
| J0114.0+6418 | 18.515100 | 64.304001 | GB6 J0113+6416 | BCU | ISP | ... | none | ... |
| J0114.8+1326 | 18.711901 | 13.434200 | GB6 J0114+1325 | BL Lac | ISP | 0.583 | opt | ... |
| J0115.1+2622 | 18.778400 | 26.373301 | 1RXS J011451.8+262337 | BCU | ISP | ... | none | ... |
| J0115.1-0129 | 18.785900 | -1.496200 | PKS 0112-017 | FSRQ | LSP | 1.365 | none | ... |
| J0115.8+2519 | 18.953899 | 25.332399 | RX J0115.7+2519 | BL Lac | HSP | 0.358 | opt | ... |

| 4FGL Name | RA deg | Dec deg | Association | Class | SED class | redshift | Flares | Lags days |
|--------------|-----------|------------|-------------------------|--------|-----------|----------|--------|-----------------|
| J0116.0-1136 | 19.006601 | -11.606000 | PKS 0113-118 | FSRQ | LSP | 0.670 | opt | ... |
| J0117.8-2109 | 19.454300 | -21.157801 | PKS 0115-214 | FSRQ | LSP | 1.490 | none | ... |
| J0118.7-0848 | 19.688400 | -8.808000 | AT20G J011844-085058 | BCU | LSP | ... | none | ... |
| J0118.9-2141 | 19.725401 | -21.694799 | PKS 0116-219 | FSRQ | LSP | 1.165 | both | 0.92 (21.47) |
| J0120.4-2701 | 20.122700 | -27.022900 | PKS 0118-272 | BL Lac | ISP | ... | none | ... |
| J0124.8-0625 | 21.217800 | -6.432800 | PMN J0124-0624 | BL Lac | LSP | 2.117 | none | ... |
| J0125.3-2548 | 21.347401 | -25.807400 | PKS 0122-260 | BL Lac | LSP | ... | none | ... |
| J0126.0-2221 | 21.520399 | -22.361000 | PKS 0123-226 | FSRQ | LSP | 0.720 | none | ... |
| J0127.2+0324 | 21.823700 | 3.413000 | NVSS J012713+032259 | BL Lac | HSP | ... | none | ... |
| J0128.5+4440 | 22.143801 | 44.677700 | GB6 J0128+4439 | FSRQ | LSP | 0.228 | none | ... |
| J0131.1+6120 | 22.792400 | 61.337200 | RX J0131.0+6120 | BL Lac | HSP | ... | none | ... |
| J0132.7-1654 | 23.176001 | -16.910299 | PKS 0130-17 | FSRQ | LSP | 1.020 | both | 5.32 (51.68) |
| J0133.1-5201 | 23.293800 | -52.020199 | PKS 0131-522 | FSRQ | LSP | 0.925 | both | 20.39 (3.84) |
| J0134.3-3842 | 23.588699 | -38.708500 | PMN J0134-3843 | FSRQ | LSP | 2.140 | none | ... |
| J0137.0+4751 | 24.260300 | 47.863701 | OC 457 | FSRQ | LSP | 0.859 | both | 2.22 (9.45) |
| J0137.6-2430 | 24.406900 | -24.516300 | PKS 0135-247 | FSRQ | LSP | 0.835 | opt | ... |
| J0137.9+5814 | 24.495701 | 58.249401 | TXS 0134+579 | BL Lac | HSP | ... | none | ... |
| J0138.0+2247 | 24.506300 | 22.796200 | GB6 J0138+2248 | BL Lac | HSP | ... | none | ... |
| J0140.6+8736 | 25.168800 | 87.606201 | WN B0126.6+8722 | BCU | LSP | ... | none | ... |
| J0141.4-0928 | 25.362600 | -9.482500 | PKS 0139-09 | BL Lac | LSP | 0.730 | both | 9.97 (33.89) |
| J0143.1-3622 | 25.785601 | -36.367401 | PMN J0143-3623 | BCU | LSP | ... | gam | ... |
| J0143.7-5846 | 25.948000 | -58.771801 | SUMSS J014347-584550 | BL Lac | HSP | ... | opt | ... |
| J0144.6+2705 | 26.150200 | 27.089899 | TXS 0141+268 | BL Lac | LSP | ... | none | ... |
| J0145.0-2732 | 26.258499 | -27.536301 | PKS 0142-278 | FSRQ | LSP | 1.148 | none | ... |
| J0146.0-6746 | 26.518200 | -67.774803 | SUMSS J014554-674646 | BL Lac | ISP | ... | none | ... |
| J0152.2+2206 | 28.072701 | 22.113300 | PKS 0149+21 | FSRQ | LSP | 1.320 | opt | ... |
| J0152.2+3714 | 28.063101 | 37.234100 | B2 0149+37 | BCU | LSP | 0.761 | none | ... |
| J0152.6+0147 | 28.161400 | 1.789400 | PMN J0152+0146 | BL Lac | HSP | 0.080 | opt | ... |
| J0153.9+0823 | 28.497200 | 8.393100 | GB6 J0154+0823 | BL Lac | ISP | 0.681 | none | ... |
| J0156.5+3914 | 29.132500 | 39.249298 | MG4 J015630+3913 | FSRQ | LSP | ... | none | ... |
| J0156.9-5301 | 29.232800 | -53.030800 | 1RXS J015658.6-530208 | BL Lac | HSP | ... | none | ... |
| J0157.7-4614 | 29.435301 | -46.243099 | PMN J0157-4614 | FSRQ | LSP | 2.287 | none | ... |
| J0158.5-3932 | 29.646000 | -39.535801 | PMN J0158-3932 | BL Lac | ISP | ... | none | ... |
| J0159.5+1046 | 29.885799 | 10.773700 | RX J0159.5+1047 | BL Lac | HSP | 0.195 | none | ... |
| J0200.6-6637 | 30.159901 | -66.625999 | PMN J0201-6638 | FSRQ | LSP | ... | none | ... |
| J0202.7+4204 | 30.686199 | 42.071400 | B3 0159+418 | BL Lac | LSP | ... | opt | ... |
| J0203.6+7233 | 30.911400 | 72.553001 | S5 0159+723 | BL Lac | LSP | ... | none | ... |
| J0203.7+3042 | 30.932699 | 30.713900 | NVSS J020344+304238 | BL Lac | LSP | 0.761 | opt | ... |
| J0204.8+1513 | 31.218201 | 15.232600 | 4C +15.05 | BCU | LSP | 0.833 | none | ... |
| J0205.0-1700 | 31.263700 | -17.002199 | PKS 0202-17 | FSRQ | LSP | 1.740 | both | 4.83 (17.01) |
| J0205.2+3212 | 31.308901 | 32.202999 | B2 0202+31 | FSRQ | LSP | 1.466 | gam | ... |
| J0206.4-1151 | 31.601801 | -11.857600 | PMN J0206-1150 | FSRQ | LSP | 1.663 | both | 10.29 (23.41) |
| J0207.5-2402 | 31.898899 | -24.048401 | NVSS J020733-240202 | BCU | ... | ... | none | ... |
| J0209.9+7229 | 32.497898 | 72.487701 | S5 0205+722 | BL Lac | LSP | 0.895 | none | ... |
| J0210.7-5101 | 32.694599 | -51.021801 | PKS 0208-512 | FSRQ | LSP | 1.003 | both | 5.93 (29.36) |
| J0211.2+1051 | 32.809101 | 10.856900 | MG1 J021114+1051 | BL Lac | ISP | 0.200 | both | 5.05 (12.75) |
| J0212.9+2244 | 33.242699 | 22.746599 | MG3 J021252+2246 | BL Lac | ISP | 0.459 | none | ... |
| J0214.4-5822 | 33.602402 | -58.369801 | PMN J0214-5822 | BCU | ... | ... | none | ... |
| J0216.6-1015 | 34.165298 | -10.266200 | PMN J0216-1017 | BCU | LSP | ... | both | 999.90 (999.90) |
| J0216.8-6635 | 34.216801 | -66.589699 | RBS 0300 | BL Lac | HSP | 0.330 | none | ... |
| J0217.2+0837 | 34.316299 | 8.623400 | ZS 0214+083 | BL Lac | LSP | 0.085 | opt | ... |
| J0217.4+7352 | 34.353298 | 73.880402 | S5 0212+73 | FSRQ | LSP | 2.367 | none | ... |
| J0217.8+0144 | 34.462101 | 1.734600 | PKS 0215+015 | FSRQ | LSP | 1.715 | opt | ... |
| J0218.9+3643 | 34.747299 | 36.717602 | MG3 J021846+3641 | BCU | ... | ... | gam | ... |
| J0221.1+3556 | 35.280998 | 35.935902 | B2 0218+357 | FSRQ | LSP | 0.944 | gam | ... |
| J0221.5+2513 | 35.380901 | 25.230499 | 2MASS J02212698+2514338 | BL Lac | ISP | 0.482 | none | ... |
| J0222.0-1616 | 35.519699 | -16.278700 | PKS 0219-164 | FSRQ | LSP | 0.698 | both | 4.57 (9.12) |
| J0222.6+4302 | 35.669601 | 43.035702 | 3C 66A | BL Lac | ISP | 0.444 | both | 999.90 (999.90) |
| J0224.2+0700 | 36.057701 | 7.012600 | PKS 0221+067 | FSRQ | LSP | 0.511 | opt | ... |
| J0225.1-2604 | 36.282902 | -26.077400 | PMN J0225-2603 | BCU | LSP | ... | opt | ... |
| J0226.5+0938 | 36.631302 | 9.635100 | NVSS J022634+093843 | FSRQ | LSP | 2.605 | none | ... |
| J0226.5-4441 | 36.648102 | -44.685902 | RBS 0318 | BL Lac | HSP | ... | none | ... |
| J0227.8+2246 | 36.954399 | 22.777500 | NVSS J022744+224834 | BCU | LSP | 0.428 | none | ... |
| J0229.5-3644 | 37.387699 | -36.738800 | PKS 0227-369 | FSRQ | LSP | 2.115 | both | 15.99 (9.05) |
| J0230.8+4032 | 37.708599 | 40.541599 | B3 0227+403 | FSRQ | LSP | 1.019 | gam | ... |
| J0231.2-4745 | 37.820900 | -47.765400 | PMN J0231-4746 | FSRQ | LSP | 0.765 | both | -2.05 (8.87) |
| J0231.8+1322 | 37.961601 | 13.369200 | 4C +13.14 | FSRQ | LSP | 2.065 | none | ... |
| J0236.8-6136 | 39.202099 | -61.610600 | PKS 0235-618 | FSRQ | LSP | 0.467 | opt | ... |
| J0237.6-3602 | 39.424400 | -36.042198 | RBS 0334 | BL Lac | HSP | 0.411 | none | ... |
| J0237.8+2848 | 39.473701 | 28.804399 | 4C +28.07 | FSRQ | LSP | 1.206 | both | 8.18 (23.08) |
| J0238.1-3905 | 39.529900 | -39.087399 | 1RXS J023800.5-390505 | BL Lac | HSP | 0.200 | none | ... |
| J0238.2+1531 | 39.561699 | 15.517500 | CRATES J023819+153323 | BCU | LSP | ... | gam | ... |
| J0238.4-3116 | 39.620899 | -31.282801 | 1RXS J023832.6-311658 | BL Lac | HSP | 0.232 | opt | ... |
| J0238.6+1637 | 39.667999 | 16.617901 | PKS 0235+164 | BL Lac | LSP | 0.940 | both | 1.74 (25.23) |
| J0239.5+1326 | 39.884701 | 13.436600 | GB6 J0239+1327 | BCU | ... | ... | none | ... |
| J0239.7+0415 | 39.940300 | 4.264300 | PKS 0237+040 | FSRQ | LSP | 0.978 | none | ... |
| J0243.4+7119 | 40.867901 | 71.324898 | S5 0238+711 | BL Lac | LSP | ... | none | ... |
| J0244.6-5819 | 41.157600 | -58.325600 | RBS 0351 | BL Lac | HSP | 0.265 | opt | ... |
| J0244.7+1316 | 41.192001 | 13.279900 | GB6 J0244+1320 | BCU | LSP | ... | none | ... |
| J0245.1-0257 | 41.291401 | -2.955000 | PMN J0245-0255 | BL Lac | LSP | ... | none | ... |
| J0245.4+2408 | 41.354500 | 24.149799 | B2 0242+23 | FSRQ | LSP | 2.243 | none | ... |
| J0245.9-4650 | 41.496601 | -46.846298 | PKS 0244-470 | FSRQ | LSP | 1.385 | none | ... |
| J0250.2-8224 | 42.573200 | -82.403702 | PMN J0251-8226 | BCU | LSP | ... | none | ... |

| 4FGL Name | RA deg | Dec deg | Association | Class | SED class | redshift | Flares | Lags days |
|--------------|-----------|------------|----------------------------|--------|-----------|----------|--------|-----------------|
| J0251.5-5958 | 42.897598 | -59.973900 | PKS 0250-602 | FSRQ | LSP | 1.373 | opt | ... |
| J0252.8-2219 | 43.200699 | -22.320299 | PKS 0250-225 | FSRQ | LSP | 1.419 | gam | ... |
| J0253.5+3216 | 43.382900 | 32.282600 | MG3 J025334+3217 | FSRQ | LSP | 0.859 | none | ... |
| J0253.9+5103 | 43.493301 | 51.063301 | TXS 0250+508 | FSRQ | LSP | 1.732 | none | ... |
| J0257.9-1215 | 44.492001 | -12.263700 | PMN J0257-1211 | FSRQ | LSP | 1.391 | opt | ... |
| J0258.1+2030 | 44.542198 | 20.513700 | MG3 J025805+2029 | BL Lac | LSP | ... | none | ... |
| J0259.4+0746 | 44.857800 | 7.783300 | PKS 0256+075 | FSRQ | LSP | 0.893 | both | 999.90 (999.90) |
| J0301.6-7155 | 45.403599 | -71.927902 | PKS 0301-721 | FSRQ | LSP | 0.823 | both | -5.99 (11.50) |
| J0303.4-2407 | 45.862499 | -24.122499 | PKS 0301-243 | BL Lac | HSP | 0.266 | opt | ... |
| J0303.4-5232 | 45.870602 | -52.534901 | AT20G J030328-523433 | BCU | LSP | ... | none | ... |
| J0303.6+4716 | 45.909801 | 47.275902 | 4C +47.08 | BL Lac | LSP | ... | opt | ... |
| J0303.6-6211 | 45.924500 | -62.189899 | PKS 0302-623 | FSRQ | LSP | 1.351 | both | -1.79 (4.95) |
| J0304.5+3349 | 46.137901 | 33.826099 | 4C +33.06 | BCU | LSP | ... | none | ... |
| J0309.0+1029 | 47.261700 | 10.492700 | PKS 0306+102 | FSRQ | LSP | 0.863 | none | ... |
| J0309.9-6058 | 47.492100 | -60.973301 | PKS 0308-611 | FSRQ | LSP | 1.479 | both | 9.87 (8.58) |
| J0310.6-5017 | 47.654400 | -50.290100 | 1RXS J031036.0-501615 | BL Lac | HSP | ... | none | ... |
| J0312.8+0134 | 48.222198 | 1.572400 | PKS 0310+013 | FSRQ | LSP | 0.664 | none | ... |
| J0314.3-5103 | 48.592899 | -51.055000 | PMN J0314-5104 | BL Lac | LSP | ... | none | ... |
| J0315.9-1033 | 48.992199 | -10.552200 | PKS 0313-107 | FSRQ | LSP | 1.565 | gam | ... |
| J0316.2+0905 | 49.058300 | 9.094600 | GB6 J0316+0904 | BL Lac | LSP | 0.372 | none | ... |
| J0318.7+2135 | 49.694599 | 21.596800 | MG3 J031849+2135 | BL Lac | ... | ... | none | ... |
| J0319.8+1845 | 49.972198 | 18.753201 | 1E 0317.0+1835 | BL Lac | HSP | 0.190 | none | ... |
| J0319.9-3821 | 49.997501 | -38.357700 | NVSS J031957-381527 | BCU | ... | ... | none | ... |
| J0325.5-5635 | 51.379398 | -56.591000 | 1RXS J032521.8-563543 | BL Lac | HSP | 0.060 | opt | ... |
| J0325.6-1646 | 51.417900 | -16.781000 | RBS 0421 | BL Lac | HSP | 0.291 | opt | ... |
| J0325.7+2225 | 51.442101 | 22.432600 | TXS 0322+222 | FSRQ | LSP | 2.066 | gam | ... |
| J0327.5-1805 | 51.890701 | -18.088499 | CRATES J032743.34-180342.0 | BCU | ... | ... | none | ... |
| J0330.6+0438 | 52.672699 | 4.634900 | GB6 J0330+0439 | BCU | LSP | ... | none | ... |
| J0331.3-6156 | 52.843800 | -61.936501 | PMN J0331-6155 | BL Lac | HSP | ... | none | ... |
| J0331.9+6307 | 52.990898 | 63.130901 | GB6 J0331+6307 | BL Lac | ISP | ... | none | ... |
| J0332.1-1123 | 53.033501 | -11.394900 | 1RXS J033223.2-111938 | FSRQ | LSP | 0.207 | none | ... |
| J0333.9+6537 | 53.476700 | 65.618797 | TXS 0329+654 | BL Lac | LSP | ... | none | ... |
| J0334.2-3725 | 53.555599 | -37.432701 | PMN J0334-3725 | BL Lac | LSP | ... | opt | ... |
| J0334.2-4008 | 53.556599 | -40.145000 | PKS 0332-403 | BL Lac | LSP | 1.445 | opt | ... |
| J0335.1-4459 | 53.784599 | -44.991600 | SUMSS J033513-445939 | BL Lac | HSP | ... | none | ... |
| J0336.4+3224 | 54.101501 | 32.411098 | NRAO 140 | FSRQ | LSP | 1.259 | none | ... |
| J0338.5+1302 | 54.635502 | 13.041900 | RX J0338.4+1302 | BL Lac | HSP | ... | none | ... |
| J0338.9-2848 | 54.744701 | -28.800900 | NVSS J033859-284619 | BCU | ... | ... | none | ... |
| J0339.5-0146 | 54.877102 | -1.776900 | PKS 0336-01 | FSRQ | LSP | 0.850 | both | 0.09 (13.39) |
| J0340.5-2118 | 55.147701 | -21.315800 | PKS 0338-214 | BL Lac | LSP | 0.233 | opt | ... |
| J0342.2+3858 | 55.573002 | 38.978001 | GB6 J0342+3858 | FSRQ | LSP | 0.945 | none | ... |
| J0343.2-2529 | 55.813599 | -25.494301 | PKS 0341-256 | FSRQ | LSP | 1.419 | none | ... |
| J0343.2-6444 | 55.816299 | -64.734901 | PMN J0343-6442 | BL Lac | ISP | ... | none | ... |
| J0345.2-2353 | 56.318699 | -23.885000 | NVSS J034518-235218 | BL Lac | ISP | 0.104 | none | ... |
| J0347.7-3616 | 56.946999 | -36.280800 | PKS 0346-364 | BCU | LSP | ... | none | ... |
| J0348.5-2749 | 57.153801 | -27.821501 | PKS 0346-27 | FSRQ | LSP | 0.991 | both | 6.92 (9.73) |
| J0348.6-1609 | 57.153198 | -16.165400 | PKS 0346-163 | BL Lac | LSP | ... | none | ... |
| J0349.6+2410 | 57.423000 | 24.177500 | TXS 0346+241 | BCU | ... | ... | opt | ... |
| J0349.8-2103 | 57.469898 | -21.057600 | PKS 0347-211 | FSRQ | LSP | 2.944 | none | ... |
| J0350.6-3226 | 57.659401 | -32.447300 | PKS 0348-326 | BCU | LSP | ... | none | ... |
| J0353.0+5654 | 58.271999 | 56.902599 | GB6 J0353+5654 | BL Lac | HSP | ... | none | ... |
| J0354.4+4643 | 58.609001 | 46.723099 | B3 0350+465 | BCU | ... | ... | none | ... |
| J0354.7+8009 | 58.691898 | 80.164703 | S5 0346+80 | BL Lac | LSP | ... | none | ... |
| J0354.7-1617 | 58.677898 | -16.287001 | PKS 0352-164 | FSRQ | LSP | 1.187 | none | ... |
| J0358.6+0634 | 59.665600 | 6.575900 | PMN J0358+0629 | BCU | LSP | ... | none | ... |
| J0358.9+6004 | 59.732800 | 60.076698 | TXS 0354+599 | FSRQ | LSP | 0.455 | none | ... |
| J0359.6+5057 | 59.915798 | 50.959000 | NRAO 150 | FSRQ | LSP | 1.520 | gam | ... |
| J0401.7+2112 | 60.449600 | 21.200701 | TXS 0358+210 | FSRQ | LSP | 0.834 | gam | ... |
| J0401.9-2034 | 60.486698 | -20.580400 | PMN J0401-2034 | BCU | LSP | ... | both | 999.90 (999.90) |
| J0402.0-2616 | 60.510300 | -26.273001 | PKS 0359-264 | BL Lac | LSP | 1.920 | none | ... |
| J0403.9-3605 | 60.974998 | -36.087002 | PKS 0402-362 | FSRQ | LSP | 1.417 | both | 1.20 (16.07) |
| J0405.6-1308 | 61.418900 | -13.143800 | PKS 0403-13 | FSRQ | LSP | 0.571 | gam | ... |
| J0407.0-3826 | 61.762699 | -38.439400 | PKS 0405-385 | FSRQ | LSP | 1.285 | both | 5.01 (11.59) |
| J0407.5+0741 | 61.892101 | 7.699800 | TXS 0404+075 | BL Lac | LSP | 1.133 | opt | ... |
| J0409.8-0359 | 62.462898 | -3.986500 | NVSS J040946-040003 | BL Lac | ISP | ... | opt | ... |
| J0410.9+4216 | 62.736000 | 42.277699 | B3 0407+421 | BCU | LSP | ... | none | ... |
| J0416.2-4353 | 64.072197 | -43.887901 | SUMSS J041613-435057 | FSRQ | LSP | 0.398 | none | ... |
| J0416.5-1852 | 64.137299 | -18.872400 | PKS 0414-189 | FSRQ | LSP | 1.536 | none | ... |
| J0416.9+0105 | 64.226898 | 1.088000 | 1ES 0414+009 | BL Lac | HSP | 0.287 | opt | ... |
| J0420.3-3745 | 65.093597 | -37.752201 | NVSS J042025-374443 | BCU | LSP | ... | none | ... |
| J0422.1-0644 | 65.534302 | -6.741000 | PMN J0422-0643 | FSRQ | LSP | 0.242 | both | 999.90 (999.90) |
| J0423.3-0120 | 65.825996 | -1.334200 | PKS 0420-01 | FSRQ | LSP | 0.916 | both | 999.90 (999.90) |
| J0424.7+0036 | 66.194504 | 0.602800 | PKS 0422+00 | BL Lac | LSP | 0.268 | opt | ... |
| J0424.9-5331 | 66.249802 | -53.525700 | PMN J0425-5331 | BL Lac | LSP | 0.390 | opt | ... |
| J0427.3-3900 | 66.825996 | -39.009701 | PMN J0427-3900 | BCU | LSP | ... | none | ... |
| J0428.6-3756 | 67.172997 | -37.940300 | PKS 0426-380 | BL Lac | LSP | 1.110 | both | -9.39 (50.58) |
| J0430.3+1654 | 67.590103 | 16.909300 | MG1 J043022+1655 | BCU | ... | ... | none | ... |
| J0431.8+7403 | 67.951698 | 74.055199 | GB6 J0431+7403 | BL Lac | HSP | ... | none | ... |
| J0433.6+2905 | 68.410698 | 29.097500 | MG2 J043337+2905 | BL Lac | LSP | 0.970 | gam | ... |
| J0433.6-6030 | 68.401199 | -60.511101 | PKS 0432-606 | FSRQ | LSP | 0.930 | opt | ... |
| J0434.1-2014 | 68.529297 | -20.244400 | TXS 0431-203 | BL Lac | ISP | 0.928 | none | ... |
| J0434.7+0922 | 68.688599 | 9.378300 | TXS 0431+092 | BL Lac | ... | ... | none | ... |
| J0436.8-5223 | 69.219803 | -52.393398 | AT20G J043652-521639 | BCU | LSP | ... | none | ... |

| 4FGL Name | RA deg | Dec deg | Association | Class | SED class | redshift | Flares | Lags days |
|--------------|------------|------------|----------------------------|--------|-----------|----------|--------|-----------------|
| J0438.4-1254 | 69.609901 | -12.905300 | PKS 0436-129 | FSRQ | LSP | 1.276 | none | ... |
| J0438.9-4521 | 69.744698 | -45.358398 | PKS 0437-454 | BL Lac | LSP | 2.017 | none | ... |
| J0440.3-4333 | 70.082901 | -43.544800 | PKS 0438-43 | FSRQ | ... | 2.852 | both | 3.21 (7.79) |
| J0442.6-0017 | 70.661201 | -0.296100 | PKS 0440-00 | FSRQ | LSP | 0.449 | none | ... |
| J0443.3-6652 | 70.848297 | -66.867302 | PMN J0443-6651 | FSRQ | LSP | ... | none | ... |
| J0445.1-6012 | 71.285797 | -60.212200 | PMN J0444-6014 | FSRQ | ... | 0.097 | none | ... |
| J0449.1+1121 | 72.282303 | 11.356900 | PKS 0446+11 | FSRQ | LSP | 2.153 | none | ... |
| J0449.4-4350 | 72.358200 | -43.834999 | PKS 0447-439 | BL Lac | HSP | 0.205 | both | 3.40 (39.74) |
| J0451.8-4651 | 72.955597 | -46.857498 | PKS 0450-469 | FSRQ | LSP | 0.602 | both | 15.89 (56.38) |
| J0453.1-2806 | 73.288696 | -28.114401 | PKS 0451-28 | FSRQ | LSP | 2.564 | none | ... |
| J0455.7-4617 | 73.946297 | -46.287102 | PKS 0454-46 | FSRQ | LSP | 0.858 | opt | ... |
| J0456.2+2702 | 74.067299 | 27.040300 | MG2 J045613+2702 | BCU | LSP | ... | none | ... |
| J0457.0+0646 | 74.254501 | 6.780400 | 4C +06.21 | FSRQ | LSP | 0.405 | none | ... |
| J0457.0-2324 | 74.260803 | -23.414900 | PKS 0454-234 | FSRQ | LSP | 1.003 | both | 3.02 (11.79) |
| J0501.2-0158 | 75.302299 | -1.974900 | S3 0458-02 | FSRQ | LSP | 2.291 | gam | ... |
| J0502.4+0609 | 75.618103 | 6.162700 | PKS 0459+060 | FSRQ | LSP | 1.106 | none | ... |
| J0502.5+1340 | 75.634102 | 13.668500 | PKS 0459+135 | BL Lac | LSP | ... | none | ... |
| J0502.5+3438 | 75.636597 | 34.633801 | MG2 J050234+3436 | BCU | ... | ... | none | ... |
| J0505.3+0459 | 76.343102 | 4.999400 | PKS 0502+049 | FSRQ | LSP | 0.954 | both | 3.02 (5.67) |
| J0505.6+6405 | 76.424400 | 64.087700 | TXS 0500+640 | BCU | LSP | ... | opt | ... |
| J0505.8-0419 | 76.459801 | -4.318200 | S3 0503-04 | FSRQ | LSP | 1.481 | none | ... |
| J0507.7-6104 | 76.932701 | -61.081402 | PMN J0507-6104 | FSRQ | LSP | 1.089 | none | ... |
| J0507.9+6737 | 76.995598 | 67.622299 | 1ES 0502+675 | BL Lac | HSP | 0.416 | none | ... |
| J0509.4+0542 | 77.359299 | 5.701400 | TXS 0506+056 | BL Lac | ISP | 0.336 | both | 3.61 (18.39) |
| J0509.4+1012 | 77.350998 | 10.200800 | PKS 0506+101 | FSRQ | LSP | 0.621 | none | ... |
| J0509.9-6417 | 77.487602 | -64.289101 | RBS 0625 | BL Lac | HSP | ... | none | ... |
| J0510.0+1800 | 77.518097 | 18.013500 | PKS 0507+17 | FSRQ | LSP | 0.416 | both | 999.90 (999.90) |
| J0510.4-1809 | 77.611603 | -18.164301 | CRATES J051015.50-181227.8 | BCU | LSP | ... | none | ... |
| J0512.8+4041 | 78.218597 | 40.694500 | B3 0509+406 | BCU | LSP | ... | none | ... |
| J0515.6-4556 | 78.905899 | -45.948299 | PKS 0514-459 | FSRQ | LSP | 0.194 | both | -2.02 (24.70) |
| J0515.8+1527 | 78.953003 | 15.461400 | GB6 J0515+1527 | BL Lac | ISP | ... | none | ... |
| J0516.7-6207 | 79.179802 | -62.124802 | PKS 0516-621 | BL Lac | LSP | 1.300 | both | 999.90 (999.90) |
| J0521.7+2112 | 80.444504 | 21.213100 | TXS 0518+211 | BL Lac | HSP | 0.108 | both | 21.11 (94.34) |
| J0521.8-3848 | 80.471802 | -38.806599 | PKS 0520-388 | BCU | ... | ... | none | ... |
| J0524.6-2819 | 81.173203 | -28.328800 | PMN J0524-2818 | BCU | LSP | ... | none | ... |
| J0525.8-0052 | 81.466599 | -0.870900 | PMN J0525-0051 | BL Lac | LSP | 1.200 | none | ... |
| J0526.2-4830 | 81.571404 | -48.515099 | PKS 0524-485 | FSRQ | LSP | 1.300 | both | 6.35 (14.00) |
| J0529.3-7243 | 82.329300 | -72.733002 | PKS 0530-727 | BCU | LSP | ... | none | ... |
| J0530.9+1332 | 82.736397 | 13.540200 | PKS 0528+134 | FSRQ | LSP | 2.070 | none | ... |
| J0532.0-4827 | 83.002197 | -48.460701 | PMN J0531-4827 | BL Lac | ISP | ... | none | ... |
| J0532.6+0732 | 83.171997 | 7.549300 | OG 050 | FSRQ | LSP | 1.254 | none | ... |
| J0532.8-3941 | 83.199997 | -39.685299 | PKS 0531-397 | BCU | LSP | ... | none | ... |
| J0533.0-8446 | 83.267700 | -84.778297 | PMN J0532-8447 | BCU | LSP | ... | none | ... |
| J0533.3+4823 | 83.333801 | 48.383400 | TXS 0529+483 | FSRQ | LSP | 1.160 | none | ... |
| J0533.8-3749 | 83.474899 | -37.830898 | PKS 0532-378 | FSRQ | LSP | 1.668 | none | ... |
| J0538.2-3910 | 84.574600 | -39.169601 | NVSS J053810-390844 | BL Lac | HSP | 0.440 | none | ... |
| J0538.8-4405 | 84.708900 | -44.086201 | PKS 0537-441 | BL Lac | LSP | 0.892 | both | -14.46 (7.67) |
| J0539.6+1432 | 84.905197 | 14.544300 | TXS 0536+145 | FSRQ | LSP | 2.690 | gam | ... |
| J0539.9-2839 | 84.995201 | -28.658501 | PKS 0537-286 | FSRQ | LSP | 3.104 | gam | ... |
| J0540.8-5415 | 85.206902 | -54.257500 | PKS 0539-543 | FSRQ | LSP | 1.185 | none | ... |
| J0542.9-0913 | 85.740898 | -9.220800 | PMN J0542-0913 | BCU | LSP | ... | none | ... |
| J0543.9-5531 | 85.981400 | -55.532700 | 1RXS J054357.3-553206 | BL Lac | HSP | 0.273 | opt | ... |
| J0555.6+3947 | 88.901497 | 39.787800 | B2 0552+39A | FSRQ | LSP | 2.365 | both | 999.90 (999.90) |
| J0556.2-4352 | 89.074898 | -43.869598 | SUMSS J055618-435146 | BL Lac | LSP | ... | none | ... |
| J0601.1-7035 | 90.295799 | -70.589500 | PKS 0601-70 | FSRQ | LSP | 2.409 | both | -0.28 (2.09) |
| J0607.4+4739 | 91.857101 | 47.663502 | TXS 0603+476 | BL Lac | LSP | ... | both | 999.90 (999.90) |
| J0608.0+6721 | 92.005699 | 67.351196 | S4 0602+67 | FSRQ | LSP | 1.970 | none | ... |
| J0608.0-0835 | 92.010101 | -8.585700 | PKS 0605-08 | FSRQ | LSP | 0.870 | none | ... |
| J0608.1-1521 | 92.030197 | -15.363900 | PMN J0608-1520 | FSRQ | LSP | 1.094 | none | ... |
| J0608.9-5456 | 92.238701 | -54.942501 | PKS 0607-549 | BCU | LSP | ... | none | ... |
| J0609.0-2219 | 92.262001 | -22.331600 | PKS 0606-223 | FSRQ | LSP | 1.926 | opt | ... |
| J0610.1-1848 | 92.545502 | -18.807600 | PMN J0610-1847 | BL Lac | LSP | ... | opt | ... |
| J0610.9-6054 | 92.730499 | -60.916401 | PKS 0609-609 | FSRQ | LSP | 1.773 | none | ... |
| J0611.6-2712 | 92.911499 | -27.215200 | PMN J0611-2709 | BCU | ... | ... | none | ... |
| J0612.5-3138 | 93.127998 | -31.638100 | PKS 0610-316 | FSRQ | LSP | 0.873 | none | ... |
| J0612.8+4122 | 93.221802 | 41.371700 | B3 0609+413 | BL Lac | ISP | ... | opt | ... |
| J0614.8+6136 | 93.721298 | 61.607899 | GB6 J0614+6139 | BCU | ... | ... | none | ... |
| J0615.3-3117 | 93.839401 | -31.285299 | PKS 0613-312 | BL Lac | ISP | ... | none | ... |
| J0617.2+5701 | 94.316200 | 57.024899 | 87GB 061258.1+570222 | BL Lac | LSP | ... | none | ... |
| J0620.5-2512 | 95.144501 | -25.212900 | PKS 0618-252 | BCU | LSP | 1.900 | none | ... |
| J0622.3-2605 | 95.595596 | -26.096300 | PMN J0622-2605 | BL Lac | HSP | 0.414 | both | 999.90 (999.90) |
| J0622.9+3326 | 95.729599 | 33.433498 | B2 0619+33 | BCU | LSP | 1.062 | none | ... |
| J0623.0-3010 | 95.764603 | -30.182800 | PMN J0623-3010 | BCU | ... | ... | none | ... |
| J0625.3+4439 | 96.328796 | 44.664799 | GB6 J0625+4440 | BL Lac | LSP | ... | opt | ... |
| J0625.8-5441 | 96.452301 | -54.691898 | PMN J0625-5438 | FSRQ | LSP | 2.051 | none | ... |
| J0628.8-6250 | 97.217400 | -62.840500 | PKS 0628-627 | BL Lac | LSP | ... | none | ... |
| J0629.3-1959 | 97.347801 | -19.999901 | PKS 0627-199 | BL Lac | LSP | 1.724 | none | ... |
| J0631.1+2020 | 97.776604 | 20.340599 | TXS 0628+203 | BCU | ... | ... | none | ... |
| J0633.4-2222 | 98.369598 | -22.372400 | PMN J0633-2223 | FSRQ | LSP | 1.508 | none | ... |
| J0635.6-7518 | 98.902199 | -75.304604 | PKS 0637-75 | FSRQ | LSP | 0.653 | none | ... |
| J0636.5+7138 | 99.182800 | 71.661499 | GB6 J0636+7138 | BCU | LSP | ... | none | ... |
| J0638.6+7320 | 99.671097 | 73.343803 | S5 0633+73 | FSRQ | LSP | 1.850 | none | ... |
| J0641.7-0320 | 100.437103 | -3.346600 | PMN J0641-0320 | FSRQ | LSP | 1.196 | gam | ... |

| 4FGL Name | RA deg | Dec deg | Association | Class | SED class | redshift | Flares | Lags days |
|--------------|------------|------------|----------------------------|--------|-----------|----------|--------|-----------------|
| J0643.2-5356 | 100.815399 | -53.936401 | PMN J0643-5358 | BCU | LSP | ... | none | ... |
| J0643.3+0857 | 100.834503 | 8.952500 | PMN J0643+0857 | FSRQ | LSP | 0.882 | gam | ... |
| J0644.4-6712 | 101.105301 | -67.212402 | PKS 0644-671 | FSRQ | LSP | ... | none | ... |
| J0644.6+6039 | 101.162300 | 60.656200 | NVSS J064435+603849 | BL Lac | ISP | 0.358 | none | ... |
| J0646.7-3913 | 101.678398 | -39.217701 | PKS 0644-390 | FSRQ | LSP | 0.681 | none | ... |
| J0647.7-6058 | 101.931396 | -60.978100 | PMN J0647-6058 | BL Lac | LSP | ... | none | ... |
| J0648.7+1516 | 102.190498 | 15.280800 | RX J0648.7+1516 | BL Lac | HSP | 0.179 | none | ... |
| J0649.5-3139 | 102.394501 | -31.657301 | NVSS J064933-313917 | BL Lac | ... | 0.563 | none | ... |
| J0650.5-2851 | 102.628998 | -28.861000 | PMN J0650-2849 | BCU | LSP | ... | none | ... |
| J0650.7+2503 | 102.698601 | 25.054800 | 1ES 0647+250 | BL Lac | HSP | 0.203 | opt | ... |
| J0654.3+5042 | 103.596199 | 50.702702 | GB6 J0654+5042 | FSRQ | LSP | 1.253 | none | ... |
| J0654.4+4514 | 103.606003 | 45.244598 | B3 0650+453 | FSRQ | LSP | 0.928 | none | ... |
| J0659.6-2742 | 104.906601 | -27.701300 | TXS 0657-276 | FSRQ | LSP | 1.727 | none | ... |
| J0659.9+1709 | 104.984703 | 17.152201 | TXS 0657+172 | FSRQ | ... | 1.080 | none | ... |
| J0700.5-6610 | 105.129303 | -66.180298 | PKS 0700-661 | BL Lac | ISP | ... | opt | ... |
| J0701.5-4634 | 105.390602 | -46.572899 | PKS 0700-465 | FSRQ | LSP | 0.822 | both | 4.65 (21.58) |
| J0702.7-1951 | 105.678001 | -19.851700 | TXS 0700-197 | BL Lac | LSP | ... | none | ... |
| J0703.3-0050 | 105.836700 | -0.843600 | TXS 0700-007 | BL Lac | ISP | ... | opt | ... |
| J0704.8+4907 | 106.206703 | 49.131802 | 87GB 070112.8+491056 | BCU | LSP | ... | none | ... |
| J0706.8+7742 | 106.724899 | 77.700203 | NVSS J070651+774137 | BL Lac | ISP | ... | none | ... |
| J0709.1+2241 | 107.276901 | 22.684700 | GB6 J0708+2241 | BL Lac | ISP | ... | opt | ... |
| J0709.7-0255 | 107.445099 | -2.930100 | PMN J0709-0255 | FSRQ | LSP | 1.472 | gam | ... |
| J0710.4+5908 | 107.623398 | 59.135201 | 1H 0658+595 | BL Lac | HSP | 0.125 | none | ... |
| J0710.8-3851 | 107.724503 | -38.851299 | AT20G J071043-385037 | FSRQ | LSP | 0.129 | none | ... |
| J0710.9+4733 | 107.732300 | 47.553001 | S4 0707+47 | BL Lac | LSP | 1.292 | none | ... |
| J0712.7+5033 | 108.187599 | 50.550598 | GB6 J0712+5033 | BL Lac | LSP | 0.502 | opt | ... |
| J0713.0+5738 | 108.259804 | 57.634499 | GB6 J0713+5738 | BCU | ISP | ... | gam | ... |
| J0713.8+1935 | 108.464699 | 19.587900 | MG2 J071354+1934 | FSRQ | LSP | 0.540 | none | ... |
| J0718.0+4536 | 109.515900 | 45.616299 | S4 0714+45 | FSRQ | LSP | 0.940 | none | ... |
| J0719.3+3307 | 109.839996 | 33.123199 | B2 0716+33 | FSRQ | LSP | 0.779 | both | 4.92 (14.91) |
| J0720.0-3507 | 110.004402 | -35.122601 | AT20G J071959-350448 | BCU | LSP | ... | none | ... |
| J0721.3+0405 | 110.347504 | 4.091400 | PMN J0721+0406 | FSRQ | LSP | 0.665 | none | ... |
| J0721.9+7120 | 110.488197 | 71.340500 | S5 0716+71 | BL Lac | ISP | 0.127 | both | -5.89 (33.53) |
| J0725.2+1425 | 111.323997 | 14.421200 | 4C +14.23 | FSRQ | LSP | 1.038 | none | ... |
| J0726.4-4727 | 111.613098 | -47.458900 | PMN J0726-4728 | FSRQ | LSP | 1.686 | none | ... |
| J0729.1+5703 | 112.285698 | 57.055801 | TXS 0724+571 | FSRQ | LSP | 0.426 | none | ... |
| J0730.3-1141 | 112.577599 | -11.688800 | PKS 0727-11 | FSRQ | LSP | 1.589 | none | ... |
| J0730.5-0535 | 112.635399 | -5.584200 | TXS 0728-054 | BL Lac | ISP | ... | none | ... |
| J0733.5-5445 | 113.385201 | -54.759300 | SUMSS J073334-544544 | BCU | LSP | ... | none | ... |
| J0733.6+3649 | 113.419601 | 36.822498 | GB6 J0733+3650 | BCU | LSP | ... | none | ... |
| J0733.8+0455 | 113.472198 | 4.928200 | GB6 J0733+0456 | FSRQ | LSP | 3.010 | none | ... |
| J0734.0+5021 | 113.524498 | 50.357201 | TXS 0730+504 | FSRQ | LSP | 0.720 | none | ... |
| J0734.4-7711 | 113.611801 | -77.185204 | PKS 0736-770 | BCU | LSP | ... | none | ... |
| J0738.1+1742 | 114.538696 | 17.706600 | PKS 0735+17 | BL Lac | LSP | 0.424 | both | -0.20 (44.72) |
| J0739.2+0137 | 114.820000 | 1.621600 | PKS 0736+01 | FSRQ | LSP | 0.189 | both | 11.20 (12.89) |
| J0742.6+5443 | 115.671501 | 54.727001 | GB6 J0742+5444 | FSRQ | LSP | 0.720 | opt | ... |
| J0742.9-5242 | 115.739998 | -52.703300 | PMN J0742-5241 | BCU | LSP | ... | none | ... |
| J0743.0-5622 | 115.769798 | -56.376801 | PMN J0743-5619 | FSRQ | LSP | 2.319 | none | ... |
| J0743.6-3805 | 115.906197 | -38.093700 | PMN J0743-3804 | BCU | LSP | ... | opt | ... |
| J0746.4+2546 | 116.602097 | 25.767799 | B2 0743+25 | FSRQ | LSP | 2.987 | opt | ... |
| J0746.5+2730 | 116.627602 | 27.515301 | OI 272 | FSRQ | LSP | 1.690 | none | ... |
| J0746.6-4754 | 116.669403 | -47.915501 | PMN J0746-4755 | BL Lac | HSP | ... | none | ... |
| J0747.3-3310 | 116.832802 | -33.177799 | PKS 0745-330 | BL Lac | LSP | ... | none | ... |
| J0748.0-1638 | 117.005898 | -16.643700 | TXS 0745-165 | BCU | LSP | ... | none | ... |
| J0748.3+4928 | 117.082397 | 49.474800 | NVSS J074837+493040 | BL Lac | ... | ... | none | ... |
| J0748.6+2400 | 117.163803 | 24.016600 | OI 275 | FSRQ | LSP | 0.410 | both | 999.90 (999.90) |
| J0749.3+4453 | 117.348198 | 44.891800 | SDSS J074916.88+445232.1 | BCU | LSP | 0.559 | none | ... |
| J0750.8+1229 | 117.700996 | 12.494000 | OI 280 | FSRQ | ... | 0.889 | both | 999.90 (999.90) |
| J0751.0+7908 | 117.767799 | 79.139397 | JVAS J0750+7909 | BCU | LSP | ... | none | ... |
| J0752.2+3313 | 117.982597 | 33.236099 | OI 380 | FSRQ | ... | 1.936 | both | -1.13 (7.26) |
| J0753.9+0923 | 118.490700 | 9.390400 | TXS 0751+095 | BCU | LSP | ... | opt | ... |
| J0754.4-1148 | 118.610497 | -11.805200 | TXS 0752-116 | BL Lac | LSP | ... | none | ... |
| J0754.7+4823 | 118.692902 | 48.393200 | GB1 0751+485 | BL Lac | LSP | 0.377 | opt | ... |
| J0757.1+0956 | 119.285599 | 9.949100 | PKS 0754+100 | BL Lac | LSP | 0.266 | opt | ... |
| J0800.4-2257 | 120.111298 | -22.957199 | PMN J0800-2302 | BCU | LSP | ... | none | ... |
| J0800.9+4401 | 120.245697 | 44.018101 | B3 0757+441 | BL Lac | LSP | 1.072 | none | ... |
| J0801.1+6444 | 120.293297 | 64.743797 | RX J0801.0+6444 | BL Lac | ... | 0.200 | none | ... |
| J0803.2-0337 | 120.824699 | -3.618900 | TXS 0800-034 | FSRQ | HSP | 0.365 | none | ... |
| J0803.5+2046 | 120.888298 | 20.767799 | GB6 B0800+2046 | BCU | LSP | ... | none | ... |
| J0804.0-3629 | 121.007599 | -36.485401 | NVSS J080405-362919 | BL Lac | ... | ... | none | ... |
| J0804.5+0414 | 121.132797 | 4.239300 | TXS 0802+043 | BCU | LSP | ... | none | ... |
| J0805.1+7744 | 121.289101 | 77.744102 | WN B0759.6+7754 | BCU | LSP | ... | none | ... |
| J0805.2-0110 | 121.300400 | -1.181000 | PKS B0802-010 | FSRQ | LSP | 1.388 | none | ... |
| J0805.4+6147 | 121.355698 | 61.793701 | TXS 0800+618 | FSRQ | LSP | 3.033 | none | ... |
| J0805.4+7534 | 121.361603 | 75.576599 | RX J0805.4+7534 | BL Lac | HSP | 0.121 | none | ... |
| J0806.5+4503 | 121.628403 | 45.060501 | B3 0803+452 | FSRQ | LSP | 2.102 | none | ... |
| J0807.1-0541 | 121.779800 | -5.684200 | PKS 0804-05 | BL Lac | ISP | ... | none | ... |
| J0807.7-1206 | 121.933701 | -12.104300 | CRATES J080736.06-120745.9 | BCU | LSP | ... | none | ... |
| J0808.2-0751 | 122.065002 | -7.855600 | PKS 0805-07 | FSRQ | LSP | 1.837 | both | 1.36 (9.41) |
| J0809.3+4053 | 122.330002 | 40.895401 | S4 0805+41 | FSRQ | LSP | 1.418 | none | ... |
| J0809.8+5218 | 122.461700 | 52.314301 | 1ES 0806+524 | BL Lac | HSP | 0.138 | opt | ... |
| J0811.4+0146 | 122.861000 | 1.775600 | OJ 014 | BL Lac | LSP | 1.148 | none | ... |
| J0814.2-1013 | 123.550903 | -10.217200 | NVSS J081411-101208 | BL Lac | ISP | ... | none | ... |

| 4FGL Name | RA deg | Dec deg | Association | Class | SED class | redshift | Flares | Lags days |
|--------------|------------|------------|--------------------------|--------|-----------|----------|--------|-----------------|
| J0814.6+6430 | 123.665398 | 64.504997 | GB6 J0814+6431 | BL Lac | LSP | 0.239 | opt | ... |
| J0816.3+5739 | 124.099701 | 57.661598 | SBS 0812+578 | BL Lac | ISP | 0.054 | none | ... |
| J0816.4-1311 | 124.112297 | -13.197300 | PMN J0816-1311 | BL Lac | HSP | 0.046 | none | ... |
| J0816.7-2420 | 124.191597 | -24.342699 | PMN J0816-2421 | BCU | LSP | ... | none | ... |
| J0817.8-0934 | 124.473396 | -9.577700 | TXS 0815-094 | BL Lac | LSP | ... | none | ... |
| J0818.2+4222 | 124.557198 | 42.381901 | S4 0814+42 | BL Lac | LSP | 0.530 | none | ... |
| J0821.1+1007 | 125.299301 | 10.128700 | SDSS J082054.81+100609.4 | BCU | LSP | 0.956 | none | ... |
| J0824.4+2440 | 126.108101 | 24.670900 | B2 0821+24 | FSRQ | LSP | 1.242 | none | ... |
| J0824.7+5552 | 126.197701 | 55.881599 | OJ 535 | FSRQ | LSP | 1.417 | none | ... |
| J0824.9+3915 | 126.236099 | 39.257401 | 4C +39.23 | FSRQ | LSP | 1.216 | none | ... |
| J0825.9-2230 | 126.499100 | -22.505501 | PKS 0823-223 | BL Lac | LSP | 0.910 | both | 13.27 (35.45) |
| J0830.8+2410 | 127.701500 | 24.172701 | S3 0827+24 | FSRQ | LSP | 0.939 | both | 14.94 (44.52) |
| J0831.8+0429 | 127.973198 | 4.494100 | PKS 0829+046 | BL Lac | LSP | 0.174 | both | 1.36 (21.72) |
| J0833.9+4223 | 128.475906 | 42.398899 | OJ 451 | FSRQ | LSP | 0.249 | none | ... |
| J0836.2+2141 | 129.051102 | 21.697100 | MG2 J083615+2138 | BCU | ... | ... | none | ... |
| J0836.5-2026 | 129.130905 | -20.447399 | PKS 0834-20 | FSRQ | LSP | 2.752 | none | ... |
| J0839.8+0105 | 129.963303 | 1.087700 | PKS 0837+012 | FSRQ | LSP | 1.123 | both | 1.17 (19.43) |
| J0841.3-3554 | 130.340607 | -35.904099 | NVSS J084121-355506 | BL Lac | HSP | ... | none | ... |
| J0842.3-6053 | 130.597900 | -60.891899 | PMN J0842-6053 | BCU | ... | ... | gam | ... |
| J0843.0-0853 | 130.773895 | -8.887800 | PMN J0843-0848 | BCU | ... | ... | none | ... |
| J0844.2+5312 | 131.050903 | 53.214100 | NVSS J084411+531250 | BL Lac | LSP | 0.435 | none | ... |
| J0849.4-2911 | 132.351105 | -29.186300 | NVSS J084922-291149 | BCU | ISP | ... | none | ... |
| J0849.8-3541 | 132.451599 | -35.687698 | PMN J0849-3541 | BCU | LSP | ... | both | 999.90 (999.90) |
| J0850.0+4855 | 132.508301 | 48.921700 | GB6 J0850+4855 | BL Lac | LSP | ... | both | 999.90 (999.90) |
| J0850.1-1212 | 132.541199 | -12.212100 | PMN J0850-1213 | FSRQ | LSP | 0.566 | none | ... |
| J0851.5+5528 | 132.880493 | 55.479401 | GB6 J0851+5528 | BL Lac | LSP | ... | opt | ... |
| J0852.5-5755 | 133.141800 | -57.930401 | PMN J0852-5755 | BCU | LSP | ... | both | 999.90 (999.90) |
| J0854.8+2006 | 133.707108 | 20.115900 | OJ 287 | BL Lac | LSP | 0.306 | both | 999.90 (999.90) |
| J0855.9+7144 | 133.975403 | 71.741898 | GB6 J0856+7146 | FSRQ | LSP | 0.542 | none | ... |
| J0856.6-1105 | 134.169601 | -11.099300 | PMN J0856-1105 | BL Lac | LSP | ... | none | ... |
| J0857.9-1949 | 134.491104 | -19.817499 | PKS 0855-19 | FSRQ | LSP | 0.659 | none | ... |
| J0900.6-7408 | 135.172104 | -74.143997 | AT20G J085959-741401 | BCU | LSP | ... | none | ... |
| J0900.7-1243 | 135.175095 | -12.720100 | TXS 0858-125 | BCU | ISP | ... | none | ... |
| J0902.4+2051 | 135.617203 | 20.850300 | NVSS J090226+205045 | BL Lac | ISP | 2.055 | opt | ... |
| J0904.5-3513 | 136.140396 | -35.230801 | NVSS J090442-351423 | BCU | LSP | ... | none | ... |
| J0904.9-5734 | 136.231506 | -57.583302 | PKS 0903-57 | BCU | LSP | 0.695 | both | -0.83 (21.85) |
| J0905.6+1358 | 136.401703 | 13.975000 | MG1 J090534+1358 | BL Lac | HSP | ... | opt | ... |
| J0906.3-0905 | 136.582703 | -9.092500 | PMN J0906-0905 | BL Lac | ... | ... | none | ... |
| J0909.1+0121 | 137.296707 | 1.355700 | PKS 0906+01 | FSRQ | LSP | 1.024 | none | ... |
| J0909.7-0230 | 137.446396 | -2.514300 | PKS 0907-023 | FSRQ | LSP | 0.957 | gam | ... |
| J0910.6+2247 | 137.674301 | 22.797800 | TXS 0907+230 | FSRQ | LSP | 2.661 | none | ... |
| J0910.8+3859 | 137.709106 | 38.999901 | FBQS J091052.0+390202 | BL Lac | LSP | 0.199 | opt | ... |
| J0912.2+4127 | 138.055893 | 41.456299 | B3 0908+416B | FSRQ | LSP | 2.563 | gam | ... |
| J0915.4-3027 | 138.875000 | -30.464199 | PMN J0915-3030 | BCU | LSP | ... | none | ... |
| J0915.9+2933 | 138.986206 | 29.552999 | Ton 0396 | BL Lac | HSP | 0.190 | none | ... |
| J0916.7+3856 | 139.189804 | 38.947899 | 4C +38.28 | FSRQ | LSP | 1.268 | none | ... |
| J0920.3-0443 | 140.100006 | -4.731100 | TXS 0917-044 | BCU | LSP | ... | none | ... |
| J0920.9+4441 | 140.229095 | 44.699001 | S4 0917+44 | FSRQ | LSP | 2.186 | both | 999.90 (999.90) |
| J0921.6+6216 | 140.418503 | 62.270802 | OK 630 | FSRQ | LSP | 1.446 | both | 0.88 (3.25) |
| J0922.6+0434 | 140.666901 | 4.578100 | GB6 J0922+0433 | BCU | LSP | 1.325 | none | ... |
| J0922.7-3959 | 140.691803 | -39.986698 | PKS 0920-39 | FSRQ | LSP | 0.595 | both | 1.32 (6.21) |
| J0923.5+3852 | 140.884995 | 38.874298 | B2 0920+39 | BCU | LSP | ... | none | ... |
| J0923.5+4125 | 140.894897 | 41.428299 | B3 0920+416 | FSRQ | LSP | 1.732 | none | ... |
| J0924.0+2816 | 141.004898 | 28.275499 | B2 0920+28 | FSRQ | LSP | 0.744 | none | ... |
| J0928.1-2035 | 142.047806 | -20.597300 | PKS 0925-203 | FSRQ | LSP | 0.348 | gam | ... |
| J0929.3+5014 | 142.326508 | 50.235199 | GB6 J0929+5013 | BL Lac | LSP | ... | none | ... |
| J0930.3+8612 | 142.599396 | 86.202103 | S5 0916+864 | BL Lac | LSP | ... | opt | ... |
| J0930.9-1015 | 142.740402 | -10.256500 | TXS 0928-099 | BCU | LSP | ... | none | ... |
| J0931.2-8533 | 142.817596 | -85.562599 | PKS 0936-853 | BCU | LSP | ... | none | ... |
| J0932.6+5306 | 143.158997 | 53.100800 | S4 0929+53 | FSRQ | LSP | 0.597 | opt | ... |
| J0937.1+5008 | 144.296906 | 50.143700 | GB6 J0937+5008 | FSRQ | LSP | 0.276 | opt | ... |
| J0937.9-1434 | 144.475098 | -14.570600 | NVSS J093754-143350 | BL Lac | ISP | 0.287 | opt | ... |
| J0939.3-1732 | 144.835999 | -17.541800 | TXS 0936-173 | BCU | LSP | ... | none | ... |
| J0940.0-2828 | 145.011597 | -28.480301 | TXS 0937-282 | BCU | LSP | ... | opt | ... |
| J0940.7-6105 | 145.178802 | -61.085499 | MRC 0939-608 | BCU | LSP | ... | opt | ... |
| J0940.9-1335 | 145.243805 | -13.589100 | TXS 0938-133 | FSRQ | LSP | 0.551 | none | ... |
| J0941.7+4125 | 145.449997 | 41.421600 | GB6 J0941+4121 | BCU | LSP | 0.819 | none | ... |
| J0942.3-0800 | 145.585602 | -8.007600 | PMN J0942-0800 | BL Lac | LSP | ... | opt | ... |
| J0945.2+5200 | 146.316193 | 52.005299 | WISE J094452.09+520233.4 | FSRQ | LSP | 0.563 | none | ... |
| J0945.7+5759 | 146.432007 | 57.987099 | GB6 J0945+5757 | BL Lac | LSP | 0.229 | none | ... |
| J0946.6+1016 | 146.661301 | 10.277000 | TXS 0943+105 | FSRQ | LSP | 1.007 | none | ... |
| J0947.1-2541 | 146.781296 | -25.683901 | 1RXS J094709.2-254056 | BL Lac | ... | ... | none | ... |
| J0949.0+4038 | 147.261795 | 40.636700 | 4C +40.24 | FSRQ | LSP | 1.250 | none | ... |
| J0949.2+1749 | 147.315506 | 17.830000 | TXS 0946+181 | FSRQ | LSP | 0.694 | none | ... |
| J0952.6-5048 | 148.156601 | -50.811199 | PMN J0952-5049 | BCU | ... | ... | none | ... |
| J0953.0-0840 | 148.262802 | -8.669500 | PMN J0953-0840 | BL Lac | HSP | ... | none | ... |
| J0956.7+2516 | 149.176102 | 25.281700 | OK 290 | FSRQ | LSP | 0.708 | none | ... |
| J0957.3-1348 | 149.331406 | -13.814100 | PMN J0957-1350 | FSRQ | LSP | 1.323 | none | ... |
| J0957.6+5523 | 149.416107 | 55.383801 | 4C +55.17 | FSRQ | LSP | 0.896 | none | ... |
| J0957.8+3423 | 149.470703 | 34.397499 | B2 0954+34 | BCU | LSP | 1.810 | none | ... |
| J0958.0+4728 | 149.509003 | 47.467499 | OK 492 | FSRQ | LSP | 1.882 | gam | ... |
| J0958.4+5042 | 149.605698 | 50.700001 | 7C 0955+5054 | FSRQ | LSP | 1.154 | none | ... |
| J0958.7+6534 | 149.689697 | 65.567802 | S4 0954+65 | BL Lac | LSP | 0.367 | both | -2.34 (16.15) |

| 4FGL Name | RA deg | Dec deg | Association | Class | SED class | redshift | Flares | Lags days |
|--------------|------------|------------|----------------------------|--------|-----------|----------|--------|-----------------|
| J1001.1+2911 | 150.293793 | 29.188000 | GB6 J1001+2911 | BL Lac | LSP | 0.558 | both | -13.29 (24.54) |
| J1006.7-2159 | 151.693100 | -21.990999 | PKS 1004-217 | FSRQ | LSP | 0.330 | both | -22.55 (2.88) |
| J1007.6-3332 | 151.911697 | -33.543201 | PKS 1005-333 | FSRQ | LSP | 1.837 | none | ... |
| J1008.0+0620 | 152.013596 | 6.347500 | MG1 J100800+0621 | BL Lac | LSP | 0.650 | opt | ... |
| J1008.7-2909 | 152.198898 | -29.155899 | PMN J1008-2912 | BCU | LSP | ... | none | ... |
| J1010.2-3119 | 152.571594 | -31.320700 | 1RXS J101015.9-311909 | BL Lac | HSP | 0.143 | none | ... |
| J1010.8-0158 | 152.703796 | -1.981700 | PKS 1008-01 | FSRQ | LSP | 0.896 | none | ... |
| J1011.3-0427 | 152.825302 | -4.457700 | PKS B1008-041 | FSRQ | LSP | 1.588 | none | ... |
| J1012.7+2439 | 153.198898 | 24.663799 | MG2 J101241+2439 | FSRQ | LSP | 1.805 | gam | ... |
| J1013.7+3444 | 153.448700 | 34.738400 | OL 318 | FSRQ | LSP | 0.208 | none | ... |
| J1015.0+4926 | 153.768005 | 49.433601 | 1H 1013+498 | BL Lac | HSP | 0.212 | both | 999.90 (999.90) |
| J1015.6+5553 | 153.910507 | 55.889301 | TXS 1012+560 | FSRQ | LSP | 0.677 | none | ... |
| J1016.0+0512 | 154.009293 | 5.208900 | TXS 1013+054 | FSRQ | LSP | 1.713 | opt | ... |
| J1017.8+0715 | 154.472794 | 7.263800 | GB6 J1018+0715 | BCU | ... | ... | none | ... |
| J1018.1+1905 | 154.548004 | 19.096300 | NVSS J101808+190614 | BL Lac | LSP | ... | none | ... |
| J1018.3-3124 | 154.591293 | -31.403200 | PKS 1016-311 | FSRQ | LSP | 0.794 | both | -1.05 (2.13) |
| J1018.4+0528 | 154.617203 | 5.470200 | TXS 1015+057 | FSRQ | LSP | 1.945 | none | ... |
| J1018.4+3540 | 154.607193 | 35.680199 | B2 1015+35B | FSRQ | LSP | 1.228 | none | ... |
| J1019.7+6321 | 154.926300 | 63.352699 | GB6 J1019+6319 | BL Lac | LSP | ... | opt | ... |
| J1023.1+3949 | 155.788498 | 39.822601 | 4C +40.25 | FSRQ | LSP | 1.333 | both | 0.25 (10.80) |
| J1023.8-4335 | 155.972504 | -43.595100 | RX J1023.9-4336 | BL Lac | HSP | 0.320 | none | ... |
| J1023.9-3236 | 155.996399 | -32.603401 | PKS 1021-323 | FSRQ | LSP | 1.568 | none | ... |
| J1026.9-1749 | 156.742401 | -17.821800 | 1RXS J102658.5-174905 | BL Lac | HSP | 0.267 | none | ... |
| J1027.2+7427 | 156.812103 | 74.452400 | GB6 J1027+7428 | BCU | LSP | 0.879 | none | ... |
| J1027.6+8251 | 156.922699 | 82.861099 | 2MASS J10284195+8253398 | BCU | ... | ... | none | ... |
| J1028.4-0234 | 157.121307 | -2.582900 | PMN J1028-0237 | FSRQ | LSP | 0.476 | opt | ... |
| J1031.1+7442 | 157.792496 | 74.701897 | S5 1027+74 | BL Lac | ISP | 0.123 | none | ... |
| J1031.6+6019 | 157.909103 | 60.317799 | TXS 1028+605 | FSRQ | LSP | 1.231 | none | ... |
| J1032.6+3737 | 158.173401 | 37.623402 | B3 1029+378 | BL Lac | ISP | 0.528 | none | ... |
| J1033.1+4115 | 158.275208 | 41.262001 | S4 1030+41 | FSRQ | LSP | 1.117 | none | ... |
| J1033.9+6050 | 158.484894 | 60.849300 | S4 1030+61 | FSRQ | LSP | 1.401 | both | -1.86 (20.20) |
| J1037.4-2933 | 159.356400 | -29.556801 | PKS 1034-293 | FSRQ | LSP | 0.312 | both | 5.18 (8.18) |
| J1037.7-2822 | 159.427399 | -28.381599 | PKS B1035-281 | FSRQ | LSP | 1.066 | both | 3.87 (4.97) |
| J1038.2-2425 | 159.558807 | -24.423901 | NVSS J103824-242355 | BCU | ... | ... | none | ... |
| J1038.8-5312 | 159.712906 | -53.206902 | MRC 1036-529 | FSRQ | LSP | 1.450 | none | ... |
| J1040.5+0617 | 160.149506 | 6.284800 | GB6 J1040+0617 | BL Lac | LSP | ... | both | 999.90 (999.90) |
| J1043.2+2408 | 160.805298 | 24.146000 | B2 1040+24A | FSRQ | LSP | 0.560 | opt | ... |
| J1045.8-2928 | 161.468399 | -29.479500 | PKS B1043-291 | FSRQ | LSP | 2.128 | none | ... |
| J1047.2-5517 | 161.800201 | -55.293098 | PMN J1047-5513 | BCU | ... | ... | none | ... |
| J1047.7+7238 | 161.938797 | 72.641998 | GB6 J1047+7238 | BL Lac | ISP | ... | none | ... |
| J1047.8-6216 | 161.960907 | -62.274502 | PMN J1047-6217 | BCU | LSP | ... | none | ... |
| J1048.4+7143 | 162.106705 | 71.729698 | S5 1044+71 | FSRQ | LSP | 1.150 | both | -2.80 (15.42) |
| J1049.8+1429 | 162.467499 | 14.483500 | MG1 J104945+1429 | BCU | LSP | 1.630 | both | -8.64 (16.21) |
| J1050.1+0432 | 162.546402 | 4.537700 | MG1 J105009+0433 | FSRQ | LSP | 1.217 | none | ... |
| J1054.5+2211 | 163.627899 | 22.191299 | 87GB 105148.6+222705 | BL Lac | ISP | 2.055 | none | ... |
| J1056.8+7012 | 164.207596 | 70.201897 | S5 1053+70 | FSRQ | LSP | 2.492 | both | 6.83 (29.25) |
| J1057.2+5510 | 164.318298 | 55.180401 | SDSS J105707.47+551032.2 | BL Lac | HSP | 2.085 | none | ... |
| J1057.3-2341 | 164.342300 | -23.688900 | PKS B1054-234 | FSRQ | LSP | 1.125 | none | ... |
| J1058.0+4305 | 164.518097 | 43.093800 | B3 1055+433 | BL Lac | LSP | ... | none | ... |
| J1058.4+0133 | 164.623993 | 1.564100 | 4C +01.28 | BL Lac | LSP | 0.890 | both | -7.64 (25.17) |
| J1058.5+8115 | 164.625504 | 81.254700 | S5 1053+81 | FSRQ | LSP | 0.706 | opt | ... |
| J1058.6+2817 | 164.650299 | 28.286600 | GB6 J1058+2817 | BL Lac | LSP | 0.479 | both | -1.01 (11.62) |
| J1058.6+5627 | 164.665207 | 56.463402 | TXS 1055+567 | BL Lac | ISP | 0.143 | opt | ... |
| J1058.6-8003 | 164.660004 | -80.064003 | PKS 1057-79 | BL Lac | LSP | 0.569 | none | ... |
| J1059.2-1134 | 164.806305 | -11.572000 | PKS B1056-113 | BL Lac | LSP | ... | both | 999.90 (999.90) |
| J1059.5+2057 | 164.878296 | 20.952400 | MG2 J105938+2057 | FSRQ | ... | 0.400 | none | ... |
| J1102.6+5251 | 165.673004 | 52.856899 | GB6 J1102+5249 | FSRQ | ISP | 0.690 | none | ... |
| J1103.0+1157 | 165.772202 | 11.965400 | TXS 1100+122 | FSRQ | ISP | 0.914 | both | 999.90 (999.90) |
| J1103.9-5357 | 165.975693 | -53.964699 | PKS 1101-536 | BL Lac | LSP | ... | both | 999.90 (999.90) |
| J1104.4+0730 | 166.116806 | 7.510000 | MG1 J110424+0730 | BL Lac | ISP | 0.630 | gam | ... |
| J1104.4+3812 | 166.118698 | 38.207001 | Mkn 421 | BL Lac | HSP | 0.030 | both | 19.78 (43.58) |
| J1106.0+2813 | 166.501999 | 28.225401 | MG2 J110606+2812 | FSRQ | LSP | 0.844 | none | ... |
| J1106.5-3646 | 166.627396 | -36.772301 | PMN J1106-3647 | BL Lac | ... | 1.080 | none | ... |
| J1107.0-4449 | 166.774902 | -44.832298 | PKS 1104-445 | FSRQ | LSP | 1.598 | none | ... |
| J1110.5-1836 | 167.641098 | -18.605801 | CRATES J111027.78-183552.6 | BL Lac | ISP | ... | opt | ... |
| J1112.5+3448 | 168.146896 | 34.802200 | TXS 1109+350 | FSRQ | LSP | 1.949 | none | ... |
| J1113.6-1920 | 168.404800 | -19.335899 | NVSS J111348-192252 | BCU | ISP | ... | none | ... |
| J1114.5-0819 | 168.642105 | -8.322400 | PKS B1112-080 | FSRQ | LSP | 2.078 | none | ... |
| J1117.0+2013 | 169.270798 | 20.229401 | RBS 0958 | BL Lac | HSP | 0.139 | none | ... |
| J1118.2-4634 | 169.557907 | -46.579498 | PKS 1116-46 | FSRQ | ISP | 0.713 | none | ... |
| J1119.0+1235 | 169.765503 | 12.586600 | OM 127 | FSRQ | LSP | 2.126 | none | ... |
| J1121.4-0553 | 170.364105 | -5.899700 | PKS 1118-05 | FSRQ | LSP | 1.297 | opt | ... |
| J1123.4-2529 | 170.868301 | -25.488001 | NVSS J112325-252858 | FSRQ | ... | 0.148 | none | ... |
| J1124.9+4934 | 171.242798 | 49.567402 | GB6 J1124+4933 | BL Lac | HSP | ... | none | ... |
| J1125.5-3557 | 171.392899 | -35.958099 | PMN J1125-3556 | BL Lac | ISP | 0.284 | opt | ... |
| J1125.9+2005 | 171.491196 | 20.091200 | 4C +20.25 | FSRQ | LSP | 0.133 | opt | ... |
| J1127.0-1857 | 171.763397 | -18.964001 | PKS 1124-186 | FSRQ | LSP | 1.048 | opt | ... |
| J1127.4+5648 | 171.864807 | 56.803200 | S4 1124+57 | FSRQ | LSP | 2.890 | none | ... |
| J1127.8+3618 | 171.963898 | 36.313999 | MG2 J112758+3620 | FSRQ | LSP | 0.884 | none | ... |
| J1128.0+5924 | 172.003403 | 59.401501 | TXS 1125+596 | FSRQ | LSP | 1.795 | none | ... |
| J1129.1+3703 | 172.295898 | 37.064400 | CRATES J112916+370317 | BL Lac | LSP | 0.445 | none | ... |
| J1129.2-0529 | 172.311493 | -5.487400 | NVSS J112914-052856 | BCU | ... | ... | none | ... |
| J1129.5+3034 | 172.380402 | 30.578899 | 87GB 112657.9+305242 | BCU | ISP | 0.435 | none | ... |

| 4FGL Name | RA deg | Dec deg | Association | Class | SED class | redshift | Flares | Lags days |
|--------------|------------|------------|------------------------------|--------|-----------|----------|--------|-----------------|
| J1131.0+3815 | 172.754501 | 38.256500 | B2 1128+38 | FSRQ | LSP | 1.733 | both | 11.26 (5.71) |
| J1132.7+0034 | 173.196106 | 0.573700 | PKS B1130+008 | BL Lac | ISP | 1.223 | none | ... |
| J1135.1+3014 | 173.788406 | 30.234400 | CRATES J113514+301001 | BL Lac | LSP | ... | none | ... |
| J1136.2+3407 | 174.074997 | 34.129002 | MG2 J113627+3408 | FSRQ | LSP | 1.337 | none | ... |
| J1136.4+6736 | 174.117905 | 67.612701 | RX J1136.5+6737 | BL Lac | HSP | 0.136 | none | ... |
| J1136.4+7009 | 174.121902 | 70.153702 | Mkn 180 | BL Lac | HSP | 0.045 | opt | ... |
| J1139.0+4033 | 174.763702 | 40.561699 | CRATES J113903+403303 | BCU | LSP | 2.360 | none | ... |
| J1143.1+6122 | 175.788101 | 61.380100 | GB6 J1143+6122 | BL Lac | LSP | 0.475 | none | ... |
| J1145.7-6949 | 176.438202 | -69.831398 | PKS 1143-696 | FSRQ | LSP | 0.244 | gam | ... |
| J1146.9+3958 | 176.740494 | 39.977501 | S4 1144+40 | FSRQ | LSP | 1.089 | gam | ... |
| J1147.0-3812 | 176.759995 | -38.200600 | PKS 1144-379 | BL Lac | LSP | 1.048 | both | 999.90 (999.90) |
| J1147.2-2627 | 176.811401 | -26.464899 | PMN J1147-2625 | BCU | LSP | ... | none | ... |
| J1147.8-0724 | 176.960800 | -7.414400 | PKS 1145-071 | FSRQ | LSP | 1.342 | none | ... |
| J1148.5+2629 | 177.141296 | 26.498600 | TXS 1145+268 | FSRQ | LSP | 0.867 | none | ... |
| J1149.5-4029 | 177.386505 | -40.491001 | PMN J1149-4029 | BCU | LSP | ... | opt | ... |
| J1150.4+2418 | 177.602905 | 24.301600 | OM 280 | BL Lac | ISP | 0.200 | opt | ... |
| J1150.6+4154 | 177.656296 | 41.909599 | RBS 1040 | BL Lac | HSP | 0.320 | none | ... |
| J1152.3-0839 | 178.080795 | -8.666300 | PKS B1149-084 | FSRQ | LSP | 2.370 | gam | ... |
| J1153.0+8056 | 178.266403 | 80.935699 | S5 1150+81 | FSRQ | LSP | 1.250 | none | ... |
| J1153.3-1104 | 178.342300 | -11.078700 | PKS B1150-108 | BCU | LSP | 0.269 | gam | ... |
| J1153.4+4931 | 178.350494 | 49.516899 | 4C +49.22 | FSRQ | LSP | 0.334 | none | ... |
| J1154.0+4037 | 178.514496 | 40.632000 | B3 1151+408 | FSRQ | LSP | 0.925 | none | ... |
| J1154.0+6018 | 178.518997 | 60.310699 | RX J1154.0+6022 | FSRQ | LSP | 1.120 | none | ... |
| J1154.1-3243 | 178.542297 | -32.718899 | PKS 1151-324 | BL Lac | LSP | ... | none | ... |
| J1156.6+0640 | 179.163605 | 6.672800 | TXS 1154+069 | BCU | LSP | ... | none | ... |
| J1158.5+4824 | 179.636505 | 48.416100 | GB1 1155+486 | FSRQ | LSP | 2.028 | none | ... |
| J1159.2-2227 | 179.810699 | -22.460501 | PKS 1156-221 | BCU | LSP | 0.565 | both | 3.57 (11.94) |
| J1159.3-2142 | 179.843201 | -21.703800 | PMN J1159-2142 | FSRQ | LSP | 0.617 | opt | ... |
| J1159.5+2914 | 179.884003 | 29.244801 | Ton 599 | FSRQ | LSP | 0.729 | both | -2.52 (15.95) |
| J1200.2+0201 | 180.055099 | 2.017200 | 87GB 115739.6+021927 | BCU | LSP | ... | none | ... |
| J1200.6+1229 | 180.173401 | 12.492200 | GB6 J1200+1230 | BL Lac | ... | 0.415 | none | ... |
| J1200.7+2008 | 180.186600 | 20.135401 | TXS 1158+204 | BCU | LSP | ... | none | ... |
| J1202.5-0528 | 180.629105 | -5.470900 | PKS 1200-051 | FSRQ | LSP | 0.381 | none | ... |
| J1203.1+6031 | 180.788101 | 60.518002 | SBS 1200+608 | BL Lac | LSP | 0.065 | none | ... |
| J1204.2-0709 | 181.074097 | -7.162700 | 1RXS J120417.0-070959 | BL Lac | ISP | 0.184 | none | ... |
| J1205.7-2635 | 181.432205 | -26.594601 | PKS 1203-26 | FSRQ | LSP | 0.789 | none | ... |
| J1207.7-0106 | 181.927597 | -1.106300 | AT20G J120741-010630 | FSRQ | LSP | 1.006 | both | -4.87 (18.23) |
| J1208.9+5441 | 182.226105 | 54.699501 | TXS 1206+549 | FSRQ | LSP | 1.345 | none | ... |
| J1209.4+7608 | 182.362503 | 76.137001 | 2MASS J12093020+7609120 | BCU | ISP | ... | none | ... |
| J1209.8+1810 | 182.466400 | 18.177601 | MG1 J120953+1809 | FSRQ | LSP | 0.845 | opt | ... |
| J1211.0-3800 | 182.762100 | -38.015598 | PMN J1211-3754 | BCU | LSP | ... | none | ... |
| J1212.0-2326 | 183.000900 | -23.449400 | PMN J1212-2327 | BL Lac | ... | 0.666 | none | ... |
| J1215.0+1656 | 183.774200 | 16.937201 | TXS 1212+171 | FSRQ | LSP | 1.132 | none | ... |
| J1217.9+3007 | 184.476196 | 30.117701 | B2 1215+30 | BL Lac | HSP | 0.130 | both | -12.97 (15.16) |
| J1218.0-0028 | 184.513596 | -0.483200 | PKS 1215-002 | BL Lac | LSP | 0.419 | none | ... |
| J1218.5-0119 | 184.638794 | -1.327000 | PKS 1216-010 | BL Lac | LSP | ... | opt | ... |
| J1220.1+3432 | 185.046204 | 34.538300 | GB2 1217+348 | BL Lac | LSP | ... | none | ... |
| J1220.1+7105 | 185.043793 | 71.092003 | S5 1217+71 | FSRQ | LSP | 0.451 | both | -0.33 (10.37) |
| J1221.3+3010 | 185.344894 | 30.167700 | PG 1218+304 | BL Lac | HSP | 0.184 | opt | ... |
| J1221.5+2814 | 185.378403 | 28.238199 | W Comae | BL Lac | ISP | 0.102 | none | ... |
| J1222.5+0414 | 185.627106 | 4.238900 | 4C +04.42 | FSRQ | LSP | 0.964 | gam | ... |
| J1223.8+8039 | 185.970703 | 80.659798 | S5 1221+80 | BL Lac | LSP | ... | none | ... |
| J1223.9+5000 | 185.988007 | 50.008900 | SBS 1221+503 | FSRQ | LSP | 1.064 | opt | ... |
| J1224.4+2436 | 186.116104 | 24.614201 | MS 1221.8+2452 | BL Lac | HSP | 0.219 | opt | ... |
| J1224.7-8313 | 186.199005 | -83.225899 | PKS 1221-82 | BCU | LSP | ... | none | ... |
| J1224.9+2122 | 186.227707 | 21.381399 | 4C +21.35 | FSRQ | LSP | 0.434 | both | -0.33 (26.43) |
| J1225.0+0330 | 186.251907 | 3.509800 | 4C +03.23 | FSRQ | LSP | 0.956 | none | ... |
| J1225.5-2851 | 186.392197 | -28.862499 | AT20G J122515-284956 | BCU | LSP | ... | none | ... |
| J1226.8-1329 | 186.718796 | -13.494000 | PMN J1226-1328 | BL Lac | LSP | 0.456 | none | ... |
| J1228.7+4858 | 187.179199 | 48.982700 | TXS 1226+492 | FSRQ | LSP | 1.716 | opt | ... |
| J1229.0+0202 | 187.267502 | 2.045400 | 3C 273 | FSRQ | LSP | 0.158 | both | 999.90 (999.90) |
| J1229.7-5304 | 187.444199 | -53.070400 | AT20G J122939-530332 | BL Lac | ... | ... | none | ... |
| J1230.2+2517 | 187.559906 | 25.298300 | ON 246 | BL Lac | ISP | 0.135 | both | 4.75 (38.09) |
| J1231.7+2847 | 187.934906 | 28.791700 | B2 1229+29 | BL Lac | ISP | 0.236 | none | ... |
| J1233.7-0144 | 188.433899 | -1.742800 | NVSS J123341-014426 | BL Lac | ISP | ... | none | ... |
| J1234.0-5735 | 188.519394 | -57.596100 | AT20G J123407-573552 | BCU | ISP | ... | none | ... |
| J1238.1-4541 | 189.545303 | -45.686100 | PMN J1238-4541 | BL Lac | ISP | ... | none | ... |
| J1238.3-1959 | 189.593597 | -19.994499 | PMN J1238-1959 | BL Lac | LSP | ... | opt | ... |
| J1239.5+0443 | 189.885406 | 4.728400 | MG1 J123931+0443 | FSRQ | LSP | 1.761 | gam | ... |
| J1243.9-0218 | 190.984497 | -2.308200 | PMN J1243-0218 | BCU | LSP | ... | none | ... |
| J1245.1+5709 | 191.288300 | 57.158001 | 1RXS J124510.5+571020 | BL Lac | ISP | 1.545 | none | ... |
| J1246.7-2548 | 191.688705 | -25.801800 | PKS 1244-255 | FSRQ | LSP | 0.635 | both | 0.38 (29.79) |
| J1248.9+4840 | 192.244291 | 48.669998 | 87GB 124632.9+485605 | BCU | LSP | 1.852 | none | ... |
| J1249.3-0545 | 192.326401 | -5.762100 | GALEXASC J124919.46-054539.7 | BCU | ... | ... | none | ... |
| J1249.8+3707 | 192.459793 | 37.130600 | 2MASS J12494675+3707474 | BL Lac | ... | 0.286 | none | ... |
| J1251.3-0201 | 192.835999 | -2.027100 | TXS 1248-017 | BCU | LSP | 0.335 | none | ... |
| J1253.2+5301 | 193.306702 | 53.017300 | S4 1250+53 | BL Lac | LSP | ... | opt | ... |
| J1253.8+6242 | 193.466599 | 62.705200 | 1RXS J125400.1+624303 | BL Lac | LSP | 0.867 | none | ... |
| J1254.2-2205 | 193.552094 | -22.087200 | NVSS J125422-220413 | BCU | ... | ... | none | ... |
| J1254.5+2210 | 193.636993 | 22.180799 | TXS 1252+224 | BL Lac | HSP | 0.509 | none | ... |
| J1254.9+1138 | 193.733398 | 11.649500 | ON 187 | FSRQ | LSP | 0.872 | none | ... |
| J1254.9-7141 | 193.726700 | -71.693100 | PKS 1251-71 | BCU | ... | ... | none | ... |
| J1256.1-0547 | 194.041504 | -5.788700 | 3C 279 | FSRQ | LSP | 0.536 | both | -0.89 (8.71) |

| 4FGL Name | RA deg | Dec deg | Association | Class | SED class | redshift | Flares | Lags days |
|--------------|------------|------------|--------------------------|--------|-----------|----------|--------|-----------------|
| J1257.2+3646 | 194.310303 | 36.770599 | RX J1257.3+3647 | BL Lac | ISP | 0.531 | none | ... |
| J1257.8+3228 | 194.472794 | 32.472099 | ON 393 | FSRQ | LSP | 0.806 | both | -1.31 (14.33) |
| J1258.6-1759 | 194.663498 | -17.995800 | PKS B1256-177 | FSRQ | LSP | 1.956 | gam | ... |
| J1258.8-2219 | 194.717194 | -22.325701 | PKS 1256-220 | FSRQ | LSP | 1.303 | both | 1.31 (15.83) |
| J1259.1-2311 | 194.779800 | -23.192499 | PKS B1256-229 | BL Lac | LSP | 0.481 | none | ... |
| J1259.7-3223 | 194.944901 | -32.389801 | LEDA 4075145 | BL Lac | LSP | 0.014 | gam | ... |
| J1300.4+1416 | 195.119507 | 14.270100 | OW 197 | FSRQ | LSP | 1.109 | none | ... |
| J1301.6+3336 | 195.417603 | 33.609699 | MG2 J130126+3337 | FSRQ | LSP | 1.008 | none | ... |
| J1302.8+5748 | 195.720901 | 57.814602 | TXS 1300+580 | BL Lac | LSP | 1.088 | none | ... |
| J1303.0+2434 | 195.757095 | 24.582100 | MG2 J130304+2434 | BL Lac | LSP | 0.993 | both | 999.90 (999.90) |
| J1303.6-4622 | 195.923798 | -46.367500 | PMN J1303-4621 | FSRQ | LSP | 1.664 | none | ... |
| J1304.3-4353 | 196.088303 | -43.895699 | 1RXS J130421.2-435308 | BL Lac | HSP | ... | opt | ... |
| J1304.6-0348 | 196.171799 | -3.813900 | PKS 1302-035 | FSRQ | LSP | 1.250 | none | ... |
| J1307.6-4259 | 196.909607 | -42.994999 | 1RXS J130737.8-425940 | BL Lac | HSP | ... | none | ... |
| J1308.4-6706 | 197.110397 | -67.108101 | PKS 1304-668 | BCU | LSP | ... | none | ... |
| J1308.5+3547 | 197.128601 | 35.791801 | 5C 12.291 | FSRQ | LSP | 1.055 | gam | ... |
| J1309.4+4305 | 197.362595 | -43.084999 | B3 1307+433 | BL Lac | ISP | 0.691 | opt | ... |
| J1310.5+3221 | 197.632401 | 32.354698 | OP 313 | FSRQ | LSP | 0.997 | both | 999.90 (999.90) |
| J1310.7-5553 | 197.683701 | -55.886700 | PMN J1310-5552 | BCU | HSP | 0.104 | none | ... |
| J1312.4-2156 | 198.110794 | -21.938000 | PKS 1309-216 | BL Lac | HSP | 1.491 | opt | ... |
| J1312.6+4828 | 198.169403 | 48.470100 | GB 1310+487 | BCU | LSP | 0.501 | none | ... |
| J1312.8-0425 | 198.216995 | -4.419600 | PKS B1310-041 | FSRQ | LSP | 0.825 | gam | ... |
| J1314.7+2348 | 198.687897 | 23.812401 | TXS 1312+240 | BL Lac | ISP | ... | opt | ... |
| J1315.1-5333 | 198.797806 | -53.564899 | PMN J1315-5334 | BL Lac | LSP | ... | gam | ... |
| J1315.9-0732 | 198.986603 | -7.546000 | NVSS J131552-073301 | BL Lac | HSP | ... | none | ... |
| J1316.1-3338 | 199.025208 | -33.636501 | PKS 1313-333 | FSRQ | LSP | 1.210 | both | -5.33 (20.12) |
| J1317.6+3428 | 199.400803 | 34.467602 | S4 1315+34 | FSRQ | LSP | 1.050 | none | ... |
| J1318.2+6754 | 199.555801 | 67.915199 | 87GB 131701.6-681031 | BCU | LSP | ... | none | ... |
| J1319.5-0045 | 199.877304 | -0.761300 | PKS B1317-005 | BCU | LSP | 0.891 | none | ... |
| J1319.8+7759 | 199.965805 | 77.988197 | NVSS J131921+775823 | BL Lac | ISP | ... | none | ... |
| J1320.7+3314 | 200.185394 | 33.237801 | 87GB 131814.4+332742 | FSRQ | ISP | 0.924 | none | ... |
| J1321.1+2216 | 200.295807 | 22.280800 | TXS 1318+225 | FSRQ | LSP | 0.943 | opt | ... |
| J1322.0+8317 | 200.501495 | 83.284500 | S5 1322+83 | FSRQ | LSP | 1.024 | none | ... |
| J1322.2+0842 | 200.550995 | 8.703600 | NVSS J132210+084231 | FSRQ | LSP | 0.325 | none | ... |
| J1322.6-0936 | 200.663696 | -9.607500 | PKS B1319-093 | FSRQ | LSP | 1.864 | gam | ... |
| J1323.9+1405 | 200.976196 | 14.087100 | RX J1323.9+1406 | BL Lac | HSP | 0.470 | none | ... |
| J1326.8-5256 | 201.720093 | -52.937599 | PMN J1326-5256 | BL Lac | LSP | ... | none | ... |
| J1326.9+2210 | 201.729507 | 22.173201 | B2 1324+22 | FSRQ | LSP | 1.398 | none | ... |
| J1329.0-5607 | 202.267197 | -56.118599 | PMN J1329-5608 | BL Lac | LSP | ... | gam | ... |
| J1330.2+7002 | 202.572693 | 70.040604 | NVSS J133025+700141 | BL Lac | HSP | ... | none | ... |
| J1330.2-7003 | 202.561600 | -70.058601 | PKS 1326-697 | BCU | LSP | ... | none | ... |
| J1330.7+2933 | 202.693497 | 29.553600 | FIRST J133101.8+293216 | BCU | LSP | ... | gam | ... |
| J1332.0-0509 | 203.019608 | -5.161100 | PKS 1329-049 | FSRQ | LSP | 2.150 | gam | ... |
| J1332.2+4722 | 203.059494 | 47.372799 | B3 1330+476 | FSRQ | LSP | 0.669 | none | ... |
| J1332.6-1256 | 203.154297 | -12.943600 | PMN J1332-1256 | FSRQ | LSP | 1.492 | gam | ... |
| J1333.2+2725 | 203.322693 | 27.422100 | MG2 J133305+2725 | FSRQ | LSP | 0.731 | none | ... |
| J1333.7+5056 | 203.439499 | 50.936600 | CLASS J1333+5057 | FSRQ | LSP | 1.362 | gam | ... |
| J1337.4+5502 | 204.366806 | 55.041801 | S4 1335+55 | FSRQ | LSP | 1.100 | none | ... |
| J1337.6-1257 | 204.423996 | -12.951700 | PKS 1335-127 | FSRQ | LSP | 0.539 | both | 8.05 (22.84) |
| J1337.9-1956 | 204.488297 | -19.945000 | PMN J1337-1958 | BCU | LSP | ... | none | ... |
| J1338.0+6534 | 204.515594 | 65.569603 | 87GB 133543.8+654752 | FSRQ | LSP | 0.946 | none | ... |
| J1338.9+1153 | 204.732300 | 11.895600 | SDSS J133859.05+115316.7 | BL Lac | ISP | ... | none | ... |
| J1339.0-2400 | 204.756302 | -24.008499 | PKS 1336-237 | BCU | LSP | 0.657 | opt | ... |
| J1339.1-2620 | 204.799103 | -26.335100 | PKS 1336-260 | FSRQ | LSP | 1.510 | none | ... |
| J1339.9-0138 | 204.975601 | -1.637800 | PKS 1337-013 | FSRQ | LSP | 1.620 | none | ... |
| J1340.4+6926 | 205.109894 | 69.444603 | TXS 1339+696 | BCU | LSP | ... | none | ... |
| J1341.8-2053 | 205.460999 | -20.890100 | PKS B1339-206 | FSRQ | LSP | 1.582 | none | ... |
| J1344.2-1723 | 206.060104 | -17.397800 | PMN J1344-1723 | FSRQ | LSP | 2.490 | none | ... |
| J1345.6-3356 | 206.408493 | -33.945301 | NVSS J134543-335643 | BL Lac | ISP | ... | none | ... |
| J1345.8+0706 | 206.464798 | 7.107200 | TXS 1343+073 | FSRQ | LSP | 1.093 | none | ... |
| J1347.6-3751 | 206.913498 | -37.863300 | PMN J1347-3750 | FSRQ | LSP | 1.300 | opt | ... |
| J1349.5-1131 | 207.386902 | -11.518800 | PKS 1346-112 | FSRQ | ISP | 0.340 | none | ... |
| J1350.8+3033 | 207.714798 | 30.558800 | B2 1348+30B | FSRQ | LSP | 0.712 | none | ... |
| J1351.0+0029 | 207.757004 | 0.487300 | PKS 1348+007 | FSRQ | LSP | 2.084 | none | ... |
| J1351.3+1115 | 207.843399 | 11.250200 | RX J1351.3+1115 | BL Lac | HSP | ... | none | ... |
| J1351.7-2912 | 207.942505 | -29.210600 | PKS 1348-289 | BCU | LSP | 1.034 | none | ... |
| J1352.7-2742 | 208.190399 | -27.705200 | PMN J1352-2745 | BCU | LSP | ... | none | ... |
| J1353.3+1434 | 208.335495 | 14.575500 | OP 186 | BL Lac | LSP | 0.405 | none | ... |
| J1354.8-1041 | 208.718002 | -10.693200 | PKS 1352-104 | FSRQ | LSP | 0.330 | gam | ... |
| J1358.1+7642 | 209.528305 | 76.706398 | S5 1357+76 | FSRQ | LSP | 1.585 | none | ... |
| J1359.1+5544 | 209.784500 | 55.747898 | 87GB 135720.6+555936 | FSRQ | LSP | 1.014 | opt | ... |
| J1359.7+4012 | 209.927597 | 40.215302 | 87GB 135731.7+402612 | FSRQ | LSP | 0.407 | none | ... |
| J1359.8-3746 | 209.966797 | -37.768101 | PMN J1359-3746 | BL Lac | ISP | 0.334 | none | ... |
| J1404.8+6554 | 211.215805 | 65.904800 | NVSS J140450+655428 | BL Lac | LSP | 0.363 | none | ... |
| J1406.1-2508 | 211.544495 | -25.138599 | NVSS J140609-250808 | BL Lac | ISP | ... | none | ... |
| J1406.6-3934 | 211.665497 | -39.572701 | 1RXS J140630.3-393508 | BL Lac | ISP | 0.370 | none | ... |
| J1407.6-4301 | 211.919403 | -43.023399 | SUMSS J140739-430231 | BL Lac | LSP | ... | opt | ... |
| J1408.9-0751 | 212.235596 | -7.857500 | PKS B1406-076 | FSRQ | LSP | 1.493 | both | 22.77 (38.87) |
| J1410.1+0202 | 212.528702 | 2.035400 | PKS 1407+022 | BL Lac | LSP | ... | none | ... |
| J1411.8+5249 | 212.969193 | 52.827801 | SBS 1410+530 | BL Lac | HSP | 0.076 | none | ... |
| J1412.9+5018 | 213.240906 | 50.300999 | SDSS J141302.28+501927.4 | BCU | ... | 1.529 | none | ... |
| J1415.5+4830 | 213.899200 | 48.514198 | RX J1415.5+4830 | BL Lac | LSP | 0.496 | none | ... |
| J1418.4+3543 | 214.622894 | 35.719200 | 87GB 141615.9+355650 | FSRQ | HSP | 2.085 | gam | ... |

| 4FGL Name | RA deg | Dec deg | Association | Class | SED class | redshift | Flares | Lags days |
|--------------|------------|------------|-----------------------|--------|-----------|----------|--------|-----------------|
| J1418.4-0233 | 214.605804 | -2.559400 | NVSS J141826-023336 | BL Lac | HSP | 0.356 | opt | ... |
| J1419.4-0838 | 214.860001 | -8.641700 | NVSS J141922-083830 | FSRQ | LSP | 0.903 | both | -2.18 (16.04) |
| J1419.5+3821 | 214.894394 | 38.365700 | B3 1417+385 | FSRQ | LSP | 1.831 | none | ... |
| J1419.8+5423 | 214.955002 | 54.393700 | OQ 530 | BL Lac | LSP | 0.153 | opt | ... |
| J1421.1-1120 | 215.287201 | -11.339300 | PMN J1420-1118 | BCU | ... | ... | none | ... |
| J1422.3+3223 | 215.637100 | 32.384998 | OQ 334 | FSRQ | LSP | 0.682 | both | -1.70 (14.05) |
| J1423.1+3738 | 215.792099 | 37.645199 | NVSS J142304+373729 | BL Lac | ISP | ... | none | ... |
| J1423.5-7829 | 215.883301 | -78.498398 | PKS 1418-782 | FSRQ | LSP | 0.788 | both | -0.92 (5.47) |
| J1424.1-1750 | 216.029404 | -17.844700 | NVSS J142412-175010 | BL Lac | HSP | 0.082 | none | ... |
| J1424.2+0433 | 216.050797 | 4.562800 | TXS 1421+048 | BL Lac | LSP | 0.665 | none | ... |
| J1424.8-6808 | 216.216904 | -68.148903 | PKS 1420-679 | BCU | LSP | ... | none | ... |
| J1427.0+2348 | 216.755798 | 23.801300 | PKS 1424+240 | BL Lac | HSP | 0.604 | opt | ... |
| J1427.6-3305 | 216.912994 | -33.094002 | PKS 1424-328 | BL Lac | LSP | ... | both | 999.90 (999.90) |
| J1427.7-3215 | 216.946106 | -32.253700 | NVSS J142750-321515 | BL Lac | ISP | ... | none | ... |
| J1427.9-4206 | 216.986603 | -42.105999 | PKS 1424-41 | FSRQ | LSP | 1.522 | both | 8.38 (23.28) |
| J1428.9+5406 | 217.228897 | 54.111401 | S4 1427+543 | FSRQ | LSP | 3.013 | none | ... |
| J1431.1-3120 | 217.796204 | -31.346800 | PKS 1428-311 | BL Lac | LSP | ... | none | ... |
| J1433.0-1801 | 218.253494 | -18.019600 | PKS 1430-178 | FSRQ | LSP | 2.331 | none | ... |
| J1434.7+1950 | 218.675003 | 19.847799 | OQ 253 | FSRQ | LSP | 1.382 | both | 0.38 (7.69) |
| J1436.9+5638 | 219.229004 | 56.648998 | RBS 1409 | BL Lac | ... | 0.150 | none | ... |
| J1438.9+3710 | 219.740204 | 37.175201 | B2 1436+37B | FSRQ | LSP | 2.401 | gam | ... |
| J1439.7+4958 | 219.941101 | 49.977501 | GB6 J1439+4958 | BL Lac | LSP | ... | opt | ... |
| J1440.0-1530 | 220.007202 | -15.515400 | PKS 1437-153 | BL Lac | LSP | ... | opt | ... |
| J1440.9+0609 | 220.242004 | 6.163100 | PMN J1440+0610 | BL Lac | ISP | 0.435 | none | ... |
| J1443.9+2501 | 220.993301 | 25.029100 | PKS 1441+25 | FSRQ | LSP | 0.939 | both | -27.27 (28.54) |
| J1443.9-3908 | 220.990799 | -39.148102 | PKS 1440-389 | BL Lac | HSP | 0.065 | both | 999.90 (999.90) |
| J1445.9-1626 | 221.497803 | -16.449800 | PKS B1443-162 | BL Lac | LSP | ... | none | ... |
| J1446.0-3039 | 221.522598 | -30.661800 | PMN J1445-3036 | BCU | LSP | ... | none | ... |
| J1446.3+3111 | 221.590698 | 31.195499 | MG2 J144640+3110 | BCU | LSP | ... | none | ... |
| J1446.7+1719 | 221.688400 | 17.323700 | S3 1444+17 | FSRQ | LSP | 1.024 | none | ... |
| J1448.0+3608 | 222.017105 | 36.134399 | RBS 1432 | BL Lac | HSP | ... | opt | ... |
| J1449.6-2137 | 222.421997 | -21.627100 | PKS B1446-214 | FSRQ | LSP | 0.938 | none | ... |
| J1450.4+0910 | 222.623505 | 9.181800 | TXS 1448+093 | FSRQ | LSP | 2.611 | none | ... |
| J1451.4+6355 | 222.855392 | 63.917198 | RX J1451.4+6354 | BL Lac | LSP | 0.650 | none | ... |
| J1453.5+3505 | 223.391998 | 35.088402 | MG2 J145315+3506 | FSRQ | LSP | 0.721 | none | ... |
| J1454.1+1622 | 223.544296 | 16.374701 | CLASS J1454+1623 | FSRQ | LSP | 1.276 | none | ... |
| J1454.4-3744 | 223.615799 | -37.749901 | PKS 1451-375 | FSRQ | LSP | 0.314 | none | ... |
| J1457.4-3539 | 224.365707 | -35.652699 | PKS 1454-354 | FSRQ | LSP | 1.424 | both | 5.82 (5.73) |
| J1458.6+3722 | 224.673294 | 37.372601 | B3 1456+375 | BL Lac | LSP | 0.333 | none | ... |
| J1501.0+2238 | 225.256699 | 22.636400 | MS 1458.8+2249 | BL Lac | ISP | 0.235 | opt | ... |
| J1503.5+4759 | 225.895493 | 47.995899 | TXS 1501+481 | BL Lac | LSP | 0.345 | none | ... |
| J1503.6-6427 | 225.910004 | -64.451698 | AT20G J150350-642539 | BCU | ... | ... | none | ... |
| J1504.4+1029 | 226.103302 | 10.497800 | PKS 1502+106 | FSRQ | LSP | 1.839 | both | 0.77 (21.70) |
| J1505.0-3433 | 226.258102 | -34.554600 | PMN J1505-3432 | BL Lac | LSP | ... | none | ... |
| J1506.1+3731 | 226.534698 | 37.518299 | B2 1504+37 | FSRQ | LSP | 0.673 | gam | ... |
| J1506.6+0813 | 226.674103 | 8.225600 | PMN J1506+0814 | BL Lac | ISP | 0.376 | none | ... |
| J1507.2+1721 | 226.820694 | 17.351900 | NVSS J150716+172103 | BL Lac | ISP | 0.565 | none | ... |
| J1508.4+7717 | 227.102005 | 77.292900 | NVSS J150811+771819 | BCU | ISP | ... | none | ... |
| J1509.8-2906 | 227.462601 | -29.106899 | AT20G J150945-290502 | BCU | ... | ... | none | ... |
| J1510.1+5702 | 227.542496 | 57.039799 | GB 1508+5714 | FSRQ | ... | 4.313 | none | ... |
| J1510.8+7959 | 227.704697 | 79.990997 | 1RXS J151026.3+795946 | BCU | LSP | ... | none | ... |
| J1510.8-0542 | 227.706696 | -5.710600 | PKS 1508-05 | FSRQ | LSP | 1.191 | none | ... |
| J1512.2+0202 | 228.070206 | 2.040300 | PKS 1509+022 | FSRQ | LSP | 0.220 | opt | ... |
| J1512.9-5639 | 228.249496 | -56.655300 | PMN J1512-5640 | BCU | LSP | ... | none | ... |
| J1513.2-7131 | 228.314896 | -71.520798 | PMN J1512-7131 | BCU | ... | ... | none | ... |
| J1513.4-3231 | 228.369003 | -32.526501 | PKS 1510-324 | FSRQ | LSP | 1.153 | none | ... |
| J1514.7-3617 | 228.681198 | -36.294899 | PMN J1514-3617 | BCU | LSP | ... | none | ... |
| J1514.8-0949 | 228.715698 | -9.817000 | PMN J1514-0948 | BL Lac | LSP | ... | gam | ... |
| J1514.8-4748 | 228.700195 | -47.814098 | PMN J1514-4748 | FSRQ | LSP | 1.551 | none | ... |
| J1516.1+4351 | 229.049301 | 43.852699 | 87GB 151444.4+4440102 | BL Lac | ISP | ... | none | ... |
| J1516.8+3651 | 229.221695 | 36.850498 | MG2 J151646+3650 | BL Lac | LSP | ... | none | ... |
| J1516.9+1934 | 229.244202 | 19.580500 | PKS 1514+197 | BL Lac | LSP | ... | none | ... |
| J1517.7+6525 | 229.435593 | 65.424004 | 1H 1515+660 | BL Lac | HSP | 0.702 | none | ... |
| J1517.7-2422 | 229.425400 | -24.372999 | AP Librae | BL Lac | LSP | 0.048 | both | -5.80 (33.85) |
| J1518.0-2731 | 229.512405 | -27.531300 | TXS 1515-273 | BL Lac | HSP | ... | opt | ... |
| J1520.5+4209 | 230.134705 | 42.160000 | B3 1518+423 | FSRQ | ... | 0.484 | none | ... |
| J1521.8+4338 | 230.464493 | 43.634399 | B3 1520+437 | FSRQ | LSP | 2.168 | none | ... |
| J1522.1+3144 | 230.545395 | 31.739500 | B2 1520+31 | FSRQ | LSP | 1.489 | gam | ... |
| J1522.6-2730 | 230.664200 | -27.505899 | PKS 1519-273 | BL Lac | LSP | 1.297 | none | ... |
| J1532.7-1319 | 233.197205 | -13.326100 | TXS 1530-131 | BCU | LSP | ... | gam | ... |
| J1534.8+0131 | 233.724701 | 1.522400 | PKS 1532+01 | FSRQ | LSP | 1.428 | gam | ... |
| J1537.7-7957 | 234.439499 | -79.957497 | PMN J1537-7958 | BCU | ... | ... | none | ... |
| J1539.6+2743 | 234.901901 | 27.727699 | MG2 J153938+2744 | FSRQ | LSP | 2.196 | none | ... |
| J1544.3-0649 | 236.078506 | -6.825500 | NVSS J154419-064913 | BCU | ... | ... | opt | ... |
| J1546.1-1003 | 236.541397 | -10.051000 | PMN J1546-1003 | BL Lac | HSP | ... | none | ... |
| J1548.3+1456 | 237.099899 | 14.946100 | NVSS J154824+145702 | BL Lac | ISP | 0.230 | gam | ... |
| J1548.8-2250 | 237.201096 | -22.847099 | PMN J1548-2251 | BL Lac | HSP | 0.192 | none | ... |
| J1549.5+0236 | 237.385101 | 2.608400 | PKS 1546+027 | FSRQ | LSP | 0.414 | opt | ... |
| J1550.7+0528 | 237.696503 | 5.472500 | 4C +05.64 | FSRQ | LSP | 1.422 | both | 999.90 (999.90) |
| J1553.5-3118 | 238.392303 | -31.311300 | 1RXS J155333.4-311841 | BL Lac | HSP | ... | none | ... |
| J1553.6+1257 | 238.401505 | 12.952400 | PKS 1551+130 | FSRQ | LSP | 1.290 | none | ... |
| J1553.6-2422 | 238.402603 | -24.368700 | PKS 1550-242 | FSRQ | ... | 0.332 | gam | ... |
| J1555.2-4149 | 238.824402 | -41.828201 | PMN J1555-4150 | BCU | LSP | ... | none | ... |

| 4FGL Name | RA deg | Dec deg | Association | Class | SED class | redshift | Flares | Lags days |
|--------------|------------|------------|-----------------------|--------|-----------|----------|--------|-----------------|
| J1555.7+1111 | 238.931305 | 11.188400 | PG 1553+113 | BL Lac | HSP | 0.360 | both | 26.87 (38.10) |
| J1559.9+2319 | 239.977707 | 23.319599 | 87GB 155744.0+232525 | BL Lac | ... | 1.034 | opt | ... |
| J1603.8-4903 | 240.966507 | -49.061699 | PMN J1603-4904 | BL Lac | ISP | ... | none | ... |
| J1604.5-4441 | 241.127701 | -44.690300 | PMN J1604-4441 | BL Lac | LSP | ... | gam | ... |
| J1604.6+5714 | 241.158493 | 57.238098 | GB6 J1604+5714 | FSRQ | LSP | 0.720 | both | 22.62 (6.93) |
| J1606.9+5919 | 241.734100 | 59.320099 | 1RXS J160709.7+592115 | BL Lac | ISP | 0.132 | none | ... |
| J1608.7+1029 | 242.176407 | 10.493800 | 4C +10.45 | FSRQ | LSP | 1.226 | gam | ... |
| J1610.3-3958 | 242.598099 | -39.973701 | PMN J1610-3958 | FSRQ | LSP | 0.518 | none | ... |
| J1610.7-6648 | 242.691895 | -66.814697 | PMN J1610-6649 | BL Lac | HSP | ... | none | ... |
| J1612.4-3100 | 243.100098 | -31.001101 | NVSS J161219-305937 | BL Lac | LSP | ... | none | ... |
| J1613.6+3411 | 243.421097 | 34.198200 | OS 319 | FSRQ | LSP | 1.399 | gam | ... |
| J1617.3-5849 | 244.348602 | -58.825699 | MRC 1613-586 | FSRQ | LSP | 1.414 | none | ... |
| J1617.9-7718 | 244.480606 | -77.304001 | PKS 1610-77 | FSRQ | LSP | 1.710 | both | -3.25 (4.46) |
| J1618.0+5139 | 244.515594 | 51.665298 | TXS 1616+517 | FSRQ | LSP | 2.556 | none | ... |
| J1621.7-1103 | 245.427307 | -11.059200 | PMN J1621-1101 | BCU | ... | ... | none | ... |
| J1625.7+4134 | 246.447296 | 41.570900 | 4C +41.32 | FSRQ | LSP | 2.550 | none | ... |
| J1625.7-2527 | 246.445297 | -25.465000 | PKS 1622-253 | FSRQ | LSP | 0.786 | none | ... |
| J1626.0-2950 | 246.514999 | -29.848600 | PKS B1622-297 | FSRQ | LSP | 0.815 | gam | ... |
| J1626.6-7639 | 246.655304 | -76.650200 | PKS 1619-765 | BL Lac | ISP | 0.105 | none | ... |
| J1628.6+7706 | 247.154495 | 77.109901 | 6C B163030.4+771303 | BL Lac | LSP | 0.400 | none | ... |
| J1628.8-6149 | 247.217102 | -61.831299 | LQAC 247-061 | FSRQ | ... | 2.578 | none | ... |
| J1630.7+5221 | 247.681503 | 52.354301 | TXS 1629+524 | BL Lac | ... | 1.545 | none | ... |
| J1631.2+1046 | 247.803604 | 10.775300 | MG1 J163119+1051 | BCU | LSP | ... | none | ... |
| J1632.2+0854 | 248.059692 | 8.904400 | NVSS J163211+085608 | BCU | LSP | ... | none | ... |
| J1635.2+3808 | 248.816803 | 38.140099 | 4C +38.41 | FSRQ | LSP | 1.814 | both | -0.75 (17.37) |
| J1635.6+3628 | 248.922897 | 36.479500 | MG3 J163554+3629 | FSRQ | LSP | 3.648 | none | ... |
| J1637.7+4717 | 249.434204 | 47.291302 | 4C +47.44 | FSRQ | LSP | 0.735 | gam | ... |
| J1637.7+7326 | 249.447998 | 73.441299 | RX J1637.9+7326 | BL Lac | ... | ... | none | ... |
| J1638.1+5721 | 249.525101 | 57.357700 | OS 562 | FSRQ | LSP | 0.751 | none | ... |
| J1639.2+4129 | 249.823807 | 41.496399 | MG4 J163918+4127 | FSRQ | LSP | 0.691 | none | ... |
| J1640.4+3945 | 250.119003 | 39.762600 | NRAO 512 | FSRQ | LSP | 1.660 | none | ... |
| J1641.9-0621 | 250.489197 | -6.352900 | TXS 1639-062 | BL Lac | LSP | ... | none | ... |
| J1642.9+3948 | 250.734100 | 39.816399 | 3C 345 | FSRQ | LSP | 0.593 | both | -3.72 (6.07) |
| J1643.5-0646 | 250.883408 | -6.774900 | NVSS J164328-064619 | BL Lac | ... | 0.082 | opt | ... |
| J1645.6+6329 | 251.405106 | 63.495800 | TXS 1645+635 | FSRQ | LSP | 2.379 | none | ... |
| J1647.4-6438 | 251.870499 | -64.645401 | PMN J1647-6437 | BL Lac | LSP | ... | none | ... |
| J1647.5+4950 | 251.892303 | 49.833599 | SBS 1646+499 | BL Lac | LSP | 0.049 | opt | ... |
| J1648.0+2221 | 252.022598 | 22.352301 | MG2 J164800+2224 | BCU | LSP | 0.823 | none | ... |
| J1649.4+5235 | 252.363693 | 52.590099 | 87GB 164812.2+524023 | BL Lac | ISP | ... | opt | ... |
| J1650.3-5045 | 252.589401 | -50.751499 | PMN J1650-5044 | BL Lac | LSP | ... | none | ... |
| J1653.8+3945 | 253.473801 | 39.759499 | Mkn 501 | BL Lac | HSP | 0.033 | opt | ... |
| J1656.0+2047 | 254.004593 | 20.784100 | MG2 J165546+2043 | BCU | LSP | ... | none | ... |
| J1657.0+6010 | 254.257507 | 60.167599 | RGB J1656+602 | FSRQ | LSP | 0.623 | none | ... |
| J1657.7+4808 | 254.438293 | 48.136799 | 4C +48.41 | FSRQ | LSP | 1.669 | gam | ... |
| J1659.7-3131 | 254.945496 | -31.520901 | NVSS J165949-313047 | BCU | LSP | ... | none | ... |
| J1700.0+6830 | 255.021500 | 68.504204 | TXS 1700+685 | FSRQ | LSP | 0.301 | both | 2.18 (15.46) |
| J1701.0+6613 | 255.260101 | 66.225502 | 7C 1700+6616 | BCU | ... | ... | none | ... |
| J1703.6-6213 | 255.911697 | -62.221500 | MRC 1659-621 | FSRQ | LSP | 1.755 | none | ... |
| J1704.1+7647 | 256.036713 | 76.792297 | NVSS J170357+764611 | BCU | LSP | ... | both | 999.90 (999.90) |
| J1704.2+1234 | 256.059906 | 12.575200 | NVSS J170409+123421 | BL Lac | LSP | 0.450 | none | ... |
| J1706.1+1000 | 256.539093 | 10.007900 | NVSS J170556+100006 | BCU | ... | ... | none | ... |
| J1707.5+1649 | 256.881012 | 16.820601 | MG1 J170732+1649 | FSRQ | LSP | 0.291 | opt | ... |
| J1707.9+0016 | 256.988586 | 0.273100 | NVSS J170744+001750 | BCU | LSP | ... | none | ... |
| J1709.7+4318 | 257.431610 | 43.310902 | B3 1708+433 | FSRQ | LSP | 1.027 | none | ... |
| J1714.0-2029 | 258.522491 | -20.485500 | 1RXS J171405.2-202747 | BCU | HSP | ... | none | ... |
| J1716.1+6836 | 259.031494 | 68.606300 | S4 1716+68 | FSRQ | ... | 0.777 | opt | ... |
| J1717.5-3342 | 259.398499 | -33.700298 | TXS 1714-336 | BL Lac | LSP | ... | none | ... |
| J1717.6-5154 | 259.402588 | -51.909000 | PMN J1717-5155 | FSRQ | LSP | 1.158 | none | ... |
| J1719.2+1745 | 259.806213 | 17.753300 | PKS 1717+177 | BL Lac | LSP | 0.137 | both | -4.45 (83.66) |
| J1722.6+6104 | 260.662415 | 61.073399 | GB6 J1722+6105 | FSRQ | LSP | 2.058 | none | ... |
| J1722.7+1014 | 260.686005 | 10.234600 | TXS 1720+102 | FSRQ | LSP | 0.732 | opt | ... |
| J1723.6-7714 | 260.921906 | -77.237602 | PKS 1716-771 | BCU | LSP | ... | both | 999.90 (999.90) |
| J1724.2+4005 | 261.050903 | 40.089100 | S4 1722+40 | FSRQ | LSP | 1.049 | none | ... |
| J1724.9+7654 | 261.233093 | 76.915199 | S5 1726+76 | FSRQ | LSP | 0.680 | none | ... |
| J1725.0+1152 | 261.271301 | 11.874800 | 1H 1720+117 | BL Lac | HSP | 0.180 | opt | ... |
| J1725.5+5851 | 261.387604 | 58.857800 | 7C 1724+5854 | BL Lac | ISP | 0.297 | opt | ... |
| J1727.4+4530 | 261.852112 | 45.510799 | S4 1726+45 | FSRQ | LSP | 0.717 | both | -3.40 (7.67) |
| J1728.0+1216 | 262.020203 | 12.275600 | PKS 1725+123 | FSRQ | LSP | 0.583 | none | ... |
| J1728.3+5013 | 262.077911 | 50.226700 | I Zw 187 | BL Lac | HSP | 0.055 | none | ... |
| J1728.4+0427 | 262.122009 | 4.460600 | PKS 1725+044 | FSRQ | LSP | 0.293 | none | ... |
| J1728.6-7448 | 262.152893 | -74.803497 | MRC 1722-748 | BCU | ... | ... | none | ... |
| J1730.6+0024 | 262.662811 | 0.409500 | PKS 1728+004 | FSRQ | LSP | 1.335 | none | ... |
| J1733.0-1305 | 263.263214 | -13.085800 | PKS 1730-13 | FSRQ | LSP | 0.902 | none | ... |
| J1733.6-6054 | 263.424591 | -60.906502 | PMN J1733-6055 | BCU | LSP | ... | none | ... |
| J1734.3+3858 | 263.598389 | 38.976299 | B2 1732+38A | FSRQ | LSP | 0.976 | both | 5.76 (22.04) |
| J1736.0+2033 | 264.018585 | 20.555901 | NVSS J173605+203301 | BL Lac | HSP | ... | none | ... |
| J1738.0+8717 | 264.500885 | 87.285103 | 6C B175708+871924 | BCU | ... | ... | none | ... |
| J1738.2+4000 | 264.559988 | 40.009899 | NVSS J173807+400312 | BCU | ISP | ... | none | ... |
| J1739.5+4955 | 264.885986 | 49.931999 | S4 1738+49 | FSRQ | LSP | 1.545 | both | 999.90 (999.90) |
| J1740.5+5211 | 265.135712 | 52.192699 | 4C +51.37 | FSRQ | LSP | 1.381 | both | 999.90 (999.90) |
| J1740.6+5346 | 265.159088 | 53.770100 | 87GB 173932.3+534742 | BL Lac | LSP | ... | none | ... |
| J1744.6-5713 | 266.155487 | -57.232101 | PMN J1744-5715 | BL Lac | ISP | ... | none | ... |
| J1746.8-5235 | 266.719910 | -52.586800 | PMN J1747-5236 | BCU | LSP | ... | none | ... |

| 4FGL Name | RA deg | Dec deg | Association | Class | SED class | redshift | Flares | Lags days |
|--------------|------------|------------|-----------------------|--------|-----------|----------|--------|----------------|
| J1747.1-5453 | 266.786713 | -54.894402 | PMN J1747-5450 | BCU | LSP | ... | none | ... |
| J1748.0+3403 | 267.010590 | 34.064098 | MG2 J174803+3403 | FSRQ | LSP | 2.763 | opt | ... |
| J1748.6+7005 | 267.157990 | 70.096901 | S4 1749+70 | BL Lac | ISP | 0.770 | opt | ... |
| J1749.0+4321 | 267.255402 | 43.361599 | B3 1747+433 | BL Lac | LSP | ... | none | ... |
| J1751.5+0938 | 267.877594 | 9.645600 | OT 081 | BL Lac | LSP | 0.322 | both | 2.02 (15.08) |
| J1751.6+2921 | 267.903900 | 29.358200 | MG2 J175143+2921 | BCU | ... | ... | none | ... |
| J1753.7+2847 | 268.433289 | 28.796700 | B2 1751+28 | FSRQ | LSP | 1.118 | gam | ... |
| J1754.2+3212 | 268.553192 | 32.200699 | RX J1754.1+3212 | BL Lac | ISP | ... | opt | ... |
| J1754.7+3444 | 268.678986 | 34.741699 | MG2 J175448+3442 | BCU | ... | 0.016 | none | ... |
| J1759.1-4822 | 269.783203 | -48.377701 | PMN J1758-4820 | BCU | ... | ... | none | ... |
| J1800.6+7828 | 270.173004 | 78.467400 | S5 1803+784 | BL Lac | LSP | 0.680 | both | 1.14 (11.79) |
| J1801.5+4404 | 270.377106 | 44.074699 | S4 1800+44 | FSRQ | LSP | 0.663 | both | -0.26 (20.25) |
| J1802.6-3940 | 270.671112 | -39.668701 | PMN J1802-3940 | FSRQ | LSP | 0.296 | none | ... |
| J1803.4-6510 | 270.864014 | -65.173203 | PKS 1758-651 | FSRQ | LSP | 1.199 | none | ... |
| J1806.8+6949 | 271.710785 | 69.827003 | 3C 371 | BL Lac | LSP | 0.050 | opt | ... |
| J1807.2+6429 | 271.808685 | 64.498802 | 7C 1807+6428 | BL Lac | ISP | ... | none | ... |
| J1808.1-5013 | 272.032196 | -50.220699 | PMN J1808-5011 | FSRQ | LSP | 1.606 | none | ... |
| J1808.2+3500 | 272.065704 | 35.010399 | MG2 J180813+3501 | BL Lac | ISP | ... | opt | ... |
| J1809.7+2910 | 272.441498 | 29.170900 | MG2 J180948+2910 | BL Lac | ... | ... | none | ... |
| J1811.0+1608 | 272.750000 | 16.147800 | 87GB 180835.5+160714 | BL Lac | ISP | ... | none | ... |
| J1811.3+0340 | 272.825989 | 3.679400 | NVSS J181118+034113 | BL Lac | HSP | ... | none | ... |
| J1813.5+3144 | 273.387207 | 31.749701 | B2 1811+31 | BL Lac | HSP | 0.117 | both | -6.97 (42.66) |
| J1813.6+0614 | 273.408386 | 6.240800 | TXS 1811+062 | BL Lac | LSP | ... | none | ... |
| J1814.4+2953 | 273.615204 | 29.894300 | B2 1811+29 | FSRQ | ... | 1.351 | none | ... |
| J1816.9-4942 | 274.243896 | -49.715801 | PMN J1816-4943 | FSRQ | LSP | 1.700 | none | ... |
| J1818.6+0903 | 274.674805 | 9.065000 | MG1 J181841+0903 | FSRQ | LSP | 0.354 | none | ... |
| J1823.6-3453 | 275.910889 | -34.895199 | NVSS J182338-345412 | BCU | HSP | ... | none | ... |
| J1824.1+5651 | 276.039307 | 56.858501 | 4C +56.27 | BL Lac | LSP | 0.663 | both | 1.64 (7.99) |
| J1825.1-5231 | 276.294586 | -52.528999 | PKS 1821-525 | BCU | LSP | ... | none | ... |
| J1829.2-5813 | 277.310791 | -58.232300 | PKS 1824-582 | FSRQ | ... | 1.531 | both | -4.67 (3.97) |
| J1830.0+1324 | 277.511993 | 13.413800 | MG1 J183001+1323 | BL Lac | ISP | ... | none | ... |
| J1830.1+0617 | 277.536285 | 6.287800 | TXS 1827+062 | FSRQ | LSP | 0.745 | none | ... |
| J1830.2-4443 | 277.550415 | -44.720001 | PMN J1830-4441 | BCU | LSP | ... | none | ... |
| J1834.7-5858 | 278.687408 | -58.981800 | PKS 1830-589 | BL Lac | LSP | ... | none | ... |
| J1838.8+4802 | 279.714111 | 48.041199 | GB6 J1838+4802 | BL Lac | HSP | 0.300 | opt | ... |
| J1839.6-7107 | 279.914215 | -71.124298 | PKS 1831-711 | FSRQ | LSP | 1.356 | none | ... |
| J1840.6-5545 | 280.174805 | -55.751801 | PMN J1841-5544 | BCU | ... | ... | none | ... |
| J1841.0+6115 | 280.253113 | 61.252201 | 87GB 184000.4+611120 | BCU | ... | ... | none | ... |
| J1841.8+3218 | 280.453003 | 32.300999 | RX J1841.7+3218 | BL Lac | HSP | ... | none | ... |
| J1842.4-5840 | 280.611206 | -58.680199 | 1RXS J184230.6-584202 | BL Lac | ... | 0.421 | none | ... |
| J1844.4+1547 | 281.117401 | 15.788800 | NVSS J184425+154646 | BL Lac | HSP | ... | none | ... |
| J1848.4+3217 | 282.105011 | 32.294998 | B2 1846+32A | FSRQ | LSP | 0.798 | none | ... |
| J1848.5+3243 | 282.145599 | 32.730900 | B2 1846+32B | FSRQ | LSP | 0.981 | both | 0.81 (2.88) |
| J1848.5+6537 | 282.133209 | 65.631302 | NVSS J184822+653702 | BL Lac | ... | 0.364 | none | ... |
| J1849.2+6705 | 282.319214 | 67.090897 | S4 1849+67 | FSRQ | LSP | 0.657 | both | -11.22 (16.73) |
| J1849.4+2745 | 282.354309 | 27.754200 | MG2 J184929+2748 | BL Lac | LSP | ... | none | ... |
| J1849.4-4313 | 282.362305 | -43.221401 | PMN J1849-4314 | BL Lac | LSP | ... | opt | ... |
| J1852.4+4856 | 283.115997 | 48.935001 | S4 1851+48 | FSRQ | LSP | 1.250 | none | ... |
| J1858.3-2511 | 284.575195 | -25.199100 | PMN J1858-2511 | BCU | LSP | ... | none | ... |
| J1902.9-6748 | 285.743195 | -67.806801 | PMN J1903-6749 | FSRQ | LSP | 0.255 | both | 0.60 (31.88) |
| J1903.2+5540 | 285.807709 | 55.677299 | TXS 1902+556 | BL Lac | LSP | ... | none | ... |
| J1904.1+3627 | 286.034302 | 36.452599 | MG2 J190411+3627 | BL Lac | ... | 0.078 | none | ... |
| J1911.2-2006 | 287.807800 | -20.113701 | PKS B1908-201 | FSRQ | LSP | 1.119 | gam | ... |
| J1912.1-0803 | 288.028412 | -8.058900 | PMN J1912-0804 | BCU | ... | ... | none | ... |
| J1912.4-1222 | 288.118500 | -12.367800 | TXS 1909-124 | BCU | ... | ... | opt | ... |
| J1913.0-8009 | 288.269989 | -80.157402 | PKS 1903-80 | FSRQ | LSP | 1.756 | gam | ... |
| J1913.4-3629 | 288.350708 | -36.488499 | PMN J1913-3630 | BCU | LSP | ... | none | ... |
| J1917.7-1921 | 289.438385 | -19.362801 | 1H 1914-194 | BL Lac | HSP | 0.137 | opt | ... |
| J1918.2-4111 | 289.564301 | -41.189301 | PMN J1918-4111 | BL Lac | LSP | ... | none | ... |
| J1921.8-1607 | 290.463287 | -16.123100 | PMN J1921-1607 | BL Lac | ISP | ... | none | ... |
| J1922.5-7453 | 290.627899 | -74.887604 | 1RXS J192244.1-74541 | BCU | HSP | ... | none | ... |
| J1923.5-2104 | 290.876312 | -21.070999 | TXS 1920-211 | FSRQ | LSP | 0.874 | none | ... |
| J1924.8-2914 | 291.213593 | -29.246799 | PKS B1921-293 | FSRQ | LSP | 0.353 | none | ... |
| J1926.8+6154 | 291.709686 | 61.914600 | 87GB 192614.4+614823 | BL Lac | HSP | ... | opt | ... |
| J1927.5+6117 | 291.882202 | 61.293999 | S4 1926+61 | BL Lac | LSP | ... | opt | ... |
| J1931.1+0937 | 292.783997 | 9.631400 | RX J1931.1+0937 | BL Lac | HSP | ... | none | ... |
| J1933.2-4539 | 293.314301 | -45.650799 | PKS 1929-457 | FSRQ | LSP | 0.652 | none | ... |
| J1934.3+6541 | 293.595215 | 65.688797 | TXS 1933+655 | FSRQ | LSP | 1.687 | gam | ... |
| J1936.9-4720 | 294.241608 | -47.340000 | PMN J1936-4719 | BL Lac | ... | 0.265 | none | ... |
| J1937.2-3958 | 294.309204 | -39.982498 | PKS 1933-400 | FSRQ | LSP | 0.965 | none | ... |
| J1939.5-1525 | 294.877197 | -15.425600 | PKS 1936-15 | FSRQ | LSP | 1.657 | gam | ... |
| J1941.3-6210 | 295.346802 | -62.175301 | PKS 1936-623 | BL Lac | LSP | ... | gam | ... |
| J1942.1+4011 | 295.539001 | 40.198399 | 87GB 194033.4+400351 | BCU | ISP | ... | none | ... |
| J1942.7+1033 | 295.696014 | 10.558400 | 87GB 194024.3+102612 | BL Lac | HSP | ... | none | ... |
| J1944.9-2143 | 296.229492 | -21.721600 | 1RXS J194455.3-214318 | BL Lac | ... | 0.410 | none | ... |
| J1945.1-4007 | 296.292206 | -40.120899 | AT20G J194519-400557 | BCU | LSP | ... | none | ... |
| J1949.5+0906 | 297.390198 | 9.105400 | 1RXS J194934.1+090655 | BL Lac | HSP | ... | none | ... |
| J1951.8-0511 | 297.964996 | -5.184400 | PMN J1951-0509 | FSRQ | LSP | 1.083 | opt | ... |
| J1954.6-1122 | 298.669312 | -11.381500 | TXS 1951-115 | BL Lac | LSP | 0.683 | opt | ... |
| J1955.1-1604 | 298.777405 | -16.071501 | 1RXS J195500.6-160328 | BL Lac | HSP | ... | none | ... |
| J1955.2+1358 | 298.820099 | 13.982400 | 87GB 195252.4+135009 | FSRQ | LSP | 0.743 | none | ... |
| J1957.1-3231 | 299.286407 | -32.524601 | PKS 1953-325 | FSRQ | LSP | 1.242 | none | ... |
| J1958.0-3845 | 299.502594 | -38.754700 | PKS 1954-388 | FSRQ | LSP | 0.630 | both | 9.30 (16.55) |

| 4FGL Name | RA deg | Dec deg | Association | Class | SED class | redshift | Flares | Lags days |
|--------------|------------|------------|-------------------------|--------|-----------|----------|--------|-----------------|
| J1958.1-0711 | 299.533813 | -7.192600 | NVSS J195801-071348 | BCU | ... | ... | none | ... |
| J1958.3-3010 | 299.581207 | -30.181000 | 1RXS J195815.6-301119 | BL Lac | ... | 0.119 | opt | ... |
| J1959.0+3844 | 299.766296 | 38.736801 | LQAC 299+038 | BCU | LSP | ... | none | ... |
| J1959.1-4247 | 299.796295 | -42.785198 | PMN J1959-4246 | FSRQ | LSP | 2.174 | none | ... |
| J2000.0+6508 | 300.010986 | 65.147903 | IES 1959+650 | BL Lac | HSP | 0.047 | both | 999.90 (999.90) |
| J2000.9-1748 | 300.234589 | -17.816401 | PKS 1958-179 | FSRQ | LSP | 0.652 | both | -2.72 (19.24) |
| J2001.2+4353 | 300.301788 | 43.886200 | MG4 J200112+4352 | BL Lac | HSP | ... | none | ... |
| J2005.1+7003 | 301.277588 | 70.062401 | 1RXS J200504.0+700445 | BL Lac | HSP | ... | none | ... |
| J2005.5+7752 | 301.393005 | 77.882896 | S5 2007+77 | BL Lac | LSP | 0.342 | both | 999.90 (999.90) |
| J2005.8+6424 | 301.463989 | 64.400200 | 87GB 200541.3+641601 | FSRQ | LSP | 1.574 | none | ... |
| J2005.9-2309 | 301.476196 | -23.153099 | TXS 2002-233 | FSRQ | LSP | 0.830 | none | ... |
| J2007.2+6607 | 301.814789 | 66.117798 | TXS 2007+659 | FSRQ | LSP | 1.325 | gam | ... |
| J2007.3-7728 | 301.846588 | -77.477997 | PKS 2000-776 | BCU | LSP | ... | none | ... |
| J2009.4-4849 | 302.359497 | -48.824799 | PKS 2005-489 | BL Lac | HSP | 0.071 | opt | ... |
| J2009.9+3544 | 302.489197 | 35.745998 | B2 2008+35 | BCU | ... | ... | none | ... |
| J2010.0+7229 | 302.515900 | 72.487396 | 4C +72.28 | BL Lac | LSP | ... | none | ... |
| J2012.0+4629 | 303.020386 | 46.487999 | 7C 2010+4619 | BL Lac | ISP | ... | both | 999.90 (999.90) |
| J2012.2-1646 | 303.071899 | -16.772900 | PMN J2012-1646 | BL Lac | LSP | ... | none | ... |
| J2015.3-1432 | 303.826111 | -14.541700 | NVSS J201525-143202 | BL Lac | ... | ... | none | ... |
| J2016.3-0903 | 304.098206 | -9.062200 | PMN J2016-0903 | BL Lac | ISP | 0.367 | opt | ... |
| J2022.3-4513 | 305.591095 | -45.222801 | PMN J2022-4513 | BL Lac | ISP | ... | opt | ... |
| J2022.5+7612 | 305.645905 | 76.200699 | S5 2023+760 | BL Lac | LSP | 0.594 | opt | ... |
| J2023.6-1139 | 305.903198 | -11.658500 | PMN J2023-1140 | FSRQ | LSP | 0.698 | none | ... |
| J2024.6-3252 | 306.158112 | -32.874001 | PKS 2021-330 | FSRQ | LSP | 1.465 | none | ... |
| J2024.8-6459 | 306.200989 | -64.991302 | PMN J2024-6458 | BCU | LSP | ... | none | ... |
| J2025.2+0317 | 306.308502 | 3.289300 | PKS 2022+031 | FSRQ | LSP | 2.210 | none | ... |
| J2025.3+3341 | 306.341187 | 33.689098 | B2 2023+33 | BL Lac | LSP | 0.219 | none | ... |
| J2025.6-0735 | 306.421997 | -7.594500 | PKS 2023-07 | FSRQ | LSP | 1.388 | both | 4.40 (9.72) |
| J2029.5+4925 | 307.375000 | 49.422100 | MG4 J202932+4925 | BL Lac | LSP | ... | none | ... |
| J2030.2-0620 | 307.564087 | -6.343200 | TXS 2027-065 | FSRQ | LSP | 0.667 | none | ... |
| J2031.2-4121 | 307.811188 | -41.357399 | SUMSS J203056-411906 | BCU | ... | ... | none | ... |
| J2032.0+1219 | 308.003998 | 12.327900 | PKS 2029+121 | BL Lac | LSP | 1.215 | none | ... |
| J2034.6+1154 | 308.650391 | 11.903500 | TXS 2032+117 | FSRQ | LSP | 0.607 | both | 1.79 (5.76) |
| J2035.4+1056 | 308.851715 | 10.938000 | PKS 2032+107 | FSRQ | LSP | 0.601 | gam | ... |
| J2036.4+6553 | 309.103210 | 65.883400 | 87GB 203539.4+654245 | BL Lac | ISP | ... | none | ... |
| J2038.7+5117 | 309.693787 | 51.285099 | 3C 418 | FSRQ | LSP | 1.686 | none | ... |
| J2039.0-1046 | 309.758087 | -10.773100 | TXS 2036-109 | BL Lac | LSP | ... | none | ... |
| J2040.5-1705 | 310.136414 | -17.090099 | TXS 2037-172 | BCU | LSP | ... | none | ... |
| J2046.8-4258 | 311.720490 | -42.969398 | 2MASS J20464397-4257134 | BL Lac | ... | ... | none | ... |
| J2049.9+1002 | 312.478210 | 10.040700 | PKS 2047+098 | BL Lac | LSP | ... | none | ... |
| J2050.4-2627 | 312.610413 | -26.465900 | PMN J2050-2628 | FSRQ | LSP | 1.633 | none | ... |
| J2052.2-5533 | 313.067413 | -55.562401 | PMN J2052-5533 | BCU | ... | ... | gam | ... |
| J2056.2-4714 | 314.071503 | -47.236900 | PKS 2052-47 | FSRQ | LSP | 1.489 | both | 4.67 (11.43) |
| J2056.5-0202 | 314.142212 | -2.035500 | PMN J2056-0205 | BCU | LSP | ... | none | ... |
| J2103.8-6233 | 315.954712 | -62.556301 | PMN J2103-6232 | BL Lac | ISP | ... | none | ... |
| J2104.0-3546 | 316.009613 | -35.767799 | NVSS J210353-354620 | BCU | LSP | ... | opt | ... |
| J2108.2-2454 | 317.061493 | -24.908100 | AT20G J210812-245233 | BCU | ... | ... | none | ... |
| J2108.5+1434 | 317.147614 | 14.581200 | OX 110 | FSRQ | LSP | 2.017 | none | ... |
| J2110.3+0808 | 317.575989 | 8.149800 | PMN J2110+0810 | FSRQ | LSP | 1.580 | none | ... |
| J2114.8+2831 | 318.716492 | 28.522200 | B2 2112+28B | FSRQ | LSP | 2.345 | opt | ... |
| J2115.4+2932 | 318.873688 | 29.545601 | B2 2113+29 | FSRQ | LSP | 1.514 | both | 999.90 (999.90) |
| J2119.6-1105 | 319.924103 | -11.091000 | PKS 2116-11 | FSRQ | LSP | 1.844 | none | ... |
| J2120.6-1254 | 320.153595 | -12.909700 | NVSS J212035-125443 | BCU | ... | 0.582 | none | ... |
| J2121.0+1901 | 320.259796 | 19.032400 | OX 131 | FSRQ | LSP | 2.180 | none | ... |
| J2123.6+0535 | 320.920593 | 5.592000 | OX 036 | FSRQ | LSP | 1.941 | none | ... |
| J2126.3-4605 | 321.594788 | -46.097801 | PKS 2123-463 | FSRQ | LSP | 1.670 | none | ... |
| J2127.7+3612 | 321.931091 | 36.212502 | B2 2125+35 | BL Lac | HSP | ... | none | ... |
| J2130.4-4241 | 322.601196 | -42.690399 | SUMSS J213017-424319 | BCU | ... | ... | none | ... |
| J2131.0-2746 | 322.752991 | -27.772699 | RBS 1751 | BL Lac | HSP | 0.380 | none | ... |
| J2131.5-0916 | 322.891113 | -9.268400 | RBS 1752 | BL Lac | HSP | 0.449 | none | ... |
| J2133.9+6646 | 323.479309 | 66.777603 | NVSS J213349+664706 | BL Lac | HSP | ... | none | ... |
| J2134.2-0154 | 323.569885 | -1.904200 | PKS 2131-021 | BL Lac | LSP | 1.283 | opt | ... |
| J2134.5-2130 | 323.641388 | -21.502899 | NVSS J213430-213032 | BL Lac | ISP | ... | none | ... |
| J2135.3-5006 | 323.836212 | -50.101501 | PMN J2135-5006 | FSRQ | LSP | 2.181 | none | ... |
| J2136.5+4259 | 324.141113 | 42.993801 | TXS 2134+428 | BCU | LSP | ... | gam | ... |
| J2139.4-4235 | 324.854614 | -42.589500 | MH 2136-428 | BL Lac | ISP | ... | both | 999.90 (999.90) |
| J2141.7-6410 | 325.430511 | -64.179199 | PMN J2141-6411 | BCU | LSP | ... | gam | ... |
| J2141.8-3727 | 325.462189 | -37.454498 | PKS 2138-377 | FSRQ | LSP | 0.423 | none | ... |
| J2143.1-3929 | 325.793091 | -39.488201 | PMN J2143-3929 | BL Lac | HSP | 0.429 | none | ... |
| J2143.5+1743 | 325.894196 | 17.730600 | OX 169 | FSRQ | LSP | 0.211 | gam | ... |
| J2144.2+3132 | 326.064606 | 31.545700 | MG3 J214415+3132 | BL Lac | ISP | ... | none | ... |
| J2145.0-3356 | 326.253296 | -33.943901 | PMN J2145-3357 | FSRQ | LSP | 1.360 | none | ... |
| J2146.5-1344 | 326.644897 | -13.734700 | NVSS J214637-134359 | BL Lac | ... | 0.420 | none | ... |
| J2146.8+0425 | 326.708008 | 4.426600 | MG1 J214653+0427 | BCU | LSP | ... | none | ... |
| J2147.1+0931 | 326.782898 | 9.518100 | PKS 2144+092 | FSRQ | LSP | 1.113 | none | ... |
| J2147.3-7536 | 326.826813 | -75.602402 | PKS 2142-75 | FSRQ | LSP | 1.138 | both | 1.67 (2.48) |
| J2149.1+6104 | 327.289703 | 61.070499 | 4C +60.32 | BCU | ... | ... | none | ... |
| J2149.6+0323 | 327.423615 | 3.395900 | PKS B2147+031 | BL Lac | LSP | ... | none | ... |
| J2149.7+1917 | 327.444092 | 19.285900 | TXS 2147+191 | BCU | LSP | ... | none | ... |
| J2150.7-2810 | 327.698395 | -28.172800 | PMN J2150-2812 | FSRQ | LSP | 0.865 | none | ... |
| J2151.7-2749 | 327.925110 | -27.823400 | PMN J2151-2742 | FSRQ | LSP | 1.485 | none | ... |
| J2151.8-3027 | 327.965515 | -30.459999 | PKS 2149-306 | FSRQ | LSP | 2.345 | none | ... |
| J2153.8-1137 | 328.460907 | -11.630600 | PMN J2153-1136 | FSRQ | LSP | 1.582 | none | ... |

| 4FGL Name | RA deg | Dec deg | Association | Class | SED class | redshift | Flares | Lags days |
|--------------|------------|------------|------------------------------|--------|-----------|----------|--------|---------------|
| J2156.3-0036 | 329.079712 | -0.603900 | PKS B2153-008 | FSRQ | LSP | 0.495 | none | ... |
| J2157.5+3127 | 329.386200 | 31.455200 | B2 2155+31 | FSRQ | LSP | 1.486 | none | ... |
| J2158.1-1501 | 329.527496 | -15.023700 | PKS 2155-152 | FSRQ | LSP | 0.672 | opt | ... |
| J2158.8-3013 | 329.714111 | -30.225100 | PKS 2155-304 | BL Lac | HSP | 0.116 | both | 5.57 (52.07) |
| J2159.8-4751 | 329.962311 | -47.851799 | PMN J2200-4751 | BCU | LSP | ... | none | ... |
| J2200.1+2138 | 330.030701 | 21.638201 | TXS 2157+213 | BL Lac | LSP | ... | none | ... |
| J2201.5-8339 | 330.378693 | -83.663101 | PKS 2155-83 | FSRQ | LSP | 1.865 | both | -0.67 (3.08) |
| J2201.8+5048 | 330.453186 | 50.805302 | NRAO 676 | FSRQ | LSP | 1.899 | none | ... |
| J2202.7+4216 | 330.694611 | 42.282101 | BL Lac | BL Lac | LSP | 0.069 | both | -0.19 (24.32) |
| J2203.4+1725 | 330.872101 | 17.431801 | PKS 2201+171 | FSRQ | LSP | 1.076 | none | ... |
| J2205.0+7432 | 331.271912 | 74.546204 | S5 2205+74 | BCU | LSP | ... | none | ... |
| J2206.8-0032 | 331.708710 | -0.546100 | PMN J2206-0031 | BL Lac | LSP | 1.053 | opt | ... |
| J2207.5-5346 | 331.892212 | -53.771900 | PKS 2204-54 | FSRQ | LSP | 1.215 | none | ... |
| J2207.6+0053 | 331.913696 | 0.890700 | PMN J2207+0052 | FSRQ | ... | ... | none | ... |
| J2209.8-5028 | 332.473511 | -50.470200 | PMN J2210-5030 | BCU | ... | ... | none | ... |
| J2211.2-1325 | 332.816803 | -13.418900 | PKS 2208-137 | FSRQ | LSP | 0.392 | opt | ... |
| J2212.9-2526 | 332.226105 | -25.433500 | PKS 2210-25 | FSRQ | LSP | 1.833 | opt | ... |
| J2216.9+2421 | 334.238007 | 24.357500 | B2 2214+24B | BL Lac | LSP | 0.505 | none | ... |
| J2219.2+1806 | 334.812714 | 18.102600 | MG1 J221916+1806 | FSRQ | LSP | 1.071 | none | ... |
| J2221.5-5225 | 335.390900 | -52.430698 | PMN J2221-5224 | BL Lac | HSP | 0.340 | none | ... |
| J2221.9-3504 | 335.497009 | -35.071201 | NVSS J222227-350942 | FSRQ | ... | 0.298 | none | ... |
| J2222.8+1209 | 335.709808 | 12.156800 | TXS 2220+119 | BCU | LSP | ... | none | ... |
| J2225.6+2120 | 336.413605 | 21.341801 | PKS 2223+21 | FSRQ | LSP | 1.959 | none | ... |
| J2225.7-0457 | 336.432098 | -4.953700 | 3C 446 | FSRQ | LSP | 1.404 | none | ... |
| J2228.6-1636 | 337.165894 | -16.607300 | 2MASS J22283018-1636432 | BL Lac | ISP | 0.525 | none | ... |
| J2229.7-0832 | 337.425812 | -8.544700 | PKS 2227-08 | FSRQ | LSP | 1.560 | gam | ... |
| J2230.9-7815 | 337.728210 | -78.259399 | PKS 2225-785 | FSRQ | LSP | ... | none | ... |
| J2231.0-4416 | 337.757996 | -44.279099 | PKS 2227-445 | FSRQ | LSP | 1.326 | opt | ... |
| J2232.6+1143 | 338.152496 | 11.730600 | CTA 102 | FSRQ | LSP | 1.037 | both | -2.67 (31.53) |
| J2234.1-2656 | 338.542511 | -26.937500 | PMN J2234-2656 | BL Lac | LSP | ... | none | ... |
| J2235.1-0623 | 338.799408 | -6.395500 | PMN J2235-0623 | BCU | LSP | ... | none | ... |
| J2235.3-4836 | 338.840912 | -48.601501 | PKS 2232-488 | FSRQ | LSP | 0.510 | none | ... |
| J2235.8-3627 | 338.970795 | -36.460499 | NVSS J223554-362901 | BL Lac | ISP | ... | none | ... |
| J2236.3+2828 | 339.096191 | 28.483200 | B2 2234+28A | FSRQ | LSP | 0.790 | both | -0.91 (20.82) |
| J2236.4-2309 | 339.124603 | -23.155199 | PMN J2236-2309 | BCU | LSP | ... | gam | ... |
| J2236.5-1433 | 339.144409 | -14.555700 | PKS 2233-148 | BL Lac | LSP | 0.325 | both | 11.86 (21.82) |
| J2237.0-3921 | 339.268585 | -39.356998 | NVSS J223708-392137 | FSRQ | LSP | 0.297 | none | ... |
| J2243.4-2544 | 340.865387 | -25.736300 | PKS 2240-260 | BL Lac | LSP | 0.774 | opt | ... |
| J2243.9+2021 | 340.989502 | 20.356501 | RGB J2243+203 | BL Lac | HSP | ... | gam | ... |
| J2244.2+4057 | 341.061401 | 40.959702 | TXS 2241+406 | FSRQ | LSP | 1.171 | both | -2.60 (11.93) |
| J2248.7-3235 | 342.192810 | -32.592602 | PKS 2245-328 | FSRQ | LSP | 2.268 | none | ... |
| J2248.9+2106 | 342.246887 | 21.121401 | PKS 2246+208 | FSRQ | LSP | 1.274 | both | -4.65 (5.35) |
| J2250.0+3825 | 342.514191 | 38.424702 | B3 2247+381 | BL Lac | HSP | 0.119 | none | ... |
| J2250.0-1250 | 342.504913 | -12.848500 | PKS 2247-131 | BCU | LSP | ... | gam | ... |
| J2250.4-4206 | 342.606201 | -42.109501 | PMN J2250-4206 | BL Lac | ISP | 0.119 | none | ... |
| J2250.7-2806 | 342.690308 | -28.111401 | PMN J2250-2806 | BL Lac | LSP | 0.525 | none | ... |
| J2251.2+5550 | 342.803894 | 55.843102 | 87GB 224837.7+553415 | BCU | ... | ... | none | ... |
| J2251.5-4928 | 342.878906 | -49.469101 | SUMSS J225128-492912 | BL Lac | ISP | ... | none | ... |
| J2253.2-1232 | 343.308411 | -12.541600 | TXS 2250-127 | BCU | LSP | ... | opt | ... |
| J2253.9+1609 | 343.496307 | 16.150600 | 3C 454.3 | FSRQ | LSP | 0.859 | both | -1.52 (12.98) |
| J2254.8-2725 | 343.717987 | -27.417101 | NVSS J225453-272509 | BL Lac | ISP | 0.333 | none | ... |
| J2258.1-2759 | 344.528809 | -27.984301 | PKS 2255-282 | FSRQ | LSP | 0.926 | both | 6.68 (22.48) |
| J2258.5-8247 | 344.638885 | -82.784401 | PMN J2258-8246 | BCU | ISP | ... | none | ... |
| J2259.8-1552 | 344.952606 | -15.880900 | GALEXASC J225957.26-155332.5 | BCU | LSP | ... | opt | ... |
| J2300.7-2645 | 345.182312 | -26.750200 | PKS 2257-270 | FSRQ | LSP | 1.476 | none | ... |
| J2301.0-0158 | 345.262695 | -1.975800 | PKS B2258-022 | FSRQ | LSP | 0.778 | both | -1.45 (27.96) |
| J2304.6+3704 | 346.172607 | 37.082600 | 1RXS J230437.1+370506 | BL Lac | HSP | ... | none | ... |
| J2307.6+1451 | 346.922211 | 14.864400 | MG1 J230734+1449 | BL Lac | LSP | 0.503 | none | ... |
| J2311.0+0205 | 347.766113 | 2.099500 | NVSS J231101+020504 | BL Lac | LSP | ... | opt | ... |
| J2311.0+3425 | 347.768188 | 34.422298 | B2 2308+34 | FSRQ | LSP | 1.817 | both | 2.95 (13.50) |
| J2311.7+2604 | 347.930786 | 26.083099 | MG3 J231144+2604 | BCU | LSP | 1.747 | none | ... |
| J2312.5+7241 | 348.139587 | 72.692299 | CRATES J2312+7241 | BCU | LSP | ... | none | ... |
| J2313.5+3945 | 348.399689 | 39.764400 | 87GB 231102.6+393314 | BCU | ... | ... | none | ... |
| J2315.6-5018 | 348.914001 | -50.312698 | PKS 2312-505 | BL Lac | LSP | 0.811 | none | ... |
| J2317.4-4533 | 349.356506 | -45.562302 | SUMSS J231731-453400 | BL Lac | HSP | ... | none | ... |
| J2318.2+1915 | 349.556793 | 19.256001 | TXS 2315+189 | BCU | LSP | 2.163 | none | ... |
| J2321.5-1619 | 350.385406 | -16.317600 | NVSS J232137-161935 | BL Lac | ... | 0.694 | none | ... |
| J2321.7-6438 | 350.433197 | -64.645302 | PMN J2321-6438 | BL Lac | ISP | ... | none | ... |
| J2321.9+3204 | 350.477905 | 32.073700 | B2 2319+31 | FSRQ | LSP | 1.489 | gam | ... |
| J2322.6-0735 | 350.657593 | -7.590700 | PMN J2322-0736 | BCU | LSP | ... | none | ... |
| J2322.8-4916 | 350.707703 | -49.272499 | SUMSS J232254-491629 | BL Lac | HSP | 0.380 | none | ... |
| J2323.6-0617 | 350.915710 | -6.295300 | TXS 2321-065 | FSRQ | LSP | 2.144 | none | ... |
| J2323.8+4210 | 350.974915 | 42.182598 | 1ES 2321+419 | BL Lac | HSP | 0.059 | opt | ... |
| J2324.7+0801 | 351.189606 | 8.028200 | PMN J2324+0801 | BL Lac | ISP | ... | none | ... |
| J2324.7-4041 | 351.181702 | -40.683399 | 1ES 2322-409 | BL Lac | HSP | 0.174 | opt | ... |
| J2325.2+3957 | 351.315399 | 39.954201 | B3 2322+396 | BL Lac | LSP | ... | none | ... |
| J2325.4-3559 | 351.358612 | -35.987801 | CTS 0490 | FSRQ | LSP | 0.360 | none | ... |
| J2325.4-4800 | 351.350098 | -48.002201 | PKS 2322-482 | BL Lac | ISP | 0.221 | opt | ... |
| J2325.7+1821 | 351.436005 | 18.365400 | MG1 J232550+1822 | BCU | LSP | ... | opt | ... |
| J2326.2+0113 | 351.574799 | 1.221600 | SDSS J232625.63+011208.6 | BCU | LSP | 0.335 | opt | ... |
| J2327.5+0939 | 351.895905 | 9.654300 | PKS 2325+093 | FSRQ | LSP | 1.843 | opt | ... |
| J2328.3-4036 | 352.081696 | -40.603699 | PKS 2325-408 | FSRQ | LSP | 1.972 | opt | ... |
| J2329.3-4733 | 352.339386 | -47.555801 | PKS 2326-477 | FSRQ | LSP | 1.302 | none | ... |

| 4FGL Name | RA deg | Dec deg | Association | Class | SED class | redshift | Flares | Lags days |
|--------------|------------|------------|---------------------|--------|-----------|----------|--------|--------------|
| J2330.2+7759 | 352.568207 | 77.994698 | WN B2329.2+7743 | BCU | ... | ... | none | ... |
| J2330.5+1102 | 352.628693 | 11.047900 | 4C +10.73 | FSRQ | LSP | 1.489 | none | ... |
| J2331.0-2147 | 352.763214 | -21.795300 | PMN J2331-2148 | FSRQ | LSP | 0.563 | opt | ... |
| J2334.2+0736 | 353.557312 | 7.602000 | TXS 2331+073 | FSRQ | LSP | 0.401 | none | ... |
| J2334.8+1432 | 353.723297 | 14.534600 | NVSS J233453+143214 | BL Lac | LSP | 0.415 | none | ... |
| J2335.4-0128 | 353.868805 | -1.476000 | PKS 2332-017 | FSRQ | LSP | 1.182 | none | ... |
| J2336.6-4115 | 354.163605 | -41.257900 | PKS 2333-415 | FSRQ | LSP | 1.406 | none | ... |
| J2338.0-0230 | 354.508514 | -2.510600 | PKS 2335-027 | FSRQ | LSP | 1.071 | none | ... |
| J2343.7-5624 | 355.934906 | -56.404800 | PKS 2340-567 | BCU | LSP | 1.240 | none | ... |
| J2345.2-1555 | 356.303009 | -15.918200 | PMN J2345-1555 | FSRQ | LSP | 0.621 | both | 2.28 (12.38) |
| J2347.0+5141 | 356.765900 | 51.696602 | 1ES 2344+514 | BL Lac | HSP | 0.044 | none | ... |
| J2348.0-1630 | 357.015991 | -16.516100 | PKS 2345-16 | FSRQ | LSP | 0.576 | both | 8.38 (11.04) |
| J2348.1-4934 | 357.037201 | -49.570000 | PKS 2346-498 | BCU | LSP | ... | none | ... |
| J2349.2+4535 | 357.304993 | 45.597900 | TXS 2346+453 | BL Lac | ... | ... | none | ... |
| J2349.4+0534 | 357.355804 | 5.579000 | TXS 2346+052 | FSRQ | LSP | 0.419 | none | ... |
| J2350.6-3005 | 357.664886 | -30.087000 | LEDA 3231681 | BL Lac | HSP | 0.224 | none | ... |
| J2352.0+1750 | 358.013214 | 17.839399 | CLASS J2352+1749 | BL Lac | ISP | ... | none | ... |
| J2357.8-5311 | 359.463013 | -53.191898 | PKS 2355-534 | FSRQ | LSP | 1.006 | none | ... |
| J2358.3+3830 | 359.588287 | 38.509701 | B3 2355+382 | BL Lac | ... | 0.200 | none | ... |
| J2358.3-1021 | 359.582214 | -10.361600 | PKS 2355-106 | FSRQ | LSP | 1.638 | opt | ... |
| J2359.0+3922 | 359.754791 | 39.366901 | B2 2356+39 | FSRQ | LSP | 1.198 | none | ... |

Notes: The first column gives the 4FGL name, followed by its coordinates in columns 2 and 3. In Column 4, 5, 6, we list the associated source to the γ -ray emissions, the sources class (BL Lac: BL Lac type, FSRQ: flat-spectrum radio quasars, BUC: blazar candidates of uncertain type), and the SED class (LSP: low-synchrotron peaked blazars, ISP: intermediate synchrotron peaked blazars, and HSP: high-synchrotron peaked blazars). In Column 7, the redshift is given. In Columns 8, the presence of significant flares in the optical and γ -rays light curves is display (both, opt, gam, none). Finally, in Column 9, we display the rest-frame time lag in days between optical and γ -rays flares, where a positive τ_{lag} corresponds to the γ -ray emission leading to the optical emission.

900

901 **APPENDIX B: “ORPHAN” FLARES**

902 In this appendix, we list the characteristic of our “orphan” flare golden sample.

Table B1: “Orphan” flare golden sample properties.

| 4FGL Name | Band | Peak MJD | width days | label Fig. 7 |
|----------------|------|-------------|---------------|--------------|
| 20J0011.4+0057 | gam | 57564 | 15 | A |
| 20J0038.2–2459 | opt | 57930 | 45 | a |
| 20J0050.7–0929 | opt | 56477 | 19 | b |
| 20J0102.8+5824 | opt | 59124 | 171 | c |
| 20J0108.6+0134 | gam | 57581 | 258 | B |
| 20J0118.9–2141 | opt | 58349 | 109 | d |
| 20J0133.1–5201 | gam | 57764 | 12 | C |
| 20J0133.1–5201 | gam | 58077 | 19 | C |
| 20J0211.2+1051 | opt | 56882 | 48 | e |
| 20J0211.2+1051 | opt | 57050 | 27 | e |
| 20J0217.8+0144 | opt | 57758 | 30 | f |
| 20J0229.5–3644 | gam | 57212 | 22 | D |
| 20J0303.4–2407 | opt | 58701 | 66 | g |
| 20J0325.7+2225 | gam | 58460 | 6 | E |
| 20J0405.6–1308 | gam | 57574 | 22 | F |
| 20J0405.6–1308 | gam | 59571 | 9 | F |
| 20J0440.3–4333 | gam | 58365 | 54 | G |
| 20J0457.0–2324 | opt | 57037 | 16 | h |
| 20J0457.0–2324 | opt | 57252 | 60 | h |
| 20J0501.2–0158 | gam | 57258 | 9 | H |
| 20J0538.8–4405 | opt | 57744 | 51 | i |
| 20J0539.9–2839 | gam | 59208 | 15 | I |
| 20J0539.9–2839 | gam | 59319 | 9 | I |
| 20J0719.3+3307 | opt | 57324 | 27 | j |
| 20J0742.6+5443 | opt | 57106 | 27 | k |
| 20J0839.8+0105 | opt | 58448 | 36 | l |
| 20J0842.3–6053 | gam | 59600 | 12 | J |
| 20J0854.8+2006 | opt | 58947 | 142 | m |
| 20J0910.8+3859 | opt | 57090 | 69 | n |
| 20J0912.2+4127 | gam | 57318 | 12 | K |
| 20J0921.6+6216 | gam | 57752 | 30 | L |
| 20J0942.3–0800 | opt | 57722 | 37 | o |
| 20J1058.4+0133 | gam | 56700 | 63 | M |
| 20J1153.3–1104 | gam | 58467 | 21 | N |
| 20J1159.2–2227 | gam | 59332 | 34 | O |
| 20J1218.5–0119 | opt | 58872 | 36 | p |
| 20J1238.3–1959 | opt | 58545 | 84 | q |
| 20J1303.0+2434 | opt | 59366 | 48 | r |
| 20J1308.5+3547 | gam | 58970 | 18 | P |
| 20J1312.8–0425 | gam | 58658 | 18 | Q |
| 20J1333.7+5056 | gam | 59360 | 50 | R |
| 20J1423.5–7829 | opt | 59271 | 36 | s |
| 20J1427.6–3305 | opt | 58591 | 111 | t |
| 20J1438.9+3710 | gam | 57863 | 30 | S |
| 20J1506.1+3731 | gam | 57060 | 18 | T |
| 20J1517.7–2422 | opt | 58197 | 25 | u |
| 20J1532.7–1319 | gam | 56771 | 27 | U |
| 20J1635.2+3808 | gam | 56499 | 201 | V |
| 20J1700.0+6830 | opt | 56466 | 18 | v |
| 20J1740.5+5211 | gam | 59271 | 24 | W |
| 20J1748.6+7005 | opt | 56864 | 55 | w |
| 20J1748.6+7005 | opt | 59514 | 90 | w |
| 20J2158.8–3013 | opt | 57604 | 37 | x |
| 20J2236.5–1433 | opt | 58413 | 40 | y |
| 20J2250.0–1250 | gam | 57674 | 12 | X |
| 20J2250.0–1250 | gam | 58340 | 16 | X |

